

UCSF

UC San Francisco Electronic Theses and Dissertations

Title

Dissecting biological pathways in cancer and bacteria through the study and application of serine protease inhibitors

Permalink

<https://escholarship.org/uc/item/47b8k2j7>

Author

Ray, Manisha

Publication Date

2011

Peer reviewed|Thesis/dissertation

Dissecting biological pathways in cancer and bacteria through the
study and application of serine protease inhibitors

by

Manisha Ray

DISSERTATION

Submitted in partial satisfaction of the requirements for the degree of

DOCTOR OF PHILOSOPHY

in

Biochemistry and Molecular Biology

in the

GRADUATE DIVISION

of the

UNIVERSITY OF CALIFORNIA, SAN FRANCISCO



Acknowledgements

Graduate school has been an exciting and challenging adventure, and many individuals have helped me along the way. My thesis advisor, Charly Craik, has been an endless fountain of enthusiasm. Charly's love for science and incredible generosity are truly inspiring. I can only hope that in the future I love my job half as much as Charly loves running the lab.

My thesis committee, Jeff Cox and Carol Gross have been instrumental in guiding my project. I was always amazed by how many new ideas would result from our meetings. Jeff Cox in particular has gone above and beyond in mentoring my research, from opening up his lab to me to helping me write fellowship applications. I will always admire his ability to discuss small technical details while keeping track of the big picture. The entire Cox lab, especially Yamini Ohol, have always been happy to share their knowledge and resources with me.

Chris Brown has become a close friend and collaborator through our love of phosphonates, cooking and television. Having a partner in crime made the ups and downs of our project smoother, especially with a partner as intelligent and patient as Chris. Dan Hostetter has been a constant source of encouragement and advice, as well as teaching me much of what I learned in the Craik lab. I have been incredibly lucky to work with two such optimistic and supportive scientists.

Mark Lim, Min Zhou, Alegra Eroy-Reveles, and Cheryl Tajon were my chemistry mentors in the lab. They taught me everything I know about chemistry, and I certainly would never have gotten anywhere on the phosphonate project without them. In addition to being an amazing chemist, Alegra has been a wonderful mentor. I greatly appreciate her advice on everything from what to wear on job interviews to speaking Spanish.

One reason I joined the Craik lab was the amazing group of fun, intelligent, and generous scientists Charly had assembled. Though I only overlapped with Carly R. K.

Loeb, who started the PI-9 project, briefly, she has continued to provide advice about both the project and my career throughout my time in the lab. In addition to Carly, Dan and Mark, Chris Farady, Dave Goetz, and Anthony O'Donoghue were as happy to show me new techniques as they were to grab burritos or drink lab scotch late into the night. I aspire to their ability to mix teaching and sarcasm. I have been fortunate to go through all the trials and tribulations of grad school with my classmate Tina Shahian, who joined the lab at the same time as me. I always admired Tina's thoughtful, methodical, and productive approach to both science and life. Lastly, life in the Craik lab would have been way less entertaining without Sai Duriseti, my fellow baymate, futsal teammate, night owl, and my only vegetarian ally in the lab.

UCSF is an amazing institution and attracts awesome, eclectic people to its graduate programs. I truly feel that Mission Bay is the best place in the world to do innovative, collaborative science, and I have met many wonderful people along the way. My classmates Sarah Goodwin, Ben Engel, and Mike Nehil, as well as "upperclassman" Yari Sigal, Jason Huff, Chris Rivera, Ryan Raisner, and Brad Zuchero have made my time at Mission Bay fly by, often due to poorly planned adventures into the woods and endless soccer games. Jason and Chris in particular have offered a great deal of scientific advice over the years, and they have an uncanny ability to cheer me up when science gets me down.

My parents, Ruth and Sudipta Ray, have taught me the importance of education and lifelong learning, and they have always encouraged my interest in science. I am proud to be the third Dr. Ray in my family.

Lastly, I thank my wonderful boyfriend and classmate Paul Temkin. Throughout our entire graduate careers, his support, both scientifically and emotionally, has been unwavering. Thank you to everyone at UCSF who has made my time here so productive and fulfilling!

Dissecting biological pathways in cancer and bacteria through the study and application of serine protease inhibitors

by

Manisha Ray

Abstract

Serine proteases are an abundant class of enzymes that are vital to many biological processes. Proteolysis must be tightly controlled, and this regulation is frequently carried out through serine protease inhibitors. Dysregulation of either the protease or the inhibitor can have severe biological consequences, such as the development of cancer. Additionally, the role of proteases can be challenging to study, since the active form or proteases can be difficult to isolate. In this thesis, the role of the naturally occurring protease inhibitor PI-9 is examined in the development of prostate cancer. The findings presented here show that PI-9 protects prostate cancer cells from immunosurveillance early in cancer progression. Additionally, a chemical biology approach is taken to develop small molecule activity based probes for serine proteases, in order to better study active proteases in complex systems. Principles governing the design and potency of these probes were discovered, and new imaging applications for these probes were developed. These new techniques could be applied to the study of proteases in any biological system. The work described here provides new information on how to identify proteases involved in cancer and bacterial development, and such insights could be used to design new therapeutic strategies.

Table of Contents

Chapter 1: Introduction	1
Forward: Serine proteases: Biological decision makers	1
Macromolecular protease inhibitors: role in biology and therapeutics	3
Small molecule protease inhibitors: tools and drugs	7
References	11
Figures	15
 Chapter 2: PI-9 protects prostate cancer cells from immunosurveillance	 21
Introduction	22
Materials and Methods	23
Results	27
Discussion	31
References	33
Figures	37
 Chapter 3: Peptide phosphonate activity based probes: guidelines and applications <i>(Re-printed with permission from Chemistry and Biology)</i>	 45
Introduction	46
Materials and Methods	48
Results	55
Discussion	61
References	65
Figures	71
 Chapter 4: Identification and biochemical characterization of active proteases in bacteria	 79
Introduction	79
Results	83
Conclusions/ Future Directions	86
References	87
Figures	89
 Chapter 4: Conclusions and Future Directions	 100
References	104

List of Tables

Table 3-1	71
Table 3-2	72

Table 3-3	74
Supplemental Table S3-1.....	76
Supplemental Table S3-2.....	76
Table 4-1	92
Table 4-2	97

List of Figures

Figure 1-1	15
Figure 1-2.....	16
Figure 1-3.....	17
Figure 1-4.....	18
Figure 1-5.....	19
Figure 1-6.....	20
Figure 2-1	37
Figure 2-2.....	39
Figure 2-3.....	40
Figure 2-4.....	41
Figure 2-5.....	43
Supplementary Figure S2-1	44
Supplementary Figure S2-2	44
Figure 3-1	71
Figure 3-2.....	73
Figure 3-3.....	75
Supplementary Figure S3-1	77
Supplementary Figure S3-2	78
Figure 4-1	89
Figure 4-2.....	90
Figure 4-3.....	91
Figure 4-4.....	93
Figure 4-5.....	94
Figure 4-6.....	95
Figure 4-7.....	96
Figure 4-8.....	98

Figure 4-9	99
-------------------------	-----------

Introduction

Forward: Serine proteases and their inhibitors

Macromolecular protease inhibitors: roles in biology and therapeutics

Small molecule protease inhibitors: tools and drugs

Serine proteases: biological decision makers

Proteases, proteins that cleave other proteins, are an important and abundant class of enzymes. Proteases are found in every organism, from viruses to humans, and typically make up 2-4% of every genome examined. The roles of proteases can be classified in two ways: degradation and signaling. Proteases are responsible for break down and elimination of proteins, freeing amino acids for other purposes. Examples of degradative proteases include the digestive proteases found in the stomach and pancreas, and the proteasome, which acts as a cellular “garbage disposal.”

Proteases also function as signal regulators. Because proteolysis is irreversible, proteases often act as biological decision makers. For example, blood coagulation is controlled by a proteolytic cascade, which is triggered by an injury and results in the rapid formation of blood clots (Davie, 2003)(Walsh and Ahmad, 2002). Additionally, programmed cell death, or apoptosis, is a tightly regulated process controlled by two groups of proteases, the caspases and the granzymes (Budihardjo et al., 1999).

Because of their role in cellular decision-making, proteases make excellent drug targets. The HIV protease inhibitor drugs have seen great success in treating AIDS, and the FDA has recently approved protease inhibitor drugs against another virus, Hepatitis C (Lamarre et al., 2003). Velcade, a proteasome inhibitor, is now a commonly prescribed cancer drug (Moore et al., 2008), and Januvia, an inhibitor of the protease DPP-IV, is one of the most useful diabetes drugs (Thornberry and Weber, 2007). Recently approved factor Xa and thrombin inhibitors show great promise for alternative therapies for coagulation disorders (Harenberg et al., 2011). Additional anti-proteolytic therapies are in

development. Overall, proteases have emerged as an important and effective therapeutic target.

Proteases fall into five classes, based on their catalytic residue: aspartyl and metalloproteases, cysteine, serine, and threonine proteases. This thesis will focus on serine proteases (Figure 1-1). Serine proteases are an abundant and important class of proteases in most organisms (Figure 1-2), and their well established catalytic mechanism makes them relatively facile to inhibit using mechanism-based inhibitors. Serine proteases have been implicated in cancer metastasis, cardiovascular disease, blood disorders, viral assembly, and many other processes. This thesis will examine the role of serine protease inhibitors, both naturally occurring and synthetic, as agents to intervene in the biology of cancer and other diseases.

Protease regulation

Because proteolysis is irreversible, the process must be tightly regulated. Proteases are often regulated post-translationally, which allows for tight spatial and temporal control. Many proteases are made in an inactive or zymogen form, which can be activated under appropriate conditions. One well studied example of spatial regulation is trypsin, which is made as the inactive zymogen trypsinogen in the pancreas, and activated by an enteropeptidase upon entering the small intestine. Multimeric proteases are often regulated by local concentration, for example the KSHV protease, which becomes active upon reaching high enough concentrations in the viral capsid to dimerize (Nomura et al., 2005).

Protease inhibitors are a second way to control activity. For example, the protease inhibitor anti-thrombin constantly circulates in the blood to prevent aberrant clotting by low levels of active thrombin (Walsh and Ahmad, 2002). At the most basic level, protease inhibitors operate in one of two ways: either targeting the active site, which directly prevents catalysis, or targeting a non-active site location, such as an exosite or an allosteric site. There are two broad classes of serine protease inhibitors: macromolecular inhibitors, and small molecule inhibitors.

This thesis examines two functions of serine protease inhibitors: as naturally occurring targets for cancer therapy, and synthetic small molecules to study protease activity. The second chapter focuses on the role of endogenous protease inhibitors and the development of prostate cancer, and describes how the interplay between molecular levels of a protease and its natural inhibitor can have drastic consequences on the ability of the body to control cancer. The third chapter of this thesis takes a chemical biology approach to exploring how small molecule inhibitors can be functionalized to make tools to study serine proteases in cancer and other biological processes. The fourth chapter focuses on using both chemical biology and biochemical approaches to studying proteases and proteolytically controlled processes in bacteria. The work presented here demonstrates how the ability of protease inhibitors to regulate, disrupt, and interrogate biological processes can result in new insights into cancer and other human diseases.

Macromolecular protease inhibitors: roles in biology and therapeutics

Macromolecular inhibitors are proteins that are natural synthesized by cells to inhibit proteases, and utilize a variety of mechanisms. Standard mechanism inhibitors bind in a substrate-like manner to the protease, and though the scissile bond is cleaved very slowly, the products are not released (Laskowski and Kato, 1980). Many standard mechanism inhibitors contain an inhibitory protein domain, such as a Kunitz domain, or a repeating array of domains such as Kazal domains. These disulfide-rich domains bind in the substrate pocket in an extended β -sheet. These inhibitors generally have broad specificity and inhibit a wide range of serine proteases, and well studied inhibitors utilizing this motif include Bovine Pancreatic Trypsin Inhibitor (BPTI) and Tissue Factor Pathway Inhibitor (TFPI). The Kunitz domain has been used successfully as a scaffold to rationally design protease inhibitors. For example, the peptide drug Ecallantide, which was developed using this technique and inhibits plasma kallikrein, has been approved to treat angioedema (Lehmann, 2008).

Some macromolecular active site inhibitors also bind a secondary site distal to the active site, or an exosite. One well-studied example of dual site inhibition is found in the

bacterial protease inhibitor ecotin. Ecotin is a dimeric protein that inhibits the active site of serine proteases through the standard mechanism, but also binds a distal site in an antibody-like interaction (Eggers et al., 2001). Ecotin is an extremely broad inhibitor of serine proteases, but by engineering the amino acids at the binding interface, greater specificity can be achieved (Stoop et al., 2010)(Stoop and Craik, 2003). Additionally, by tagging these ecotin molecules with a label such as biotin, inhibited proteases could be enriched and identified, an approach that has met with limited success in the Craik lab.

Exosites can potentially increase the specificity of an inhibitor, such as in the case of tick anticoagulant peptide (TAP). In addition to binding to the active site, the TAP inhibitor specifically binds the autolysis loop on the clotting protease factor Xa, allowing the inhibitor to selectively block one member of the highly similar family of proteases that make up the coagulation cascade (Wei et al., 1998). A similar strategy has evolved in the medicinal leech *Hirudo medicinalis*, whose protease inhibitor hirudin selectively inhibits thrombin (Rydel et al., 1991).

Another class of protease inhibitors requires prior cleavage by the target protease in order to inhibit it. α -2-macroglobulin, another nonspecific serine protease inhibitor found in the blood, contains several reactive loops on its surface (Kolodziej et al., 2002). When one of these loops is recognized by a specific protease, the inhibitor changes conformation to expose reactive thiol-esters, which covalently crosslink to the protease (Sottrup-Jensen, 1989). In this mechanism, the active site is less accessible but remains functional.

Serpins, or **serine protease inhibitors**, use a protease-activated mechanism to directly block the active site. Serpins also contain a bait-like loop, called the reactive center loop (RCL), which is accessible for proteolytic cleavage (Gettins, 2002). The residues of the RCL confer specificity to the serpin. Cleavage of the RCL results in a major conformational change, where the loop is inserted into the main body of the inhibitor as a β -sheet. This translocates the protease across the serpin, which completely blocks the active site. The RCL remains bound to the protease in the acyl-enzyme intermediate of

catalysis, so the active site is both sterically blocked and catalytically inhibited. This inhibitory mechanism is irreversible and the resulting serpin-protease complex is stable under harsh conditions such as boiling in SDS.

Macromolecular serine protease inhibitors play critical roles in regulating serine proteases in natural biological processes. Malfunctioning proteases underlie many human diseases, including many types of cancer. However, dysregulation of these inhibitors can also cause deleterious and cancer-promoting effects. This thesis explores the relationship between the protease Granzyme B, which induces apoptosis, and its natural inhibitor, the serpin PI-9, in the progression of prostate cancer. By gaining a better understanding of the interplay between proteases and their natural inhibitors, better treatments or prognostic tools may be developed.

The Granzymes are a family of S1A serine proteases produced by immune cells such as cytotoxic lymphocytes (CLs), which include natural killer (NK) cells (Lieberman, 2003). Granzymes are located in secretory granules within CLs, and these proteases are used to induce apoptosis in cancerous or virally infected cells recognized by the CLs. The process of monitoring and eliminating aberrant cells is called immunosurveillance. When target cells are recognized by CLs, using surface receptors on both cell types, the secretory granules fuse with the plasma membrane of the CL and the granzymes are released. The granzymes enter the target cells with the help of perforin, a pore-forming protein also found in the granules, and induce apoptosis (Figure 1-3).

Granzyme B, a 32kD serine protease, is the major initiator of apoptosis (Anthony et al., 2010). It is abundantly expressed in natural killer cells, and induces apoptosis in several ways. Granzyme B cleaves and activates both initiator and execution caspases, which are responsible for carrying out apoptosis (Medema et al., 1997), (Yang et al., 1998). In addition to activating pro-apoptotic substrates, Granzyme B cleaves and inactivates pro-life substrates like the poly-A-ribosyltransferase protein (PARP) (Froelich et al., 1996) and structural proteins like tubulin (Adrain et al., 2006). By cleaving a very specific set of

substrates that either promote death or prevent proliferation, Granzyme B acts as a cellular demolition expert.

The natural inhibitor of Granzyme B is a serpin, PI-9 (Kaiserman and Bird, 2010). PI-9 is a 42kD protein normally found in CLs to protect themselves from inadvertent exposure to their own Granzyme B. PI-9 is similarly found in sites in the body that contain many CLs, such as the eyes and the testes. PI-9 is also induced in response to inflammation, a process known as the “bystander effect,” again to protect healthy cells from accidental Granzyme B exposure (Buzza et al., 2001). The ability of PI-9 to block apoptosis by inhibiting Granzyme B could potentially be harnessed by cancer cells to block immunosurveillance.

The idea that PI-9 expression may protect cancer cells has evidence in several types of cancer. PI-9 expression has been observed in many cancers, including breast cancer, cervical cancer, and colon cancer (Medema et al., 2001). It has been shown in mice and in HeLa cells that overexpression of PI-9 directly protects cells from apoptosis through GrB inhibition (Medema et al., 2001)(Cunningham et al., 2007), and evidence for this protective effect has been observed in breast cancer as well (Jiang et al., 2006).

PI-9 expression may also affect the probability of successful treatment of cancer. PI-9 has been associated with poor clinical prognosis in lymphoma and nasopharyngeal carcinoma (ten Berge et al., 2003)(Oudejans et al., 2002). PI-9 expression can interfere with hormone therapy in breast cancer (Jiang et al., 2007), and PI-9 expression is correlated with the failure of immunotherapy in melanoma (van Houdt et al., 2005). Taken together, PI-9 has emerged as an important immuno-evasive protein in many cancers that has both therapeutic and diagnostic implications.

In this thesis, the protective capabilities of PI-9 were examined in prostate cancer. PI-9 levels were measured in both prostate cancer cell lines, as well as human prostate tissue. PI-9 expression in cell lines was found to inhibit Granzyme B, and result in a decrease in cell death induced by natural killer cells. Additionally, PI-9 expression in prostate tissue

was most consistent in the earliest forms of prostate cancer (Figure 1-4), implying that PI-9 is needed early in the development of prostate cancer. These findings indicate that PI-9 could have potential as a prognostic marker used in the classification and treatment plan for prostate cancer, and warrant additional clinical studies of PI-9 and prostate cancer.

Small molecule protease inhibitors: tools and drugs

Macromolecular protease inhibitors like serpins comprise the natural pathways that have evolved to regulate proteolysis. By exploiting small molecule inhibitors of proteolysis, new tools can be developed to study protease function, which may be useful as therapeutic agents. HIV has been successfully treated by inhibiting HIV protease, and a similar approach has recently led to a new drug to treat the Hepatitis C virus (Lamarre et al., 2003). A novel approach to treating diabetes uses the drug Januvia, which inhibits the DPP-IV protease and results in a longer lifetime of insulin-stimulating peptides (Thornberry and Weber, 2007)(White, 2008).

As with macromolecular inhibitors, small molecules can be designed to target the active site, an exosite, or both. Allosteric inhibitors have seen recent advances; the Craik lab has recently shown the utility of targeting allosteric binding interfaces, rather than the active site, for inhibiting dimeric proteases (Shahian et al., 2009), and the Wells lab has developed non-active site inhibitors of caspases in their zymogen form (Hardy and Wells, 2009). However, mechanism-based serine protease inhibitors target the active site, and these inhibitors work by trapping the enzyme in a transition state.

Transition state inhibitors form stable mimics of the tetrahedral intermediate present during catalysis. The tetrahedral intermediate is formed when the nucleophilic serine attacks the carbonyl group of the scissile bond, linking the enzyme and the substrate. Many inhibitors contain electrophilic groups that mimic the carbonyl group in order to trap the enzyme in the tetrahedral intermediate, and rely on the activity of the enzyme in order to inhibit it. These competitive inhibitors can interact covalently and reversibly with the protease.

Examples of transition state inhibitors include boronic acid inhibitors, where the boronic acid moiety forms a stable tetrahedral intermediate, and aldehyde-based inhibitors, which form a hemi-acetal intermediate that mimics the tetrahedral intermediate. Peptides can be easily attached to both inhibitors, allowing greater specificity. These inhibitors are reversible, and this strategy has resulted in very specific inhibitors and successful drugs such as Bortezomib, a boronic acid-based proteasome inhibitor used to treat cancer (Moore et al., 2008).

Another effective use of small molecules to inhibit serine proteases utilizes covalent, irreversible inhibitors. There are three types of covalent inhibitors: inhibitors that alkylate or acylate the active site, inhibitors that require proteolytic activation, and inhibitors that bind the protease in a covalent transition state (Powers et al., 2002). Chloromethyl ketones, which are also amenable to peptide attachment to attain specificity, are common inhibitors of serine proteases and work by alkylating the catalytic histidine. Isocoumarin and β -lactam inhibitors are examples of activation-based inhibitors, in which proteolytic cleavage opens one of the rings of the inhibitor, and subsequent steps result in a stable enzyme-inhibitor complex. The cephalosporin inhibitors of elastase are activation-based inhibitors. However, these ring-based inhibitors are not easily functionalized, so attaining substrate specificity is more difficult.

Covalent irreversible inhibitors of serine proteases consist of vinyl sulfones and phosphonates. Both groups contain a reactive sulfur or phosphorous group surrounded by excellent electrophilic leaving groups. When the reactive center is attacked by the active site serine, forming the tetrahedral intermediate, one of the electrophilic leaving groups is displaced, resulting in the protease stably bound to the inhibitor (Figure 1-5).

These covalent, irreversible inhibitors, particularly phosphonates, offer many useful features for the development of activity-based probes (ABPs). Activity-based probes consist of a covalent inhibitor functionalized with a detection tag, such as biotin or a fluorophore (Figure 1-6). These probes provide the ability to follow single enzymes

through visualization or enrichment followed by mass spectrometric identification, an advantage over bulk protease techniques such as fluorescent substrates (Cravatt et al., 2008). Additionally, these probes only bind to active enzymes, filtering out inactive or zymogen forms of the enzyme that may be present. The inability to distinguish between active and inactive forms of enzymes is a common complication when using most molecular biology techniques like qPCR or Western blotting. Phosphonate inhibitors attach covalently, and the electrophilic leaving groups can be tuned to alter reactivity. Phosphonates are also amenable to additional chemical functionalization, such as the addition of peptides to increase specificity. Additionally, the chemical tractability of phosphonates also enables the attachment of detection tags. Overall, phosphonates are excellent candidates for the development of serine protease activity based probes.

Activity based probes have contributed extensively to the study of cysteine proteases, as well as other enzymes like kinases and histone deacetylases (Dar and Shokat, 2011), (Salisbury and Cravatt, 2007). However, their use in the serine protease field has proved challenging. Diisopropyl fluorophosphonate (DFP) has historically been used as a serine protease inhibitor, but the fluorine leaving groups render the molecule so reactive that it will bind to any serine hydrolase, including acetylcholinesterase, making the compound highly toxic. Biotinylating DFP enabled its use as an activity based probe, and the Cravatt group identified many serine hydrolases through this approach (Tully and Cravatt, 2010), (Blankman et al., 2007).

Work by the Craik, Powers, and Oleksyszyn groups has shown that adding a peptide element to the phosphonate group directs the probe toward proteases (Oleksyszyn and Powers, 1994), (Mahrus and Craik, 2005), (Sieńczyk and Oleksyszyn, 2009). Additionally, altering the leaving group properties dramatically changed the potency of a probe directed toward the protease uPA (Sieńczyk and Oleksyszyn, 2006). Despite these insights, the advances brought about by serine activity based probes remain limited to very specific instances, and still lag behind cysteine proteases and other enzymes.

In this thesis, a systematic approach was taken to explore the utility of peptide phosphonate ABPs through kinetic, structural, and imaging approaches. A series of

probes were synthesized to test the specificity and potency against three canonical proteases in the S1A family: MT-SP1, thrombin, and uPA. The contribution of the peptide element in both composition and length was tested, and the contribution of the leaving group was examined by structural and mutagenesis studies. This work found that longer peptides composed of stable, uncharged amino acids resulted in the most potent and stable ABPs. Additionally, the steric fit of the leaving group in the binding pocket of the protease dramatically altered potency in a protease-specific manner. Protease specificity was difficult to achieve using peptide sequences alone, so optimizing the leaving group may prove to be a more effective method to gain specificity for the ABPs.

The work presented here describes guidelines for the design and synthesis of peptide phosphonate ABPs, as well as insights into applications for these ABPs. Labeling of proteases *in vitro*, in lysates, and by fluorescence microscopy was observed robustly in each application. The ability to follow active proteases by imaging opens up new types of experiments into the localization and function of proteases in the cell, particularly proteases associated with metastatic cancer. Labeling worked best on cell-surface proteases, which are an abundant class of proteases important in signaling between the cell and the outside environment.

However, identification of the active proteases that are labeled has proven problematic. The work presented here shows that phosphonates are slow inhibitors that require high concentrations (high μM) over long time periods (hours) are needed to see inhibitory effects. This large excess of probe, coupled with the long reaction times, makes purifying intact proteases difficult. Future work into optimizing the ABP and the mass spectrometry will be necessary to identify proteases.

In summary, protease inhibitors can be extremely useful as tools to study the biological role of proteases in complex systems. Here, two cancer-associated applications are discussed: the use of PI-9 as a potential prognostic marker for prostate cancer, and the use of peptide phosphonate ABPs as tools to study cancer-associated proteases.

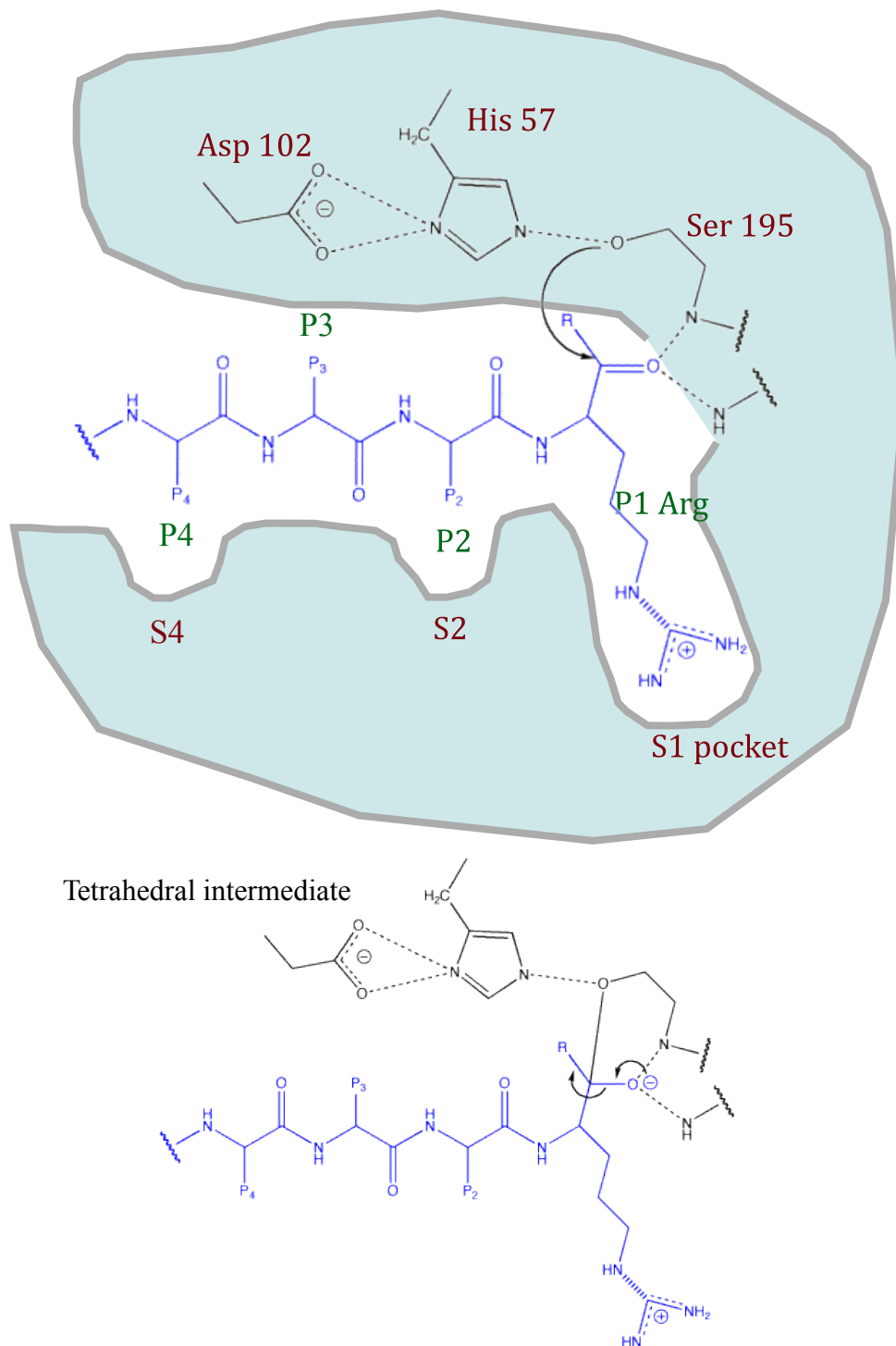
- Adrain, C., Duriez, P. J., Brumatti, G., Delivani, P., and Martin, S. J. (2006). The cytotoxic lymphocyte protease, granzyme B, targets the cytoskeleton and perturbs microtubule polymerization dynamics. *J. Biol. Chem* 281, 8118-8125.
- Anthony, D. A., Andrews, D. M., Watt, S. V., Trapani, J. A., and Smyth, M. J. (2010). Functional dissection of the granzyme family: cell death and inflammation. *Immunological Reviews* 235, 73-92.
- ten Berge, R. L., Oudejans, J. J., Ossenkoppele, G. J., and Meijer, C. J. L. M. (2003). ALK-negative systemic anaplastic large cell lymphoma: differential diagnostic and prognostic aspects--a review. *J. Pathol* 200, 4-15.
- Blankman, J. L., Simon, G. M., and Cravatt, B. F. (2007). A comprehensive profile of brain enzymes that hydrolyze the endocannabinoid 2-arachidonoylglycerol. *Chem. Biol* 14, 1347-1356.
- Budihardjo, I., Oliver, H., Lutter, M., Luo, X., and Wang, X. (1999). Biochemical Pathways of Caspase Activation During Apoptosis. *Annu. Rev. Cell Dev. Biol.* 15, 269-290.
- Buzza, M. S., Hirst, C. E., Bird, C. H., Hosking, P., McKendrick, J., and Bird, P. I. (2001). The Granzyme B Inhibitor, PI-9, Is Present in Endothelial and Mesothelial Cells, Suggesting That It Protects Bystander Cells during Immune Responses. *Cellular Immunology* 210, 21-29.
- Cravatt, B. F., Wright, A. T., and Kozarich, J. W. (2008). Activity-based protein profiling: from enzyme chemistry to proteomic chemistry. *Annu. Rev. Biochem* 77, 383-414.
- Cunningham, T. D., Jiang, X., and Shapiro, D. J. (2007). Expression of high levels of human proteinase inhibitor 9 blocks both perforin/granzyme and Fas/Fas ligand-mediated cytotoxicity. *Cellular Immunology* 245, 32-41.
- Dar, A. C., and Shokat, K. M. (2011). The Evolution of Protein Kinase Inhibitors from Antagonists to Agonists of Cellular Signaling. *Annu. Rev. Biochem.* 80, 769-795.
- Davie, E. W. (2003). A Brief Historical Review of the Waterfall/Cascade of Blood Coagulation. *Journal of Biological Chemistry* 278, 50819 -50832.
- Eggers, C. T., Wang, S. X., Fletterick, R. J., and Craik, C. S. (2001). The role of ecotin dimerization in protease inhibition. *J. Mol. Biol* 308, 975-991.
- Froelich, C. J., Hanna, W. L., Poirier, G. G., Duriez, P. J., D'amours, D., Salvesen, G. S., Alnemri, E. S., Earnshaw, W. C., and Shah, G. M. (1996). Granzyme B/Perforin-Mediated Apoptosis of Jurkat Cells Results in Cleavage of Poly(ADP-ribose) Polymerase to the 89-kDa Apoptotic Fragment and Less Abundant 64-kDa Fragment. *Biochemical and Biophysical Research Communications* 227, 658-665.

- Gettins, P. G. W. (2002). Serpin structure, mechanism, and function. *Chem. Rev* 102, 4751-4804.
- Hardy, J. A., and Wells, J. A. (2009). Dissecting an allosteric switch in caspase-7 using chemical and mutational probes. *J. Biol. Chem* 284, 26063-26069.
- Harenberg, J., Marx, S., Wehling, M., and Krejczy, M. (2011). New Anticoagulants - Promising and Failed Developments. *Br J Pharmacol*. Available at: <http://www.ncbi.nlm.nih.gov/pubmed/21740405> [Accessed July 27, 2011].
- van Houdt, I. S., Oudejans, J. J., van den Eertwegh, A. J. M., Baars, A., Vos, W., Bladergroen, B. A., Rimoldi, D., Muris, J. J. F., Hooijberg, E., Gundy, C. M., et al. (2005). Expression of the Apoptosis Inhibitor Protease Inhibitor 9 Predicts Clinical Outcome in Vaccinated Patients with Stage III and IV Melanoma. *Clinical Cancer Research* 11, 6400 -6407.
- Jiang, X., Ellison, S. J., Alarid, E. T., and Shapiro, D. J. (2007). Interplay between the levels of estrogen and estrogen receptor controls the level of the granzyme inhibitor, proteinase inhibitor 9 and susceptibility to immune surveillance by natural killer cells. *Oncogene* 26, 4106-4114.
- Jiang, X., Orr, B. A., Kranz, D. M., and Shapiro, D. J. (2006). Estrogen induction of the granzyme B inhibitor, proteinase inhibitor 9, protects cells against apoptosis mediated by cytotoxic T lymphocytes and natural killer cells. *Endocrinology* 147, 1419-1426.
- Kaiserman, D., and Bird, P. I. (2010). Control of granzymes by serpins. *Cell Death Differ* 17, 586-595.
- Kolodziej, S. J., Wagenknecht, T., Strickland, D. K., and Stoops, J. K. (2002). The three-dimensional structure of the human alpha 2-macroglobulin dimer reveals its structural organization in the tetrameric native and chymotrypsin alpha 2-macroglobulin complexes. *J. Biol. Chem* 277, 28031-28037.
- Lamarre, D., Anderson, P. C., Bailey, M., Beaulieu, P., Bolger, G., Bonneau, P., Bos, M., Cameron, D. R., Cartier, M., Cordingley, M. G., et al. (2003). An NS3 protease inhibitor with antiviral effects in humans infected with hepatitis C virus. *Nature* 426, 186-189.
- Laskowski, M., Jr, and Kato, I. (1980). Protein inhibitors of proteinases. *Annu. Rev. Biochem* 49, 593-626.
- Lehmann, A. (2008). Ecallantide (DX-88), a plasma kallikrein inhibitor for the treatment of hereditary angioedema and the prevention of blood loss in on-pump cardiothoracic surgery. *Expert Opin. Biol. Ther.* 8, 1187-1199.
- Lieberman, J. (2003). The ABCs of granule-mediated cytotoxicity: new weapons in the arsenal. *Nat Rev Immunol* 3, 361-370.

- Mahrus, S., and Craik, C. S. (2005). Selective chemical functional probes of granzymes A and B reveal granzyme B is a major effector of natural killer cell-mediated lysis of target cells. *Chem. Biol* 12, 567-577.
- Medema, J. P., de Jong, J., Peltenburg, L. T., Verdegaal, E. M., Gorter, A., Bres, S. A., Franken, K. L., Hahne, M., Albar, J. P., Melief, C. J., et al. (2001). Blockade of the granzyme B/perforin pathway through overexpression of the serine protease inhibitor PI-9/SPI-6 constitutes a mechanism for immune escape by tumors. *Proc. Natl. Acad. Sci. U.S.A* 98, 11515-11520.
- Medema, J. P., Toes, R. E., Scaffidi, C., Zheng, T. S., Flavell, R. A., Melief, C. J., Peter, M. E., Offringa, R., and Krammer, P. H. (1997). Cleavage of FLICE (caspase-8) by granzyme B during cytotoxic T lymphocyte-induced apoptosis. *Eur. J. Immunol* 27, 3492-3498.
- Moore, B. S., Eustáquio, A. S., and McGlinchey, R. P. (2008). Advances in and applications of proteasome inhibitors. *Current Opinion in Chemical Biology* 12, 434-440.
- Nomura, A. M., Marnett, A. B., Shimba, N., Dötsch, V., and Craik, C. S. (2005). Induced structure of a helical switch as a mechanism to regulate enzymatic activity. *Nat. Struct. Mol. Biol* 12, 1019-1020.
- Oleksyszyn, J., and Powers, J. C. (1994). Amino acid and peptide phosphonate derivatives as specific inhibitors of serine peptidases. *Meth. Enzymol* 244, 423-441.
- Oudejans, J. J., Harijadi, H., Kummer, J. A., Tan, I. B., Bloemena, E., Middeldorp, J. M., Bladergroen, B., Dukers, D. F., Vos, W., and Meijer, C. J. L. M. (2002). High numbers of granzyme B/CD8-positive tumour-infiltrating lymphocytes in nasopharyngeal carcinoma biopsies predict rapid fatal outcome in patients treated with curative intent. *J. Pathol* 198, 468-475.
- Powers, J. C., Asgian, J. L., Ekici, O. D., and James, K. E. (2002). Irreversible inhibitors of serine, cysteine, and threonine proteases. *Chem. Rev* 102, 4639-4750.
- Rydel, T. J., Tulinsky, A., Bode, W., and Huber, R. (1991). Refined structure of the hirudin-thrombin complex. *J. Mol. Biol* 221, 583-601.
- Salisbury, C. M., and Cravatt, B. F. (2007). Activity-based probes for proteomic profiling of histone deacetylase complexes. *Proc. Natl. Acad. Sci. U.S.A* 104, 1171-1176.
- Shahian, T., Lee, G. M., Lazic, A., Arnold, L. A., Velusamy, P., Roels, C. M., Guy, R. K., and Craik, C. S. (2009). Inhibition of a viral enzyme by a small-molecule dimer disruptor. *Nat. Chem. Biol* 5, 640-646.
- Sieńczyk, M., and Oleksyszyn, J. (2009). Irreversible inhibition of serine proteases - design and in vivo activity of diaryl alpha-aminophosphonate derivatives. *Curr. Med. Chem* 16, 1673-1687.

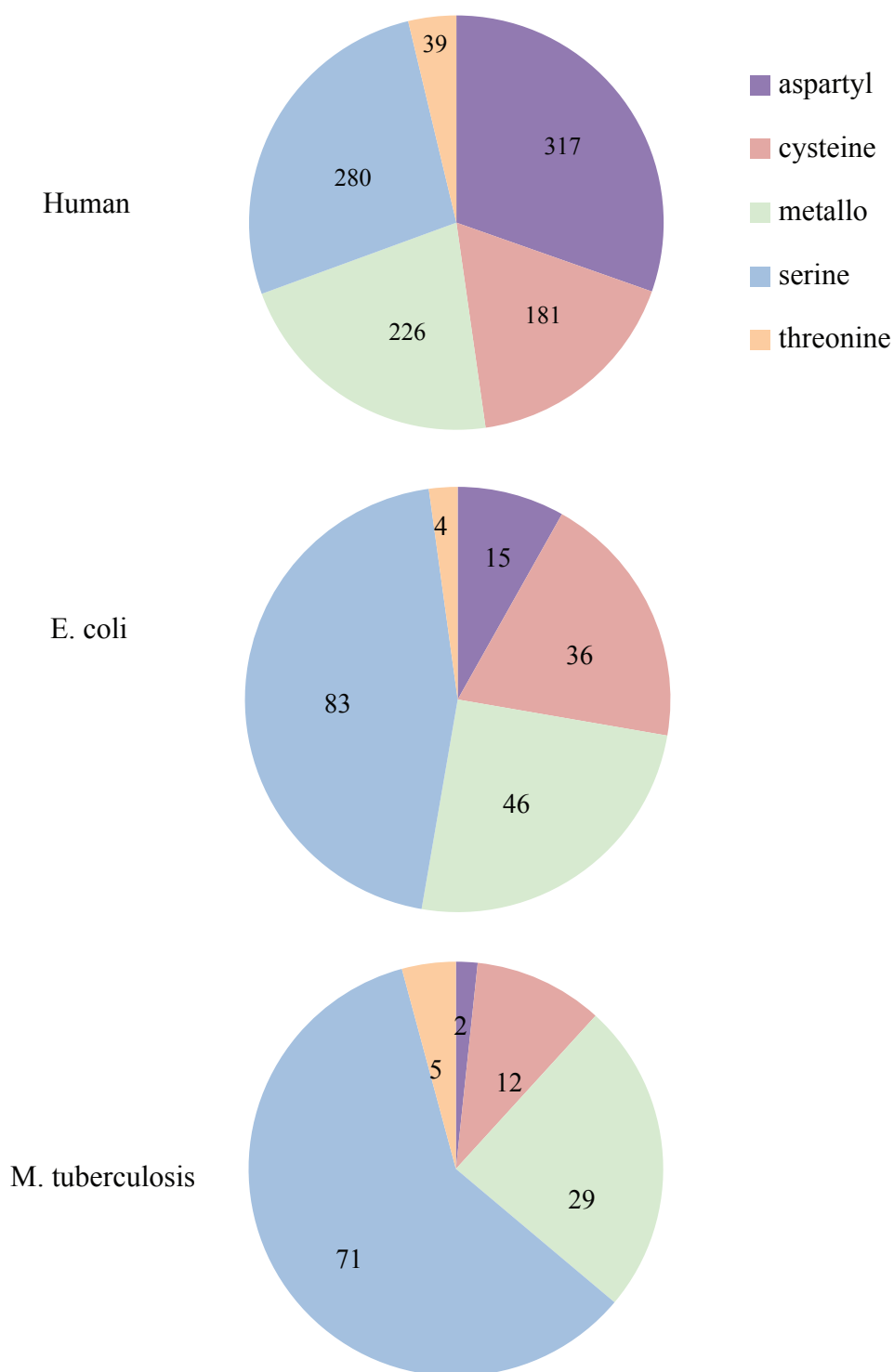
- Sieńczyk, M., and Oleksyszyn, J. (2006). Inhibition of trypsin and urokinase by Cbz-amino(4-guanidinophenyl)methanephosphonate aromatic ester derivatives: the influence of the ester group on their biological activity. *Bioorg. Med. Chem. Lett* *16*, 2886-2890.
- Sottrup-Jensen, L. (1989). Alpha-macroglobulins: structure, shape, and mechanism of proteinase complex formation. *Journal of Biological Chemistry* *264*, 11539 -11542.
- Stoop, A. A., Joshi, R. V., Eggers, C. T., and Craik, C. S. (2010). Analysis of an engineered plasma kallikrein inhibitor and its effect on contact activation. *Biol. Chem* *391*, 425-433.
- Stoop, A. A., and Craik, C. S. (2003). Engineering of a macromolecular scaffold to develop specific protease inhibitors. *Nat. Biotechnol* *21*, 1063-1068.
- Thornberry, N. A., and Weber, A. E. (2007). Discovery of JANUVIA (Sitagliptin), a Selective Dipeptidyl Peptidase IV Inhibitor for the Treatment of Type2 Diabetes. *Current Topics in Medicinal Chemistry* *7*, 557-568.
- Tully, S. E., and Cravatt, B. F. (2010). Activity-Based Probes that Target Functional Subclasses of Phospholipases in Proteomes. *J Am Chem Soc* *132*, 3264-3265.
- Walsh, P. N., and Ahmad, S. S. (2002). Proteases in blood clotting. *Essays Biochem* *38*, 95-111.
- Wei, A., Alexander, R. S., Duke, J., Ross, H., Rosenfeld, S. A., and Chang, C. H. (1998). Unexpected binding mode of tick anticoagulant peptide complexed to bovine factor Xa. *J. Mol. Biol* *283*, 147-154.
- White, J. R. (2008). Dipeptidyl Peptidase-IV Inhibitors: Pharmacological Profile and Clinical Use. *Clinical Diabetes* *26*, 53 -57.
- Yang, X., Stennicke, H. R., Wang, B., Green, D. R., Jänicke, R. U., Srinivasan, A., Seth, P., Salvesen, G. S., and Froelich, C. J. (1998). Granzyme B mimics apical caspases. Description of a unified pathway for trans-activation of executioner caspase-3 and -7. *J. Biol. Chem* *273*, 34278-34283.

Figure 1-1: Diagram of the serine protease active site and tetrahedral intermediate



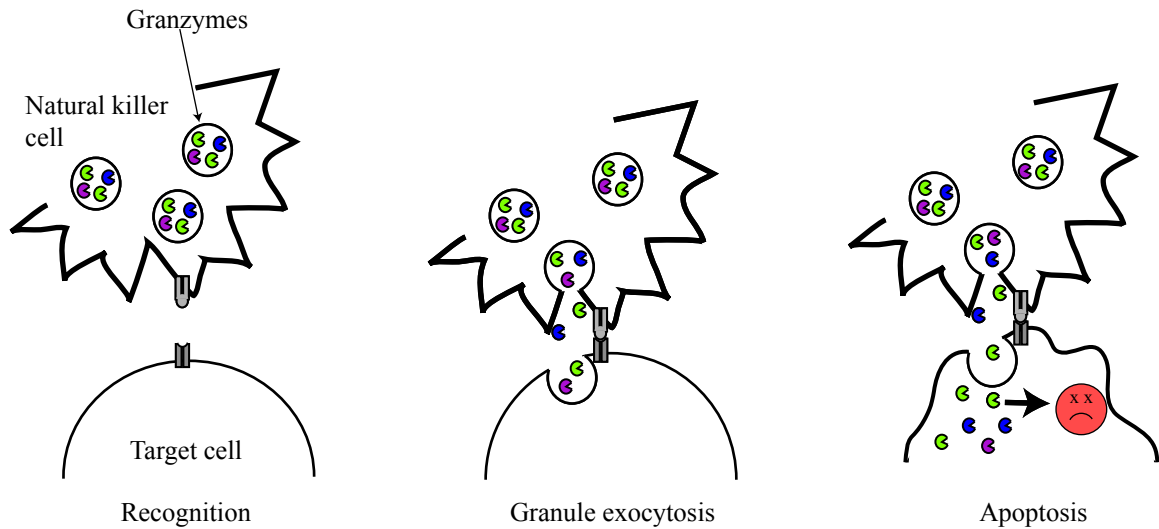
Schematic of the substrate binding pocket and active site of an S1A protease. The substrate is shown in blue, with the catalytic residues labeled in red.

Figure 1-2: Serine Proteases by Catalytic Classification



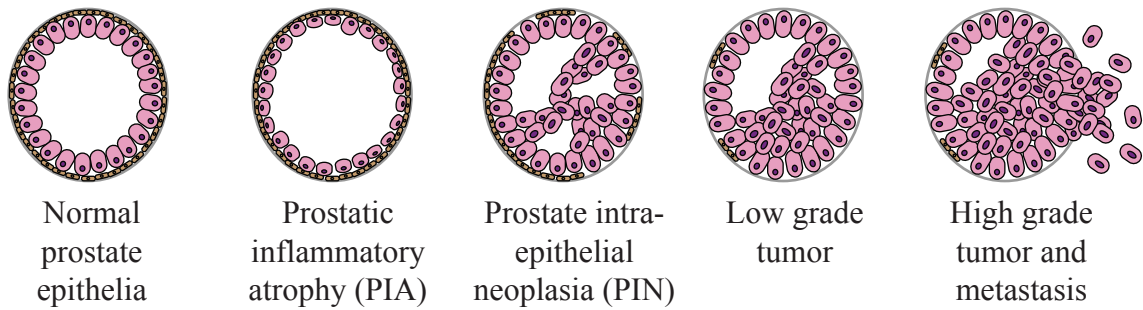
A MEROPS search for proteases in each species was conducted and graphed by catalytic class. The numbers in each segment correspond to the number of each type of protease found in the database.

Figure 1-3: Immunosurveillance



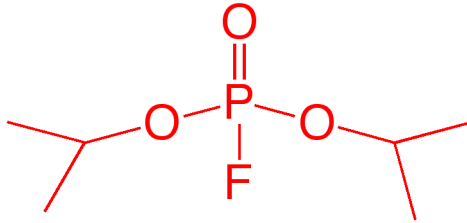
Immunosurveillance is the process by which immune cells recognize and kill cancerous or virally infected cells. Natural killer cells are filled with granules that contain proteases called granzymes. Upon recognition of a target cell, the granzymes are released into the target cell and induce apoptosis through cleavage of their substrates.

Figure 1-4: Stages of prostate cancer progression

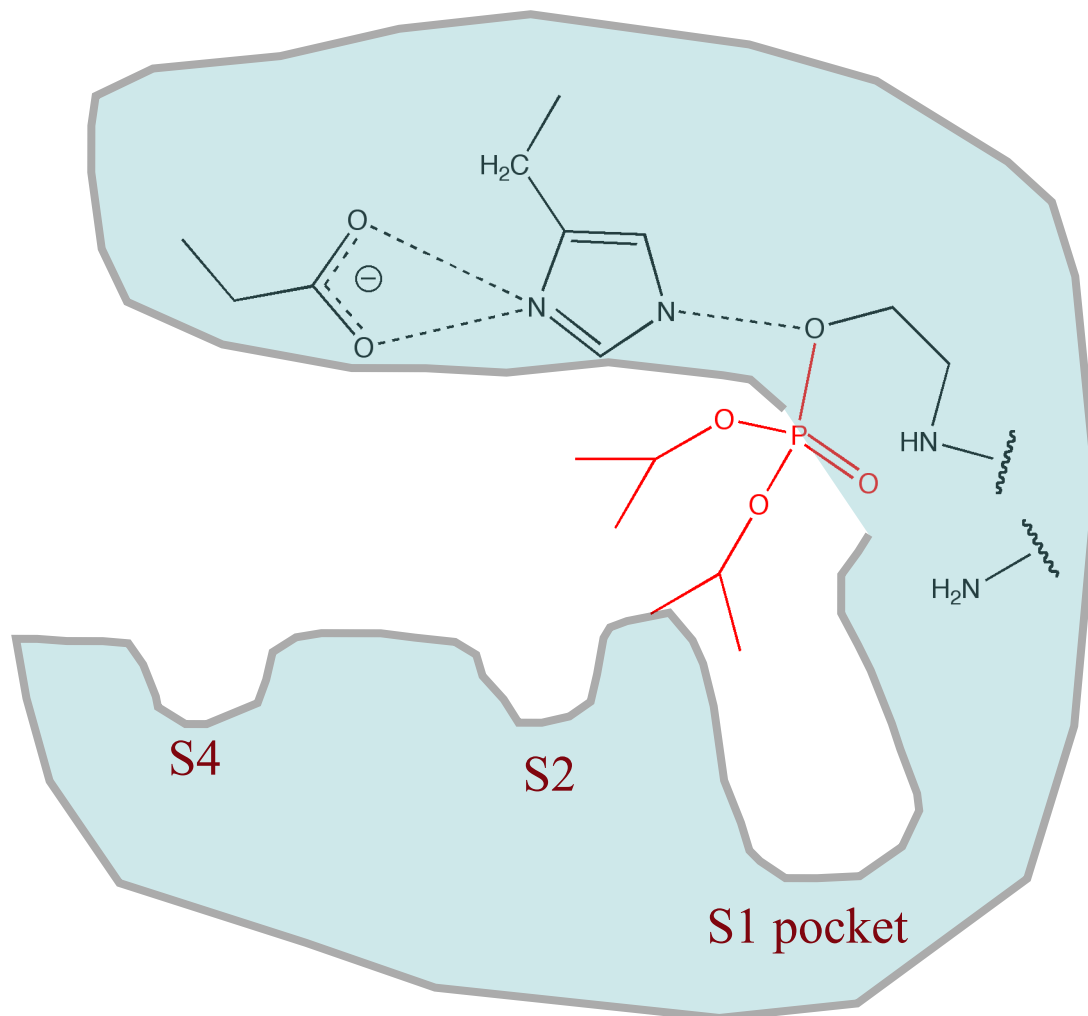


Stages of prostate cancer. The cells lining the ducts of the prostate change shape and fill in the ductal lumen as cancer progresses. Cancer is often preceded by inflammation. In the most aggressive stage of cancer, the cancerous cells can invade the surrounding tissue.

Figure 1-5: Phosphonate inhibition of serine proteases

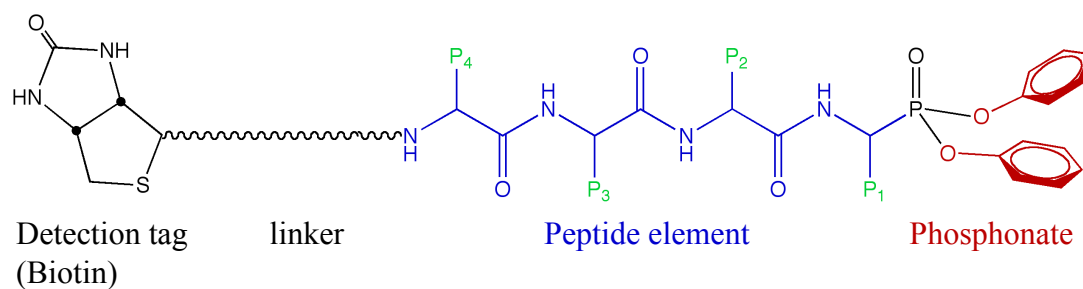


Diisopropylfluorophosphonate (DFP)



DFP covalently binds to the active site serine, mimicking the tetrahedral intermediate

Figure 1-6: Diagram of a phosphonate activity-based probe



Peptide phosphonate activity-based probes (ABPs) are modular molecules consisting of the phosphonate protease inhibitor, a peptide element to direct specificity, a linker region, and a detection tag such as biotin.

Chapter 2

Inhibition of Granzyme B by PI-9 protects prostate cancer cells from apoptosis

In order for tumors to grow and proliferate, they must avoid recognition by immune cells and subsequent death by apoptosis. Granzyme B, a protease located in natural killer cells, initiates apoptosis in target cells. Inhibition of Granzyme B by PI-9, its natural inhibitor, can prevent apoptosis. To determine whether PI-9 protects prostate cancer cells from apoptosis, we examined the function of PI-9 in several cell lines derived from prostate cancers. We found that overexpression of PI-9 in prostate cancer cells conferred protection from natural killer cell-mediated apoptosis. Additionally, examination of the levels of PI-9 in tissue from prostate tumors showed that PI-9 was more abundant early in tumor progression. These results indicate that overexpression of PI-9 can protect prostate cancer cells from apoptosis, and we suggest that early prostatic inflammation may trigger this increase in PI-9. We hypothesize that PI-9 upregulation is needed early in tumor progression, before additional protective mechanisms are in place.

Introduction

Immunosurveillance, the process by which the immune system monitors and destroys virally infected or cancerous cells, has emerged as a promising new approach to treating prostate cancer (Russell and Ley, 2002). Cytotoxic lymphocytes (CLs) carry out immunosurveillance by inducing apoptosis in target cells using two pathways: activating death ligand receptors and/or activating granule exocytosis. During granule exocytosis, CLs deliver granules filled with proteases that induce apoptosis, known as granzymes, into aberrant cells. Granzyme B (GrB), a 32 kD serine protease in the S1A family (Rawlings et al., 2008), is the main apoptotic initiator. Cleavage of GrB substrates either activates pro-death functions, such as activation of pro-caspases 3, 7 (Yang et al., 1998), and 8 (Medema et al., 1997), or deactivates pro-proliferative functions (Anthony et al., 2010) (Lieberman, 2003). GrB is the chief effector of immunosurveillance, and this mechanism must be disrupted for cancer cells to survive.

One way cancer cells could evade immunosurveillance is to prevent the initiation of apoptosis by inhibiting Granzyme B. GrB's natural inhibitor is PI-9 (serpin B9) (Sun et al., 1996), a 42 kD clade B serpin which inhibits serine proteases intracellularly. Serpins irreversibly inhibit their target protease, which can be detected by the formation of an SDS-stable complex with the target (Kaiserman and Bird, 2010) (Bird, 1998). PI-9 is abundantly expressed in the cytosol of CLs to protect them from inadvertent exposure to their own GrB (Bladergroen et al., 2001). PI-9 is also found in immune-privileged tissues, such as the placenta and the lining of blood vessels, also to protect the cells from nearby GrB (Bladergroen et al., 2001) (Buzza et al., 2001). Since expression of PI-9 in normal tissue inhibits the apoptotic activities of GrB, overexpression of PI-9 in cancer cells could inhibit GrB-mediated apoptosis. PI-9 expression has been observed in several types of cancer, including breast cancer, cervical cancer, and colon cancer (Medema et al., 2001). It has been shown in mice and in HeLa cells that overexpression of PI-9 directly protects cells from apoptosis through GrB inhibition (Medema et al., 2001) (Cunningham et al., 2007), and evidence for this protective effect has been observed in breast cancer as well (Jiang et al., 2006).

PI-9 expression may also affect the probability of successful treatment of cancer. PI-9 has been associated with poor clinical prognosis in lymphoma and nasopharyngeal carcinoma (ten Berge et al., 2003)(Oudejans et al., 2002). PI-9 expression can interfere with hormone therapy in breast cancer (Jiang et al., 2007), and PI-9 expression is correlated with the failure of immunotherapy in melanoma (van Houdt et al., 2005). Immunotherapy is of particular importance in prostate cancer, since the recently approved prostate cancer vaccine, Provenge (sipuleucel-T), uses this approach. (Harzstark and Small, 2007)(Small et al., 2006) Taken together, PI-9 has emerged as an important immunoevasive protein in many cancers that has both therapeutic and diagnostic implications.

We hypothesized that PI-9 upregulation occurs in prostate cancer, protecting the cancer cells from GrB-mediated apoptosis. Our data indicates that PI-9 dysregulation may play a protective role early in cancer progression, allowing time for the development of additional protective mechanisms as the tumor grows. This work implies that PI-9 could be a biomarker for early-stage prostate lesions that are resistance to immunotherapy. Elimination of prostate cancer from these patients will require a therapeutic strategy that bypasses PI-9 mediated inhibition of GrB.

Materials and Methods

Cell culture

All cell lines were obtained from the ATCC. LNCaP cells were grown in RPMI-1640 containing 10% FBS, 10 mM HEPES, 0.11mg/mL sodium pyruvate, 4.5g/L glucose, 10units/mL penicillin, and 10mcg/mL streptomycin. PC3 cells were grown in F-12K nutrient mixture (Gibco) containing 10% FBS, 10units/mL penicillin, and 10mcg/mL streptomycin. NK-92 cells were grown in Myelocult media (Stem Cell Technologies) containing 200 U/mL interleukin-2 (NCI).

qPCR

RNA was prepared from each cell line using the RNEasy kit (Qiagen). For prostate tissue, scrapings were taken from frozen prostate sections and sonicated in RLT buffer (Qiagen), then RNA was prepared as above. RNA was quantified using a ND-1000 Spectrophotometer (NanoDrop). Equal amounts of RNA were used to synthesize cDNA. The RNA was combined with RNase-free water, oligo-dT and random decamer primers (Ambion) and heat denatured at 70°C for 5 minutes. M-MLV reverse transcriptase and its buffer (Promega) and RNase inhibitor (Roche) were added to the reaction, which was carried out at 42°C for one hour, followed by 95°C for 10 minutes. PI-9 (Serp1B9Hs00244603_A1), α -tubulin (Hs0074482_sH), and HPRT (433768F) Taqman probe sets were purchased from Applied Biosystems/Ambion. qPCR reactions containing Taqman Universal PCR Master Mix (Applied Biosystems), one set of Taqman probes, and the appropriate cDNA were set up in triplicate. qPCR was performed on the ABI 7300 Real Time PCR system instrument. qPCR raw data (Ct) for each sample was normalized to the reference gene for comparison.

BioPorter delivery

The BioPorter kit was purchased from Genlantis. Granzyme B was expressed and purified as described previously (Harris et al., 1998). Briefly, 72 pmole of Granzyme B was incubated with the hydrated BioPorter reagent. The BioPorter/Granzyme B mixture was added to 1×10^5 cells/well in a 6-well plate at a final concentration of 2.1 μ M Granzyme B. The cells and protein mix were incubated for 4 hours at 37°C, then lysed in 0.5% NP-40 buffer containing a protease inhibitor cocktail (Roche).

Western blotting

All samples were brought up in SDS loading buffer (Invitrogen) containing 5mM Bond-Breaker TCEP Solution (Thermo Scientific). The mouse anti-Granzyme B antibody was purchased from USBiological and used at 1:1000 in 5% BSA. The polyclonal rabbit anti-PARP antibody was purchased from Cell Signaling and used at 1:1000 in 5% milk. The mouse anti-cMyc antibody was purchased from Santa Cruz Biotechnology and used at 1:1000 in 5% milk. Goat anti-mouse-HRP and goat anti-rabbit-HRP were purchased from

Bio-Rad and used at 1:2000 in 5% milk. All blots were developed using the Amersham ECL-Plus Western blotting detection system (GE Healthcare).

Flow cytometry

All flow cytometry was carried out on the FACScaliber instrument from BD Biosciences. For detection of PI-9, cells were fixed and permeabilized using the BD Cytofix/Cytoperm kit (BD) according to the manufacturer's instructions. For detection of endogenous PI-9, a mouse monoclonal (clone 7D8) anti-PI-9 (MBL Medical and Biological Labs) antibody or mouse IgG1 isotype control (BD Biosciences) were added at a final concentration of 5.0 µg/ml and incubated for 30 minutes at 4°C. Following removal of unbound primary, a FITC-conjugated goat anti-mouse IgG₁ secondary (BD Biosciences) was added to a final concentration of 10 µg/ml. After incubating for 30 min at 4°C, unbound secondary was removed and cells were analyzed. For detection of myc tagged PI-9 a similar protocol was followed except an anti-myc antibody directly conjugated to fluorochrome was used.

For detection of cell surface MIC A and MIC B, LNCaP pcDNA cells were harvested and re-suspended in Stain Buffer FBS (BD Biosciences). A mouse anti-human MIC A/MIC B antibody or its isotype control (BioLegend) were added to approximately 2×10^5 cells at a final concentration of 20.0 µg/ml and incubated for 30 minutes at 4°C. Following removal of unbound primary, a FITC-conjugated goat anti-mouse Ig secondary (BD Biosciences) was used at a final concentration of 10.0 µg/ml. Cells were incubated for 30 minutes at 4°C washed to remove unbound secondary, and resuspended in Stain Buffer FBS for flow cytometry analysis.

Transfection

The PI-9 (serpinB9) gene was synthesized with an N-terminal myc tag by GeneArt using human codon bias. After the start Met, the myc tag (EQKLISEEDL) is followed by a GGS linker. The synthesized gene was sub-cloned into pcDNA3.1(+) and the identity of the construct confirmed by HindIII and XhoI digestion and DNA sequencing.

To create the LNCaP-PI9 and LNCaP-pcDNA stables, both the PI-9 construct sub-cloned into pcDNA3.1(+) and empty pcDNA3.1(+) was linearized with PvuI restriction enzyme. Following purification, 2.0 µg of DNA was transfected into LNCaP cells using GenJet in vitro DNA transfection reagent for LNCaP cells, version II (SignaGen Labs) following the manufacturer's protocol. Approximately 48 h post-transfection, cells were switched into media containing 500 µg/ml G418 (Invitrogen). At this G418 concentration, un-transfected cells were killed in approximately 10 days. Cells that survived the G418 selection were expanded and used for all subsequent assays.

Cell death assay

LNCaP cells were washed in PBS and resuspended at 2×10^6 cells/ml in PBS. TFL4 dye (OncoImmunin) was added at 1:300,000 and the cells were incubated for 15 minutes at 37°C. LNCaP cells were washed in PBS, resuspended in Myelocult media plus 200U/mL IL-2, then aliquoted in triplicate into wells at 1×10^5 cells/well. NK-92 cells in Myelocult media plus 200U/mL IL-2 were added to the appropriate wells at ratios of 0:1, 5:1, 10:1 or 30:1 in a final volume of 200ul/well. The plate was spun at 175xG for 5 minutes, then incubated at 37°C for 4 hours. The NK-92/LNCaP cell mixture was brought up in 500ml of PBS containing a final concentration of 2µg/mL propidium iodide (BioVision). Cell death was assessed on a FACSCaliber flow cytometer (BD Biosciences) by counting the number of propidium iodide and TFL4 positive cells.

Immunohistochemistry

Immunohistochemical staining was conducted on paraffin-embedded prostate tissue sections by the UCSF Tissue Core. Tissue sections were deparaffinized with xylene and alcohol, and were then subjected to heat-based antigen retrieval in the microwave for 10 minutes in 10 mM sodium citrate buffer, pH 6.0 followed by cooling at room temperature for 30 minutes. Samples were rinsed in water and PBS and then blocked in normal horse serum for 30 minutes. Tissue sections were then incubated overnight at room temperature with a 1:10 dilution of the PI9-17 monoclonal primary anti-PI-9 antibody

(Monosan) in PBS containing 1% bovine serum albumin (BSA). On the following day, slides were rinsed in PBS and incubated for 30 minutes with the secondary biotinylated horse anti-mouse antibody at a 1:200 dilution in PBS containing 1% BSA. The ABC (Vector) stain was then applied at a 1:100 dilution and incubated for 30 minutes. After rinsing again in PBS, slides were subjected to DAB chromogen stain, hematoxylin counterstain, and were dehydrated in alcohol and xylene.

Results

PI-9 is expressed in cell lines derived from prostate cancer

To determine the role PI-9 plays in prostate cancer, we first tested whether PI-9 is expressed in cell lines derived from prostate cancers. qPCR was used to measure the amount of PI-9 mRNA in the highly invasive and androgen independent PC3 cell line, and in the non-invasive and androgen responsive LNCaP cell line. As a positive control, the amount of PI-9 mRNA was also measured in natural killer (NK-92) cells, a type of cytotoxic lymphocyte known to express high levels of PI-9. mRNA was measured using Taqman probes for PI-9 and for two reference genes, HPRT and k-a-tubulin. As shown in Figure 2-1A, DU-145 and PC3 cells expressed measureable quantities of PI-9, but LNCaP cells did not. As expected, NK-92 cells expressed PI-9 in great abundance, 324-fold more than PC3 cells. PI-9 levels were confirmed at the protein level by flow cytometry (Figure 2-1B). The androgen independent and invasive DU-145 cells were resistant to the reagents used in subsequent experiments, so functional studies were continued with the PC3 and LNCaP cell lines. These results show that PI-9 is expressed in PC3 cells but not in LNCaP cells at both the mRNA and protein levels.

PI-9 inhibits Granzyme B in PC3 cells

After demonstrating that PI-9 is made in cell lines derived from some prostate cancers, we next asked whether cellular PI-9 could inhibit its target protease, Granzyme B (GrB). Two cell lines with no detectable PI-9 (LNCaP cells) and measurable PI-9 (PC3 cells) were tested for GrB resistance. GrB was introduced into each cell line using BioPorter, a reagent for protein transfection. The cells were lysed at various time points for up to six

hours after the introduction of GrB. GrB activity was measured by monitoring cleavage of PARP, a 113kD substrate of GrB, by Western blot. As shown in Figure 2-1C, GrB cleaved PARP in LNCaP cells, which lack PI-9. However, GrB did not cleave PARP in PC3 cells, which contain PI-9. These results indicate that PI-9 inhibits GrB in a cellular context.

Since PARP cleavage suggested that PI-9 inhibited GrB activity, we next set out to directly demonstrate that PI-9 inhibited GrB. To directly test inhibition, GrB was added to PC3 cells using BioPorter, and the cells were lysed after 6 hours. Since GrB has been shown to bind to the plasma membrane of cells, lysates were prepared under denaturing conditions to prevent cell surface GrB from forming a complex with intracellular PI-9. These lysates were processed by Western blot to detect GrB. As shown in Figure 2-1D, PI-9 formed a stable complex with GrB that appeared at 85kD, and this complex was not observed in the absence of BioPorter. This result indicates that PI-9 binds to GrB and suggests that the GrB inhibition observed in PC3 cells is mediated by PI-9.

PI-9 protects prostate cancer cells from apoptosis

Having shown that PI-9 inhibited GrB *in vitro*, we next asked whether PI-9 inhibition could prevent GrB-mediated apoptosis in the context of natural killer cell mediated death. To answer this question, NK-92 cells were chosen as effectors because selective inhibition of GrB in this cell line significantly reduced target cell lysis (Willoughby et al., 2002)(Mahrus and Craik, 2005). LNCaP cells were selected as targets for two reasons: LNCaP cells express no detectable PI9, and LNCaP cells express the NK activating ligands MHC class I chain-related molecules (MICs, Supplementary Figure S2-1) (Wu et al., 2004), which suggested that NK-92 cells could recognize LNCaP cells.

To generate a PI-9 over-expression cell line, a Myc-tagged PI-9 gene or empty pcDNA vector control was transfected and stably integrated into LNCaP cells. These cell lines were referred to as LNCaP PI-9 and LNCaP pcDNA respectively. Myc-PI-9 expression was tested by immunoblotting of lysates using an anti-Myc antibody. A 45-kD band appeared in lysates from LNCaP PI-9 and was absent in lysates from LNCaP pcDNA

(Figure 2-2A). Analysis of myc staining by flow cytometry showed that greater than 80% of LNCaP PI-9 cells expressed Myc-PI-9 relative to LNCaP pcDNA cells (Figure 2-2B). An identical result was obtained when staining was performed with an anti-PI9 antibody (data not shown). This result indicated successful PI-9 overexpression.

Once LNCaPs stably expressing PI-9 were generated, the functional ability of myc-PI-9 was tested. LNCaP-pcDNA and LNCaP-PI-9 cell lysates were generated under non-denaturing conditions, then incubated with recombinant GrB. Western blotting for PI-9 using an anti-cMyc antibody showed the appearance of a 70kD band in only the LNCaP-PI-9 samples, which indicated the formation of a PI-9/GrB complex (Figure 2-2C). This complex demonstrates that myc-PI-9 is functional through its ability to bind to GrB. To further test the inhibition of GrB by myc-PI-9, the same blots were analyzed for the presence of PARP, a substrate of GrB. In the LNCaP-pcDNA samples, several PARP cleavage products were observed, and there was a 50% reduction in full length PARP (Figure 2-2D). In the LNCaP-PI-9 samples, very little PARP cleavage was observed, and 97% of the full length PARP band remained. These results indicate that overexpressed myc-PI-9 can successfully inhibit GrB and prevent cleavage of its substrates in LNCaP cells.

Once these cells lines were generated and PI-9 function verified, they were tested for resistance to NK-92-induced cell death. Fluorescently labeled LNCaP cells were co-incubated with unlabeled NK-92 cells in varying ratios for 4 hours. Cells were then stained with propidium iodide (PI) and target cell death was quantified by the percentage of PI positive, fluorescent cells by flow cytometry. All samples were normalized to LNCaP cells in the absence of NK-92 cells. LNCaP-pcDNA cells were killed by the NK-92 cells at all ratios. (Figure 2-3A). The LNCaP cells over-expressing PI-9 exhibited less cell death than the LNCaP-pcDNA cells over the entire range of ratios. This result indicates that LNCaP cells expressing PI-9 are resistant to NK-92 cell-induced cell death. The presence of PI-9 can indeed protect prostate cancer cells from NK-92-mediated apoptosis.

To further confirm the mechanism by which PI-9 prevents cell death, the target cells were examined for the degree of cleavage of the GrB substrate PARP. LNCaP cells were incubated with NK-92 cells in a ratio of 0:1 or 20:1 for 6 hours, lysed, and blotted for PARP. As shown in Figure 3B, PARP was present in both lysates, as indicated by a 113kD band present in both before and after incubation with NK-92 cells. In the LNCaP-pcDNA cells, significant PARP cleavage was observed after incubation with NK-92 cells. These PARP cleavage products were only faintly observed in the LNCaP-PI-9 cells after incubation with NK-92 cells, approximately two fold less than in the LNCaP-pcDNA lysates. These results indicate that PI-9 protected cells from apoptosis by inhibiting GrB.

PI-9 can be detected in prostate tumors

Having shown that PI-9 expression protects prostate cancer cells from NK-92 induced cell death, we undertook a small pilot study to determine whether this effect occurred in prostate tumors. PI-9 mRNA was measured in 32 prostate biopsies containing both cancerous and benign tissue. PI-9 expression was measured by qPCR using the Taqman PI-9 probe and two reference genes, and each tumor sample was normalized to its corresponding benign sample. As shown in Figure 2-4A, greater PI-9 expression was observed in low grade tumors than in the benign control. However, PI-9 expression in higher grade tumors was stochastic. These results suggest that PI-9 expression is elevated in low grade tumors but stochastically dysregulated in high grade prostate tumors, implying the function of PI-9 is needed early in cancer progression.

To confirm this observation at the protein level, 54 slices from the prostate biopsies of 24 patients were tested for the presence of PI-9 by immunohistochemistry against PI-9. As shown in Figure 2-4B, PI-9 was found in both low and high grade tumors. The tumors showed a similar pattern as the mRNA data, though fewer tumors overall stained positively than in the qPCR study, where 45% of the low grade tumors had more PI-9 than the benign tissue, but only 25% of the high grade tumors had more PI-9. Interestingly, PI-9 staining intensity was observed most consistently in high grade prostatic intraepithelial neoplasia (HGPIN, 76%), a precursor to prostate cancer, as well

as in regions of atrophy (76%). Taken together, this pilot study indicates that PI-9 is present in pre-cancerous states and remains in some tumors.

Discussion

Here we report that the protease inhibitor PI-9 can protect prostate cancer cells from NK-92 cell- induced apoptosis by inhibiting Granzyme B (GrB). We also provide tantalizing preliminary data that this protective mechanism operates early in the progression of prostate cancer. In our experiments, PI-9 expressed by prostate cancer cells inhibited GrB. LNCaP cells that overexpressed PI-9 were resistant to apoptosis mediated by NK -92 cells, but LNCaP cells that lacked PI-9 were sensitive. This observation shows that PI-9 can protect prostate cells from NK cell-mediated apoptosis, one arm of immunosurveillance. Additionally, immunohistochemistry showed that PI-9 was present in HGPIN tumors, one of the earliest forms of prostate cancer, as well as in atrophic lesions. Our results suggest that PI-9 protects prostate tumors from immunosurveillance early in cancer progression by blocking the apoptotic response, while additional mechanisms protect tumors later in their progression through blocking recognition.

Why would PI-9 initially become upregulated in prostate tumors? As shown in Figure 2-4B, not only is PI-9 upregulated in early tumors, PI-9 is also abundantly expressed during atrophy, including prostatic inflammatory atrophy (PIA, Supplemental Figure S2-2). Atrophy is a known hallmark of an inflamed prostate, and evidence has shown it can precede the development of PIN (De Nunzio et al., 2011)(Borowsky et al., 2006). A correlation between inflammation and prostate cancer has long been observed, and PI-9 could be the molecular mechanism that connects the two pathologies. PI-9 is often upregulated in response to inflammation to protect bystander cells from inadvertently introduced GrB (Buzza et al., 2001), and PI-9 expression can be induced by pro-inflammatory molecules like IL-1B and TNF-a (Kannan-Thulasiraman and Shapiro, 2002). Therefore, prostatic inflammation may provide a trigger for PI-9 upregulation. In a subset of inflamed cells, this PI-9 upregulation may become permanent, creating a cancer-prone population of cells that are resistant to immunosurveillance.

While PI-9 allows cancer cells to block the apoptotic response of immunosurveillance, prostate cancer cells have also been shown to block recognition by CLs. through the process of MIC shedding. MICs, or MHC class I chain-related molecules, are expressed on the surface of cancerous cells and target these cells for destruction. MICs bind to the NKG2D receptor on NK cells (Wu et al., 2004) which initiates granule exocytosis, killing the MIC-expressing cell (Lanier, 2001)(Raulet, 2003). MIC is expressed in HGPIN and low grade prostate tumors, however, membrane bound MIC cleaved by a metalloprotease in high grade tumors. This allows cancerous cells to evade detection by NK cells (Wu et al., 2004)(Liu et al., 2010). Early expression of PI-9 could allow prostate cancer cells to survive while MIC is present.

We hypothesize that PI-9 expression may protect prostate cancer tumors early in cancer progression, when MIC is still present on the surface of cells (Figure 2-5). We find that PI-9 is expressed in the early HGPIN stage, a stage in which MIC is also expressed, but stochastically expressed in advanced tumors (Figure 2-4B). These results imply that PI-9 is important early in cancer progression, when MIC is still present on the surface of cells. PI-9 may not be important in the later stages, after MIC is shed and cells are in less danger of NK cell-induced apoptosis. Therefore, PI-9 protects prostate cancer cells early in their progression, when surface MIC is expressed, and PI-9 is then dysregulated in later stages when MIC is shed.

In summary, prostate cancer uses both PI-9 upregulation and MIC shedding at consecutive stages in its progression to evade immunosurveillance. Treatment for prostate cancer must take into account both mechanisms, as PI-9 has been shown to affect hormone therapy in breast cancer (Jiang et al., 2007) and immunotherapy in melanoma (van Houdt et al., 2005). MIC shedding could be counteracted by inhibiting matrix metalloprotease-14 (Liu et al., 2010). PI-9 is a substrate of Granzyme M, so Granzyme M upregulation could alleviate the resistance to cell death caused by PI-9 (Mahrus et al., 2004). Targeting both MIC shedding and PI-9 expression could lead to an effective treatment strategy that enhances the immune response to cancer cells.

References:

- Anthony, D. A., Andrews, D. M., Watt, S. V., Trapani, J. A., and Smyth, M. J. (2010). Functional dissection of the granzyme family: cell death and inflammation. *Immunological Reviews* 235, 73-92.
- ten Berge, R. L., Oudejans, J. J., Ossenkoppele, G. J., and Meijer, C. J. L. M. (2003). ALK-negative systemic anaplastic large cell lymphoma: differential diagnostic and prognostic aspects--a review. *J. Pathol* 200, 4-15.
- Bird, P. I. (1998). Serpins and regulation of cell death. *Results Probl Cell Differ* 24, 63-89.
- Bladergroen, B. A., Strik, M. C. M., Bovenschen, N., van Berkum, O., Scheffer, G. L., Meijer, C. J. L. M., Hack, C. E., and Kummer, J. A. (2001). The Granzyme B Inhibitor, Protease Inhibitor 9, Is Mainly Expressed by Dendritic Cells and at Immune-Privileged Sites. *The Journal of Immunology* 166, 3218 -3225.
- Borowsky, A. D., Dingley, K. H., Ubick, E., Turteltaub, K. W., Cardiff, R. D., and DeVere-White, R. (2006). Inflammation and Atrophy Precede Prostatic Neoplasia in a PHIP-Induced Rat Model. *Neoplasia* 8, 708-715.
- Buzza, M. S., Hirst, C. E., Bird, C. H., Hosking, P., McKendrick, J., and Bird, P. I. (2001). The Granzyme B Inhibitor, PI-9, Is Present in Endothelial and Mesothelial Cells, Suggesting That It Protects Bystander Cells during Immune Responses. *Cellular Immunology* 210, 21-29.
- Cunningham, T. D., Jiang, X., and Shapiro, D. J. (2007). Expression of high levels of human proteinase inhibitor 9 blocks both perforin/granzyme and Fas/Fas ligand-mediated cytotoxicity. *Cellular Immunology* 245, 32-41.
- Harris, J. L., Peterson, E. P., Hudig, D., Thornberry, N. A., and Craik, C. S. (1998). Definition and Redesign of the Extended Substrate Specificity of Granzyme B. *Journal of Biological Chemistry* 273, 27364 -27373.
- Harzstark, A. L., and Small, E. J. (2007). Immunotherapy for prostate cancer using antigen-loaded antigen-presenting cells: APC8015 (Provenge). *Expert Opin Biol Ther* 7, 1275-1280.
- van Houdt, I. S., Oudejans, J. J., van den Eertwegh, A. J. M., Baars, A., Vos, W., Bladergroen, B. A., Rimoldi, D., Muris, J. J. F., Hooijberg, E., Gundy, C. M., et al. (2005). Expression of the Apoptosis Inhibitor Protease Inhibitor 9 Predicts Clinical Outcome in Vaccinated Patients with Stage III and IV Melanoma. *Clinical Cancer Research* 11, 6400 -6407.
- Jiang, X., Ellison, S. J., Alarid, E. T., and Shapiro, D. J. (2007). Interplay between the levels of estrogen and estrogen receptor controls the level of the granzyme inhibitor,

proteinase inhibitor 9 and susceptibility to immune surveillance by natural killer cells. *Oncogene* 26, 4106-4114.

Jiang, X., Orr, B. A., Kranz, D. M., and Shapiro, D. J. (2006). Estrogen induction of the granzyme B inhibitor, proteinase inhibitor 9, protects cells against apoptosis mediated by cytotoxic T lymphocytes and natural killer cells. *Endocrinology* 147, 1419-1426.

Kaiserman, D., and Bird, P. I. (2010). Control of granzymes by serpins. *Cell Death Differ* 17, 586-595.

Kannan-Thulasiraman, P., and Shapiro, D. J. (2002). Modulators of Inflammation Use Nuclear Factor- κ B and Activator Protein-1 Sites to Induce the Caspase-1 and Granzyme B Inhibitor, Proteinase Inhibitor 9. *Journal of Biological Chemistry* 277, 41230 -41239.

Lanier, L. L. (2001). On guard[mdash]activating NK cell receptors. *Nat Immunol* 2, 23-27.

Lieberman, J. (2003). The ABCs of granule-mediated cytotoxicity: new weapons in the arsenal. *Nat Rev Immunol* 3, 361-370.

Liu, G., Atteridge, C. L., Wang, X., Lundgren, A. D., and Wu, J. D. (2010). The membrane type matrix metalloproteinase MMP14 mediates constitutive shedding of MHC class I chain-related molecule A independent of A disintegrin and metalloproteinases. *J. Immunol* 184, 3346-3350.

Mahrus, S., Kisiel, W., and Craik, C. S. (2004). Granzyme M is a regulatory protease that inactivates proteinase inhibitor 9, an endogenous inhibitor of granzyme B. *J. Biol. Chem* 279, 54275-54282.

Mahrus, S., and Craik, C. S. (2005). Selective chemical functional probes of granzymes A and B reveal granzyme B is a major effector of natural killer cell-mediated lysis of target cells. *Chem. Biol* 12, 567-577.

Medema, J. P., de Jong, J., Peltenburg, L. T., Verdegaal, E. M., Gorter, A., Bres, S. A., Franken, K. L., Hahne, M., Albar, J. P., Melief, C. J., et al. (2001). Blockade of the granzyme B/perforin pathway through overexpression of the serine protease inhibitor PI-9/SPI-6 constitutes a mechanism for immune escape by tumors. *Proc. Natl. Acad. Sci. U.S.A* 98, 11515-11520.

Medema, J. P., Toes, R. E., Scaffidi, C., Zheng, T. S., Flavell, R. A., Melief, C. J., Peter, M. E., Offringa, R., and Krammer, P. H. (1997). Cleavage of FLICE (caspase-8) by granzyme B during cytotoxic T lymphocyte-induced apoptosis. *Eur. J. Immunol* 27, 3492-3498.

De Nunzio, C., Kramer, G., Marberger, M., Montironi, R., Nelson, W., Schröder, F., Sciarra, A., and Tubaro, A. (2011). The Controversial Relationship Between Benign Prostatic Hyperplasia and Prostate Cancer: The Role of Inflammation. *Eur Urol*. Available at: <http://www.ncbi.nlm.nih.gov/pubmed/21497433> [Accessed May 13, 2011].

- Oudejans, J. J., Harijadi, H., Kummer, J. A., Tan, I. B., Bloemena, E., Middeldorp, J. M., Bladergroen, B., Dukers, D. F., Vos, W., and Meijer, C. J. L. M. (2002). High numbers of granzyme B/CD8-positive tumour-infiltrating lymphocytes in nasopharyngeal carcinoma biopsies predict rapid fatal outcome in patients treated with curative intent. *J. Pathol* *198*, 468-475.
- Raulet, D. H. (2003). Roles of the NKG2D immunoreceptor and its ligands. *Nat Rev Immunol* *3*, 781-790.
- Rawlings, N. D., Morton, F. R., Kok, C. Y., Kong, J., and Barrett, A. J. (2008). MEROPS: the peptidase database. *Nucleic Acids Res* *36*, D320-325.
- Russell, J. H., and Ley, T. J. (2002). Lymphocyte-mediated cytotoxicity. *Annu. Rev. Immunol* *20*, 323-370.
- Small, E. J., Schellhammer, P. F., Higano, C. S., Redfern, C. H., Nemunaitis, J. J., Valone, F. H., Verjee, S. S., Jones, L. A., and Hershberg, R. M. (2006). Placebo-Controlled Phase III Trial of Immunologic Therapy with Sipuleucel-T (APC8015) in Patients with Metastatic, Asymptomatic Hormone Refractory Prostate Cancer. *Journal of Clinical Oncology* *24*, 3089 -3094.
- Sun, J., Bird, C. H., Sutton, V., McDonald, L., Coughlin, P. B., De Jong, T. A., Trapani, J. A., and Bird, P. I. (1996). A cytosolic granzyme B inhibitor related to the viral apoptotic regulator cytokine response modifier A is present in cytotoxic lymphocytes. *J. Biol. Chem* *271*, 27802-27809.
- Willoughby, C. A., Bull, H. G., Garcia-Calvo, M., Jiang, J., Chapman, K. T., and Thornberry, N. A. (2002). Discovery of potent, selective human granzyme B inhibitors that inhibit CTL mediated apoptosis. *Bioorg. Med. Chem. Lett* *12*, 2197-2200.
- Wu, J. D., Higgins, L. M., Steinle, A., Cosman, D., Haugk, K., and Plymate, S. R. (2004). Prevalent expression of the immunostimulatory MHC class I chain-related molecule is counteracted by shedding in prostate cancer. *J. Clin. Invest* *114*, 560-568.
- Yang, X., Stennicke, H. R., Wang, B., Green, D. R., Jänicke, R. U., Srinivasan, A., Seth, P., Salvesen, G. S., and Froelich, C. J. (1998). Granzyme B mimics apical caspases. Description of a unified pathway for trans-activation of executioner caspase-3 and -7. *J. Biol. Chem* *273*, 34278-34283.

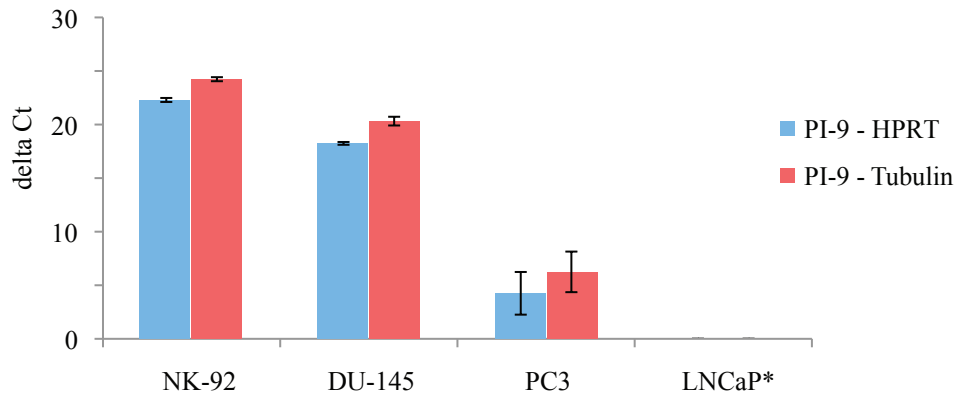
Acknowledgements

We would like to thank Dr. Peter Carroll for performing the prostate resections, Sarah Elmes for training and use of the flow cytometer, and the lab of Dr. Keith Yamamoto for the generous use of their qPCR instruments and reagents. We would also like to thank Dr.

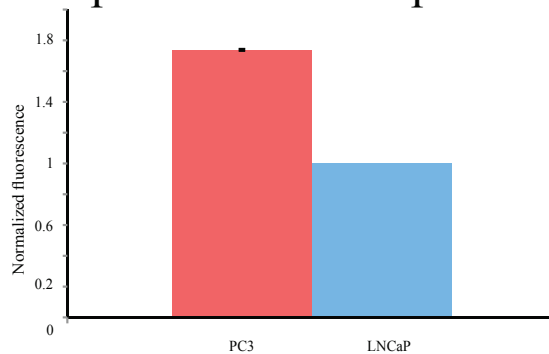
Aaron Lebeau, Dr. Marc Shuman, and Dr. Lawrence Fong for helpful discussions. This work was funded by the National Institute of Health (R01CA128765)

Figure 2-1: PI-9 inhibits Granzyme B when present in prostate cancer cell lines

2-1A: PI-9 mRNA levels in prostate cancer cell lines

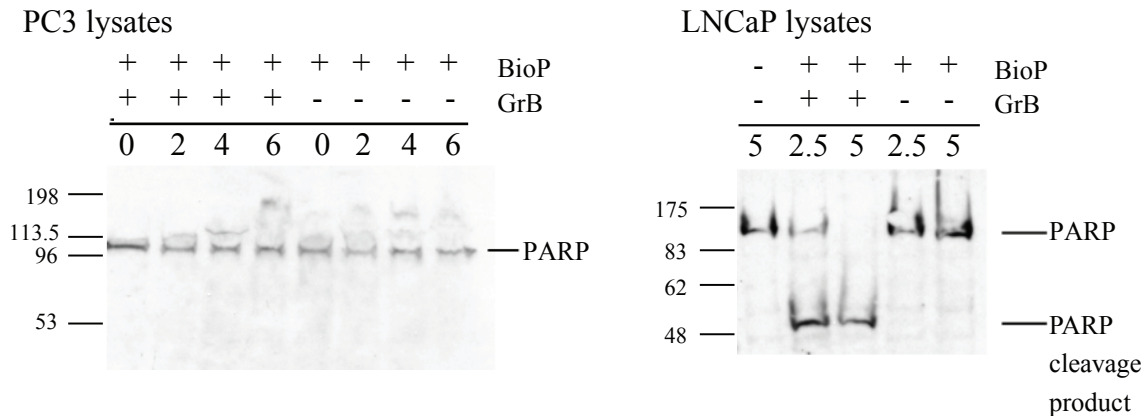


2-1B: PI-9 protein levels in prostate cancer cell lines

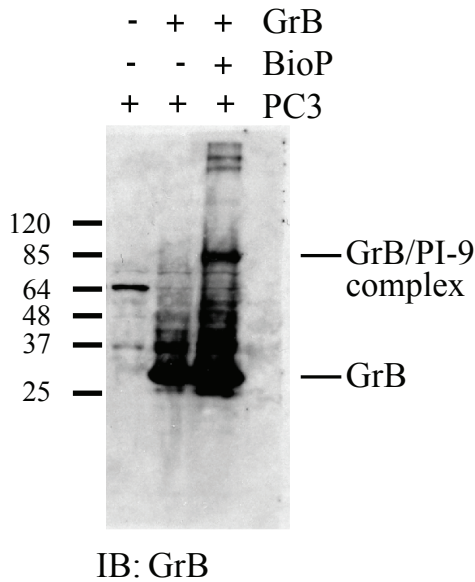


1A: PI-9 levels were measured by qPCR. The threshold cycle (Ct) of PI-9 mRNA for each cell line was normalized to the Ct two reference genes. Each cell line was then normalized to LNCaP cells. *LNCaP cells contained no detectable message. An arbitrary cutoff of 45 Ct was used as the point at which the sample contained to message, and was used for normalization. B: PI-9 levels from each cell line were measured by labeling cells with an anti-PI-9 antibody or isotype control, then measuring fluorescent intensity from 100,000 cells. Fluorescent intensity was normalized to the PI-9 staining intensity of LNCaP cells, and background fluorescence was measured using an isotype control.

2-1C: Granzyme B is inactive in PC3 cells, but active in LNCaP cells



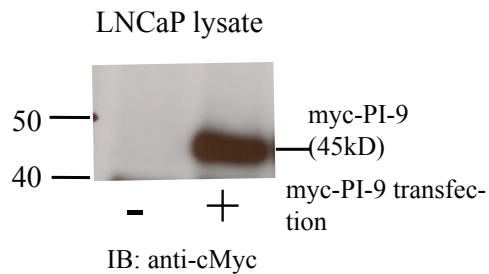
2-1D: PI-9 directly binds to Granzyme B



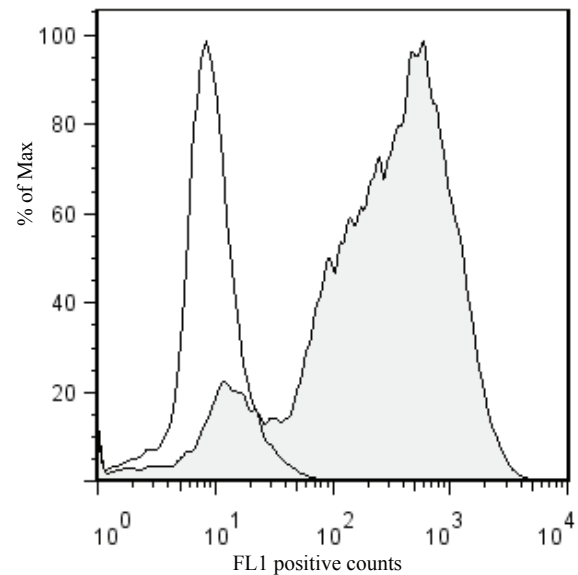
C: The protein transfection reagent BioPorter (BioP) was used to deliver recombinant GrB to both PC3 and LNCaP cells. Lysates of GrB treated cells were immunoblotted for the GrB substrate PARP to determine if GrB was active in these cell lines. D: PC3 cell lysates containing GrB delivered by BioPorter were blotted with an anti-GrB antibody. A higher molecular weight complex appears which corresponds to PI-9 bound to GrB.

Figure 2-2: myc-PI-9 overexpression in LNCaP cells

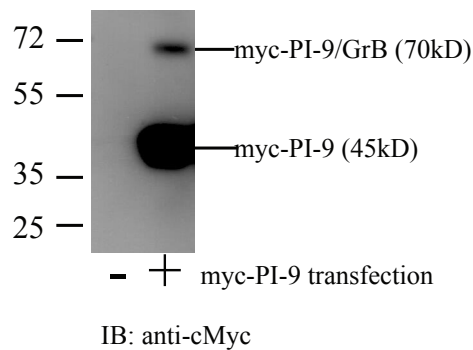
A: Myc-PI-9 expression by Western blot



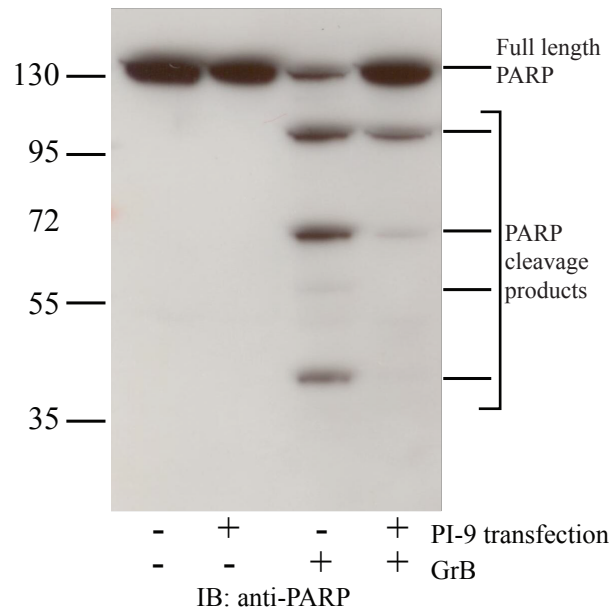
B: Myc-PI-9 expression by flow cytometry



C: Myc-PI-9 directly binds GrB

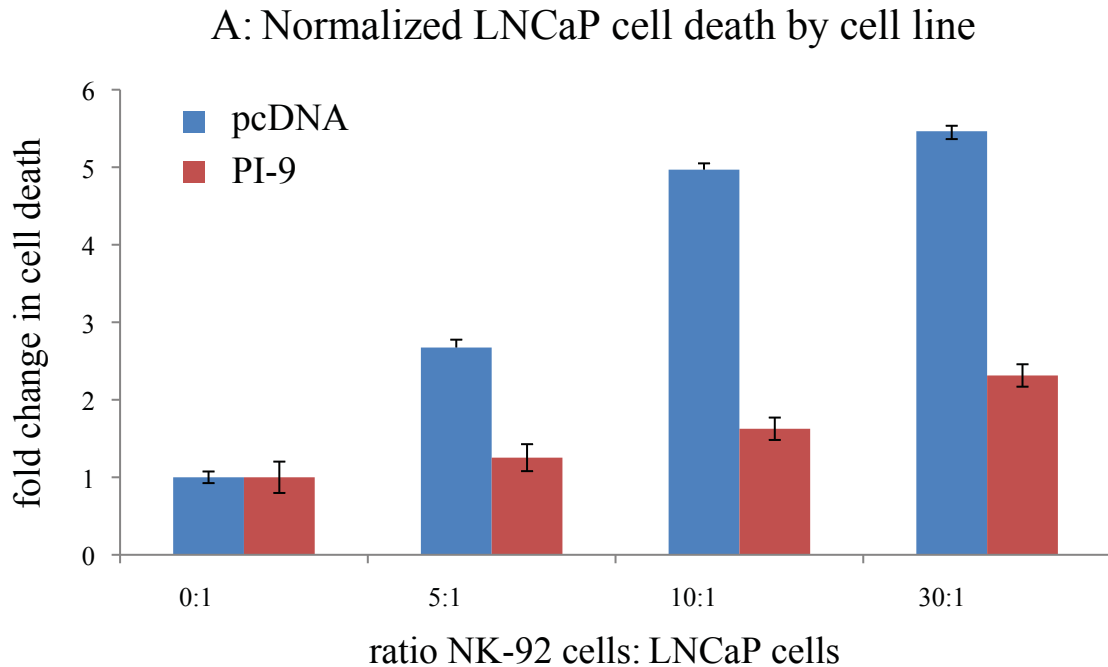


D: Myc-PI-9 inhibits GrB cleavage of PARP

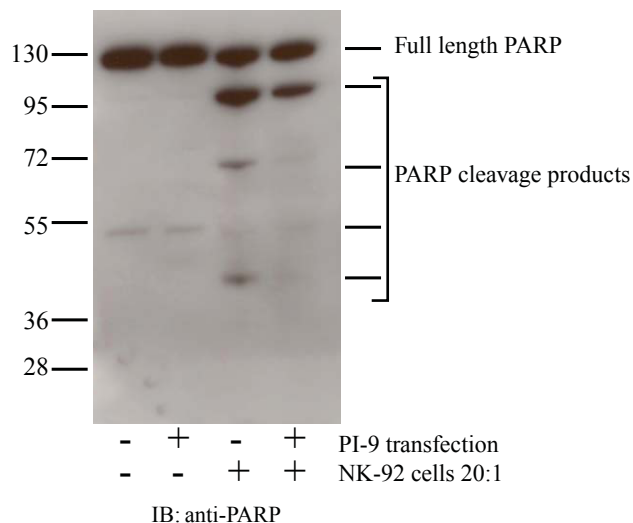


A: LNCaPs transfected with either Myc-PI-9 (+) or a pcDNA control vector (-) were lysed and blotted with anti-Myc. B: myc-PI-9 levels in LNCaP pcDNA (unfilled) and LNCaP PI9 (filled). Identical results were obtained with the anti-myc antibody and the anti-PI9 antibody. C: LNCaP lysates transfected with either Myc-PI-9 (+) or a pcDNA control vector (-) were incubated with recombinant GrB and blotted with anti-Myc. D: LNCaP lysates transfected with either Myc-PI-9 (+) or a pcDNA control vector (-) were incubated with recombinant GrB and PARP cleavage was assessed.

Figure 2-3: LNCaP cells that overexpress PI-9 are resistant to NK-mediated cell death



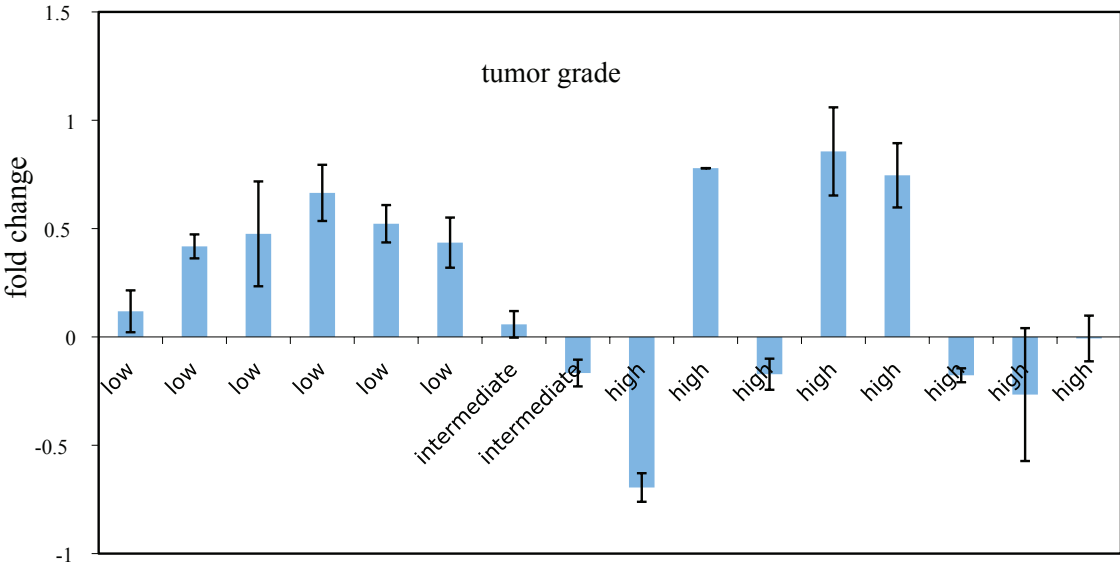
B: PARP cleavage in LNCaP cells post incubation with NK-92 cells



A: LNCaP cells transfected with either Myc-PI-9 (+) or a pcDNA control vector (-) were co-incubated varying ratios of NK-92 cells. Cell death was assayed using flow cytometry by propidium iodide staining. LNCaP-only cell death was used to normalize cell death in the presence of NK cells. B: LNCaP cells transfected with either Myc-PI-9 (+) or a pcDNA control vector (-) were co-incubated at 1:20 with NK-92 cells. LNCaPs were isolated and blotted for PARP cleavage

Figure 2-4: PI-9 is found in multiple stages of prostate tissue

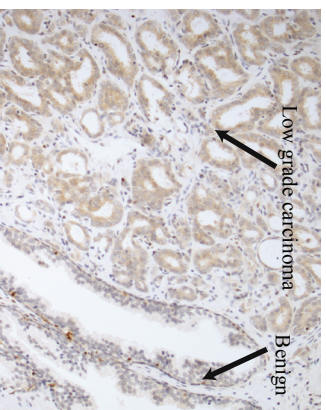
A: Change in PI-9 levels in prostate tumors relative to benign tissue by patient



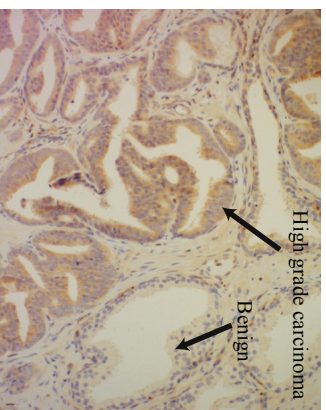
A: PI-9 is upregulated in low grade tumors, but dysregulated in high grade tumors. PI-9 levels were measured in tumor and benign patient tissue samples. PI-9 levels in tumors were then normalized to the benign levels to calculate the fold change.

2-4B: PI-9 immunohistochemistry in prostate tissue slices

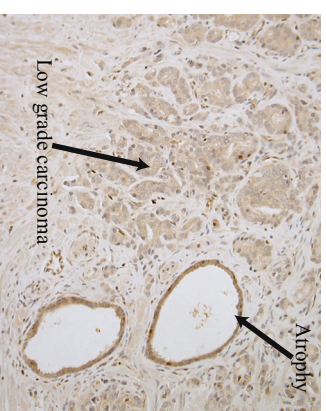
Low grade carcinoma
High PI-9



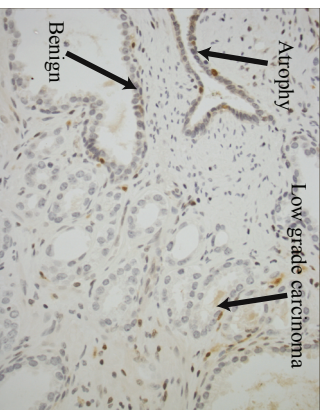
High grade carcinoma
High PI-9



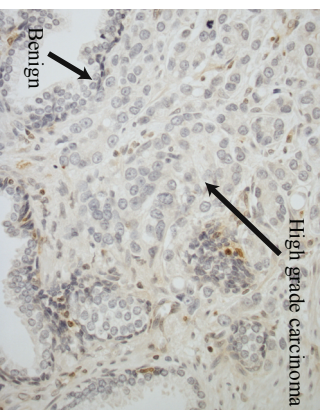
Atrophy/Inflammation



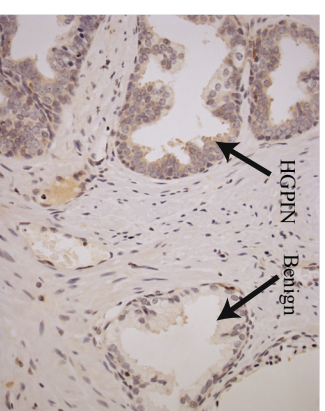
Low grade carcinoma
Low PI-9



High grade carcinoma
Low PI-9

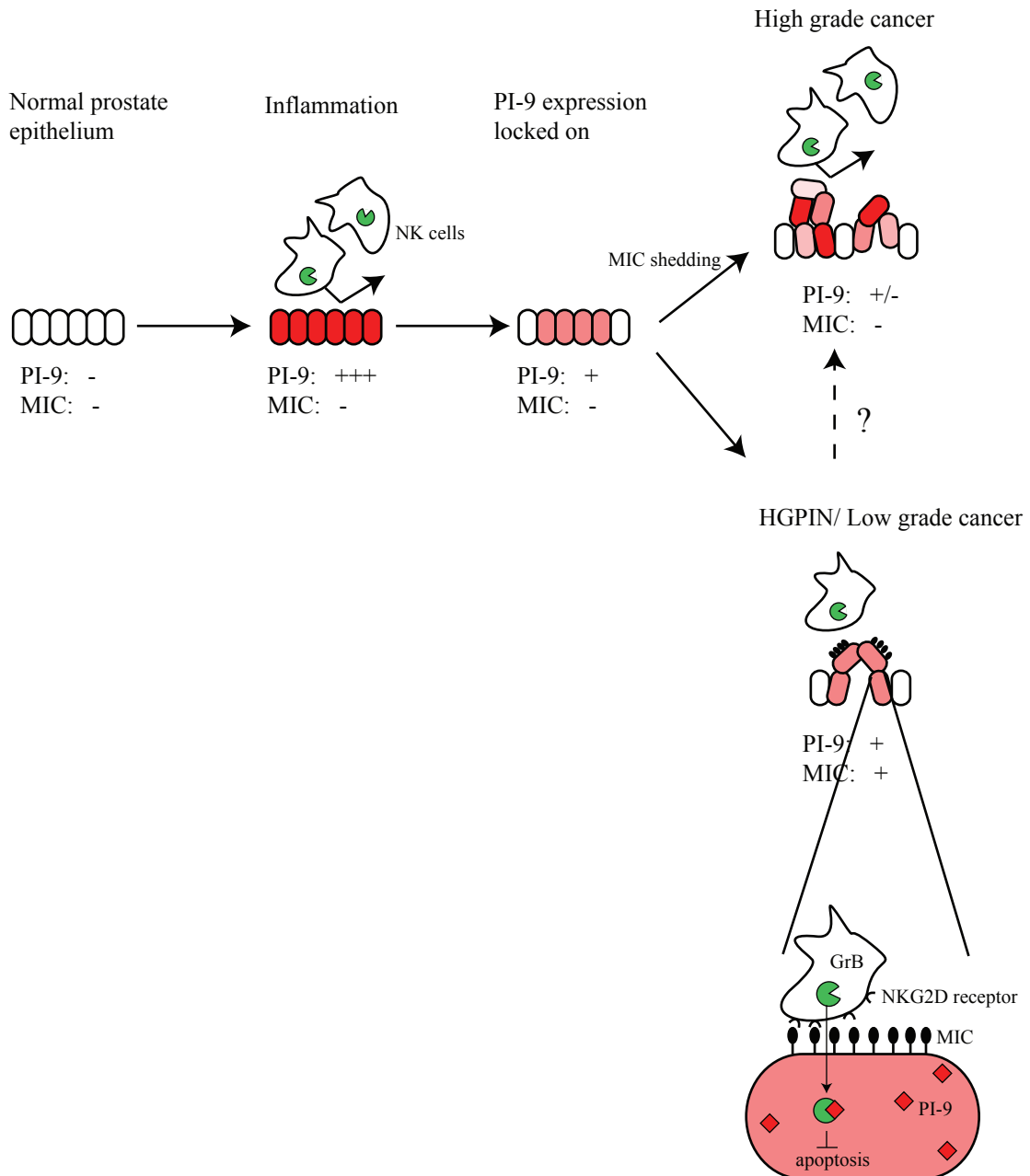


HGPIN



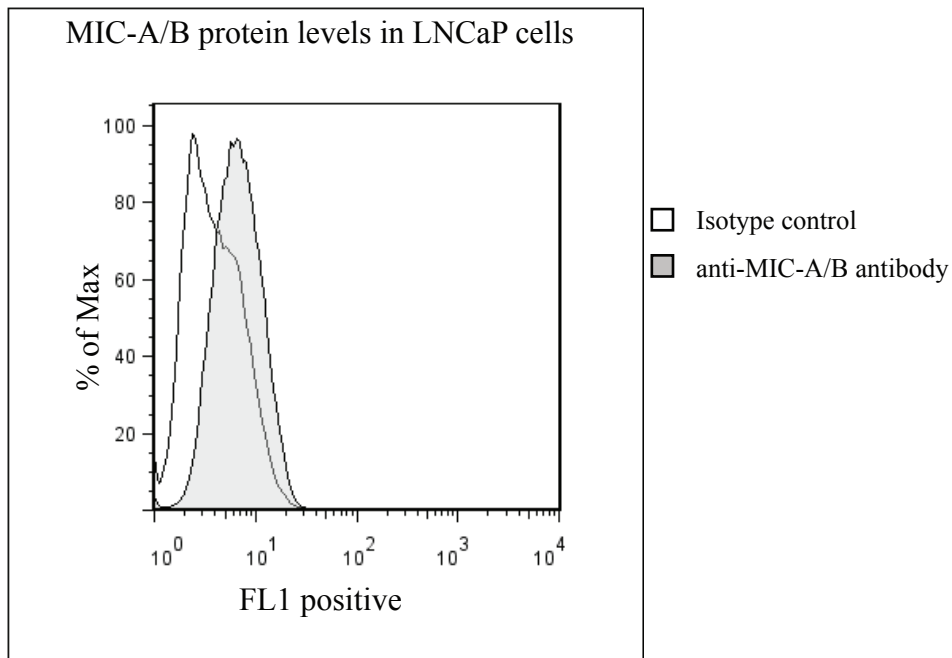
B: Immunohistochemistry for PI-9 was performed on slices of prostate tissue. PI-9 staining was heterogeneous in both benign and carcinoma regions and consistently positive in atrophy and PIN regions.

Figure 2-5: PI-9 model of prostate cancer progression



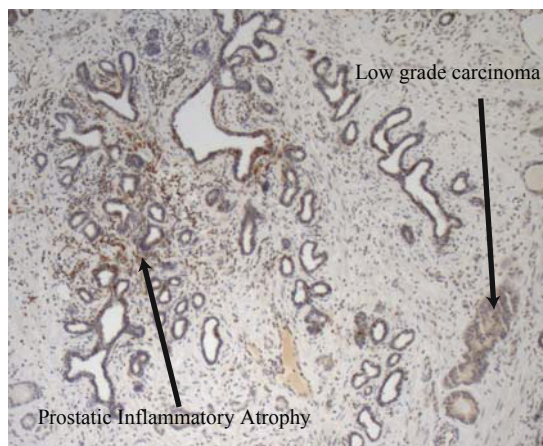
Model of immunoprotective mechanisms in prostate cancer. Normal prostate cancer cells upregulate PI-9 in response to inflammation. In a subset of cells, PI-9 remains on, creating a population of cells resistant to NK-induced apoptosis. In low grade tumors, MIC is expressed at the cell surface, binding to NK cells and leading to Granzyme B introduction, where PI-9 protects the cells from apoptosis. In high grade tumors, MIC is shed. Since PI-9 is no longer needed, its expression becomes stochastic.

Supplementary Figure S2-1: LNCaP cells contain the receptor MIC



LNCaP cells were stained with either an isotype control or an anti-MIC antibody, then fluorescent cells were counted by flow cytometry

Supplementary Figure S2-2: PI-9 staining in prostatic inflammatory atrophy



PI-9 is present in high levels in prostatic inflammatory atrophy. Also shown is PI-9 present in low grade lesions.

Chapter 3

Peptide length and leaving group sterics influence potency of peptide phosphonate protease inhibitors

Re-printed with permission from *Chemistry and Biology*, 28 January 2011.

The ability to follow enzyme activity in a cellular context represents a challenging technological frontier that impacts fields ranging from disease pathogenesis to epigenetics. Activity-based probes (ABPs) label the active form of an enzyme via covalent modification of catalytic residues. Here we present an analysis of parameters influencing potency of peptide phosphonate ABPs for trypsin-fold S1A proteases, an abundant and important class of enzymes with similar substrate specificities. We find that peptide length and stability influence potency more than sequence composition and present structural evidence that steric interactions at the prime-side of the substrate-binding cleft affect potency in a protease-dependent manner. We introduce guidelines for the design of peptide phosphonate ABPs and demonstrate their utility in a live-cell labeling application that specifically targets active S1A proteases at the cell surface of cancer cells.

Introduction

The creation and implementation of high-throughput nucleic acid analysis techniques have revolutionized medicine and biology. The developments of affinity capture and protein binding arrays have allowed similar analyses of protein levels and interactions. However, such gene and protein profiling data does not always reflect the dynamic milieu that one finds at the cellular level *in vivo*. Furthermore, enzymatic activity adds an additional layer of complexity in functionality that cannot currently be addressed using available techniques.

The need to examine enzyme activity is particularly relevant to the study of proteolytic enzymes in biological systems. While synthetic substrates can be used to study individual proteases *in vitro*, their efficacy in studying multiple proteases in a complex mixture is limited. For example, the caspase family of cysteine proteases have highly overlapping substrate specificities, thus multiple caspases can often cleave the same synthetic substrate (McStay et al., 2008). This complicates functional analyses of individual caspases during apoptosis. However, covalent labeling of active proteases allows one to monitor individual proteases in the context of the whole cell. Technologies based on covalent inhibitors are emerging for activity-based proteomics. Phosphonate inhibitors of serine proteases form the basis of one such technology (Sienczyk and Oleksyszyn, 2009).

Diisopropylfluorophosphonate (DFP) is one of the earliest irreversible inhibitors described for serine proteases, and radiolabeled DFP was one of the first activity-based probes (ABPs) described (Powers et al., 2002). More recent studies have modified DFP to include a detection tag for purification and/or visualization purposes (Liu et al., 1999). Biotin and fluorophores are the most common tags used, and active enzyme profiles of several types of human tissues and tumor types have been created using such molecules (Jessani et al., 2005). While these efforts are valuable to the field, these studies identify a preponderance of serine hydrolases that are not proteases, and ABPs specific for proteases have been difficult to achieve.

The specificity of DFP can be improved in two ways. Replacing the highly electronegative fluorine atoms with two phenoxy groups reduces reactivity and increases stability (Powers et al., 2002). Further modifying these functional groups modulates the electrophilicity and shape of the phosphonate reactive center, which can add selectivity to the compound. For example, incorporating different electron withdrawing or donating groups onto the phenyl rings of diphenyl phosphonates (DPPs) results in differential specificity between the urokinase-type plasminogen activator (uPA) and trypsin (Sienczyk and Oleksyszyn, 2006). A second way to reduce DFP promiscuity is to include a short peptide, which helps the inhibitor bind to the active site of the targeted protease. By utilizing substrate cleavage data and combinatorial peptide libraries, the peptide sequence can direct the inhibitor towards a target protease or group of proteases (Lim and Craik, 2009). This methodology was used to design specific ABPs for Granzymes A and B (Mahrus and Craik, 2005).

Despite the aforementioned tunable properties, the emergence of peptide phosphonates as the premier ABPs for specific serine proteases has yet to occur. One can imagine a platform where peptide phosphonates are incorporated into existing microarray technology to create high-throughput assays to monitor active proteases at the bench or in the clinic. However, such a technology has yet to be developed, and the utility of peptide phosphonates has come into question.

Here we describe the synthesis, evaluation, and application of peptide phosphonate inhibitors designed to target S1A family proteases. This subfamily of Clan PA proteases contains the trypsin-like enzymes, and it is the largest family of proteases in higher eukaryotes (Rawlings et al., 2010). These proteases play many important roles in biology and disease progression, and thus are of interest to many fields. This work examines the effects of peptide sequence and length on inhibition of two similar S1A proteases, thrombin and MT-SP1/matriptase, via enzymatic, structural, and imaging methods. We find that peptide length and leaving group sterics are large determinants of potency, while sequence composition contributes to a lesser degree. Our findings suggest general guidelines for the design of phosphonate ABPs that are optimized for S1A proteases. By

applying these guidelines, we demonstrate that peptide phosphonates can quantitatively label and follow proteases on the surface of cancer cells, a novel use of ABPs that can be applied to many systems.

Materials and Methods

MT-SP1 was expressed and purified as described previously and stored at -20°C in 50mM Tris pH 8.0, 50mM NaCl, 10% glycerol (Takeuchi et al., 1999). Mutants for crystallography and kinetic studies were expressed, purified, and stored in the same manner. Thrombin was purchased from Sigma and stored at -20°C in 50mM Tris pH 8.0, 50mM NaCl, 0.1 mg/mL BSA. The MT-SP1 substrates spectrazyme-tPA and spectrafluor-tPA were purchased from American Diagnostica and stored at -20 at 10 mM in H₂O.

The materials for peptide synthesis including PyBOP, EDAC, HOBt, Fmoc-PEG_{20atom}-OH, and 2-chlorotrityl chloride resin were purchased from NovaBiochem. All other chemicals were purchased from Sigma unless otherwise noted. Solvents including anhydrous ethanol (EtOH), chloroform (CHCl₃), 1,4-dioxane, diethyl ether (Et₂O), dichloromethane (DCM), trifluoroethanol (TFE), trifluoroacetic acid (TFA) and N,N-dimethylformamide (DMF) were used as received. The peptides were synthesized following standard Fmoc-SPPS procedure on 2-chlorotrityl chloride resin.

Reactions were analyzed by LC-MS performed on a Waters Alliance liquid chromatography system with a Waters Micromass ZQ single-quadrupole mass spectrometer. HPLC purifications were carried out using an Agilent 1200 series system with C18 reversed-phase columns (Waters). Mobile phase consisted of 99.9:0.1% water/trifluoroacetic acid (solvent A) and 95:4.9:0.1% acetonitrile/water/trifluoroacetic acid (solvent B). All final compounds were characterized by Matrix-assisted laser desorption ionization time-of-flight (MALDI-TOF) mass spectrometry using an ABI 4700 MALDI-TOF-TOF mass spectrometer.

Compound numbers in bold refer to the structures shown in Figure 3-1. Diphenyl [N-(benzyloxycarbonyl)amino](4-cyanophenyl)methanephosphonate (**9**) and NHS-biotin were synthesized according to literature procedure.(ref) No attempts were made to resolve the D,L-(4-AmPhGly)^P(OPh)₂ diastereomers.

Diphenyl-[N-(benzyloxycarbonyl)amino](4-ethylesterphenyl)methane phosphonate hydrochloride (10). A batch of **9** (3.0g, 6.0mmol) was dissolved in 100 mL CHCl₃ and placed in a 0° C bath. Next Ar was passed over the solution and under the flow of Ar, 3 mL of anhydrous EtOH (60mmol) and 100 mL of 4 M HCl in dioxane were added. The reaction was stirred under argon at 4°C for 5 days, after which **10** formed as a fine white precipitate formed. The precipitate was filtered, washed with Et₂O, and dried under reduced pressure (2.32g, 72%). Mass calcd for C₃₀H₂₉N₂O₆P : 544.18; found 545.45 (M+H)⁺.

Diphenyl amino(4-amidinophenyl)methanephosphonate, trifluoroacetic acid salt (12). A batch of **10** (1.0g, 1.8mmol) was dissolved in 25 mL 1,4-dioxane and 25 mL anhydrous EtOH. Next the reaction was purged with Ar and 10mL of 0.5M NH₃ in dioxane (5 mmol) was added dropwise. The reaction was stirred under argon at 23° C for two days, and the solvent was removed completely under vacuum to afford the gummy white crude intermediate, diphenyl [N-(benzyloxycarbonyl)amino](4-amidinophenyl) methanephosphonate **11**. This intermediate was dissolved in anhydrous EtOH (80mL) and concentrated HCl (305μL, 3.7mmol) and hydrogenated over 10% palladium on activated carbon for 5 h at room temperature. The catalyst was separated by filtration, and the solvent was removed under reduced pressure. The white powder thus isolated was dissolved in HPLC solvent (water with 0.1% TFA) with the aid of DMF and purified by reverse-phase HPLC. Lyophilization of fractions containing product afforded **0.49 g (27%)** of **12** as a white powder. Mass calcd for C₂₀H₂₀N₃O₃P: 381.12, *m/z* found: 382.01 (M+H)⁺.

Coupling of the biotinylated peptide to 12. General procedure. To a DCM/TFE(5:1) solution containing the biotin-PEG-peptide (0.03 mmol), EDAC (0.03 mmol) and HOBt

(0.03 mmol), was added H-Bz-DPP **12** (0.03 mmol). After 2 h, an additional eq of EDAC and HOBT was added and the mixture stirred for 8 hr. Next the solvent was removed, the isolated oil was dissolved in MeCN/water (1:3), and purified by reverse-phase HPLC. The fractions with product were lyophilized down to yield the desired product as a white powder. The final probes were dissolved in DMSO and stored at -20° C. The concentration of the solution was determined by HABA biotin quantification kit (Pierce).

Biotin-PEG-Gln-Arg-Val-Bz-DPP-TFA (1). Reaction of Biotin-PEG-Gln(Trt)-Arg(Pbf)-Val-OH (0.10 g, 0.11 mmol), with **12** yielded 39 mg (72% yield) of Biotin-PEG-Gln(Trt)-Arg(Pbf)-Val-DPP as a white powder. Mass calcd for $C_{92}H_{119}N_{14}O_{18}PS_2$: 1802.80, m/z found: 1802.10 (M+H)⁺. Next the powder was resuspended in 95% TFA, 2.5% TIS, 2.5% water and agitated for 2 hours, to obtain the desired probe **1**. The product was precipitated into cold ether, pelleted by centrifugation, and purified by reversed-phase HPLC. Lyophilization of fractions containing product afforded 22 mg (79%) afforded **1** as a white powder. Mass calcd for $C_{60}H_{89}N_{14}O_{15}PS$: 1308.61, m/z found: 656.34 (M+2H)²⁺.

Biotin-PEG-Leu-Thr-Pro-Bz-DPP (2). The protected peptide Biotin-PEG-Leu-Thr(tBu)-Pro-OH was reacted with **12** and resulted in Biotin-PEG-Leu-Thr(tBu)-Pro-Bz-DPP as a white powder (22 mg, 56% yield). Mass calcd for $C_{63}H_{93}N_{10}O_{15}PS$: 1292.63, m/z found: 1293.29 (M+H)⁺. Next the powder was resuspended in 95% TFA, 2.5% TIS, 2.5% water and agitated for 2 hours, to obtain the desired probe **2**. The product was precipitated into cold ether, pelleted by centrifugation, and purified by reversed-phase HPLC. Lyophilization of fractions containing product afforded 8 mg (36% yield). Mass calcd for $C_{59}H_{85}N_{10}O_{15}PS$: 1236.57, m/z found: 1237.12 (M+H)⁺.

Biotin-PEG-Gly-Ser-Gly-Bz-DPP (3). Reaction of Biotin-PEG-Gly-Ser-Gly-OH with **12** resulted in **3** as a white powder (22 mg, 65%). Mass calcd for $C_{51}H_{71}N_{10}O_{15}PS$: 1126.46, m/z found: 1126.92(M+H)⁺.

Biotin-PEG-Glu-Pro-Ile-Bz-DPP (4). Biotin-PEG-Glu(OtBu)-Pro-Ile-OH was reacted

with **12** to afford 23 mg (57% yield) of Biotin-PEG-Glu(OtBu)-Pro-Ile-Bz-DPP. Mass calcd for $C_{64}H_{93}N_{10}O_{16}PS$: 1320.62, m/z found: 1321.43 (M+H)⁺. Then the powder was resuspended in 95% TFA, 2.5% TIS, 2.5% water and agitated for 2 hours to obtain the desired probe. The product was precipitated into cold ether, pelleted by centrifugation, and purified by reversed-phase HPLC. Lyophilization of fractions containing product afforded 20 mg (90% yield) of **4**. Mass calcd for $C_{60}H_{85}N_{10}O_{16}PS$: 1264.56, m/z found: 1266.31 (M+H)⁺.

Biotin-PEG-Bz-DPP (5). Reaction of Biotin-PEG-OH with **12** yielded **5**, which was isolated as white powder. (7mg, 25%). Mass calcd for $C_{44}H_{60}N_7O_{11}PS$: 925.38, m/z found: 926.17 (M+H)⁺.

Biotin-PEG-Val-Bz-DPP (6). A batch of Biotin-PEG-Val-OH was reacted with **12** to afford **6** as a powder after HPLC purification (7mg, 20%). Mass calcd for $C_{49}H_{69}N_8O_{13}PS$: 1024.45, m/z found: 1025.82 (M+H)⁺.

Biotin-PEG-Arg-Val-Bz-DPP (7). Reaction of Biotin-PEG-Arg(Pbf)-Val-OH with **12** afforded Biotin-PEG-Arg(Pbf)-Val-OH as a white powder (34 mg, 77%). Mass calcd for $C_{68}H_{99}N_{12}O_{17}PS_2$, : 1450.64, m/z found: 1451.24 (M+H)⁺. Then the powder was dissolved in 95% TFA, 2.5% TIS, 2.5% water and agitated for 2 hours to obtain the desired probe. The product was precipitated into cold ether, pelleted by centrifugation, and purified by reversed-phase HPLC. Lyophilization of fractions containing product afforded 24 mg (90% yield) of **7**. Mass calcd for $C_{55}H_{81}N_{12}O_{14}PS$: 1180.55, m/z found: 1181.64 (M+H)⁺.

Biotin-PEG-Phe-Thr-Gly-Ser-Gly-Bz-DPP (13). Reaction of Biotin-PEG-Phe-Thr-Gly-Ser-Gly-OH with **12** afforded **13** as a white powder (45 mg, 40%). Mass calcd for $C_{64}H_{87}N_{12}O_{18}PS$: 1374.57, m/z found: 1376.27 (M+H)⁺.

Inhibition assays: All kinetic fluorescence measurements were taken in duplicate using a SpectraMax Gemini fluorescence spectrometer (Molecular Devices) with an excitation

wavelength of 380nm, an emission wavelength of 460 nm, and a 435 nm cutoff filter. A solution of inhibitor was serially diluted over an appropriate concentration range and incubated with enzyme. Substrate was added at the end of 4 hours to initiate the reaction, and IC-50s were calculated. MT-SP1 was used at 0.2nM in a buffer containing 50mM Tris pH 8.0, 50mM NaCl, 0.01% Tween-20, with 200μM spectrafluor-TPA as the substrate. Thrombin was used at 0.5nM in a buffer containing 50mM Tris pH 8.0, 50mM NaCl, 0.01% Tween-20, 0.1 mg/mL BSA, with 200μM Boc-β-benzyl-Asp-Pro-Arg-AMC as the substrate. All reactions were run in duplicate.

Steady-state kinetics were used to determine the observed rate constants for the inhibition reaction. The inhibitors were serially diluted in a 96 well plate at an appropriate range of concentrations. Enzyme was added in hour intervals over 8-10 hours. The reaction was initiated by the addition of 200μM substrate, and the V_{\max} recorded on a SpectraMax fluorescence spectrometer. K_{obs} was determined at each inhibitor concentration by plotting V_{\max} vs time, and K_{Iapp} was determined by plotting K_{obs} vs $[I]$. K_{inact}/K_I was determined using the equation,

$$k = \frac{k_2[I_o]}{[I_o] + K_{i^*}(1 + \frac{[S_o]}{K_M})} \quad \text{where} \quad K_{i^*} = \frac{k_{\text{inact}}}{K_I}.$$

Crystallization: Crystals were grown at room temperature by vapour diffusion in hanging drops. A combination of micro and macro seeding was used to grow large single crystals in 4.0 M Na Formate at pH=7.0 and 25 mM FeCl₃ as additive. Crystals belong to monoclinic space group C2 with one protease-inhibitor complex in the asymmetric unit corresponding to a solvent content of 50% and diffracted to better than 1.2Å resolution.

Structure resolution and refinement: Data were collected at beamline 8.3.1 at the Advanced Light Source in Berkeley on a single crystal cryoprotected in mother liquor supplemented with 20% glycerol. The data were indexed, scaled and reduced using *Mosflm* and *Scala* in *Elves* (Holton and Alber, 2004). The structure was solved by molecular replacement using *Phaser* (McCoy et al., 2007) with the previously solved

protease structure (PDB 3BN9) as search probe (Farady et al., 2008). Automatic building and refinement were performed in *Phenix* (Adams et al., 2002) using *Phenix elBow* to generate the covalently bound ligand. Manual building was carried out in *Coot* (Emsley and Cowtan, 2004). The stereochemistry of the final model was validated using *MolProbity* (Davis et al., 2007).

Western blot labeling analysis: For recombinant protease labeling, enzyme was combined with varying concentrations of phosphonate inhibitor (3mM-30μM) at room temperature overnight. The reaction was stopped by the addition of SDS loading buffer and boiling for 10 minutes. Western blots were developed using the Vectastain ABC elite kit (Vector Labs).

Fluorescent substrate synthesis: Substrates corresponding to each inhibitor were synthesized by solid phase peptide synthesis. ACC-Rink-amide resin was obtained from Kimia Corp. The first amino acid was coupled using 5 equivalents each of amino acid, HATU, and collidine in dry DMF under argon for 16 hours with agitation. The full-length peptide was synthesized using a Symphony Quartet peptide synthesizer (Protein Technologies, Inc.), acetylated with 8 equivalents each of acetic anhydride and DIPEA, and cleaved with 95% TFA/2.5% water/ 2.5% triisopropyl silane. Cleaved peptides were precipitated into cold ether, collected by centrifugation, and purified by HPLC.

Cell culture and propagation: PC3 cells were obtained from the American Type Culture Collection (ATCC) and propagated in F12K Nutrient mixture with Kaighn's Modification (1X) and L-Glutamine (GIBCO). Media was supplemented with 10% FBS and 1X Penicillin:Streptomycin. MCF7 cells were obtained from the ATCC and propagated in Dulbecco's Modified Eagle Medium with high-glucose (D-ME H21) without phenol red (GIBCO). Media was supplemented with 10% FBS, 10μg/mL Insulin, and 1X Penicillin:Streptomycin. PDAC2.1 cells were isolated from p48-Cre/+, LSL-KrasG12D/+, Trp53F/+ transgenic mice according to (Nolan-Stevaux et al., 2009). PDAC2.1 cells were propagated in D-ME H21 (GIBCO) supplemented with 10% FBS and 1X Penicillin:Streptomycin.

Flow cytometry: Cells were grown to confluency in 6-well cell culture-treated dishes using complete media appropriate for each specific cell line. Media was then aspirated and replaced with Opti-MEM serum-free medium (GIBCO). All experiments were done in triplicate. FTGSGBz-DPP (**13**) was added to the appropriate wells at a final concentration of 50 μ M. To test proteolysis, ABP was added in the presence of 1X Complete Protease Inhibitor Cocktail (Roche) dissolved in Opti-MEM. The cells were then incubated at 37°C for approximately 20hrs. After incubation, ABP-containing media was aspirated and cells were washed 3x with Opti-MEM. Cells were detached from the surface of the wells with Enzyme-free Cell Dissociation Buffer (GIBCO) for 15min. Detached cells were washed 2x with Opti-MEM, resuspended in 200 μ L, and incubated for 20min with Streptavidin:AlexaFluor 488 conjugate (Invitrogen) at 4°C. Cells were washed 3x with Opti-MEM and resuspended in 500 μ L Opti-MEM and assayed for fluorescence using a BD FACSCalibur (BD Biosciences). Data was analyzed and population mean fluorescence values were obtained using FlowJo Flow Cytometry Analysis Software (TreeStar, Inc.).

Microscopy: Cells were grown to confluency in 9.5cm² glass bottom microwell dishes (MatTek) in complete media. Media was then aspirated and replaced with Opti-MEM. Phosphonate was added to each dish to a final concentration of 50 μ M. FTGSGBz-DPP (**13**) was incubated for 20hrs at 37°C and QRVBz-DPP (**1**) was incubated for 3hrs at 37°C, respectively. Cells were washed 3x with Opti-MEM and then incubated for 20min with Streptavidin:AlexaFluor 488 conjugate and tetramethylrhodamine-conjugated wheat germ agglutinin (Invitrogen), simultaneously, at 4°C. Cells were then washed 3x with Opti-MEM and imaged. Fluorescence microscopy was carried out in the wide field using a Nikon Diaphot with a Nikon 60x lens, numerical aperture 1.4, objective and standard interference filter sets (Omega Optical). Images were collected using a 12-bit cooled charge-coupled device camera (Princeton Instruments) interfaced to a computer running Micro-Manager 1.3 software (<http://micro-manager.org>). Images were processed using Adobe Photoshop to assemble dual color image files. Brightness/Contrast was adjusted, where necessary, to improve image quality and clarity.

Results:

Improvement to the synthesis of peptide phosphonates.

Several modifications to published protocols have improved the synthesis of the diphenyl phosphonate ester of 4-amidinophenyl-glycine ($\text{H}-(\text{AmPhg})^{\text{P}}(\text{OPh})_2$, for brevity referred to herein as H-Bz-DPP, **12**) and the final biotinylated peptide phosphonate probes (Oleksyszyn et al., 1994). The synthesis of **12** (Figure 3-1) has been reported previously, though isolation of pure compound has been difficult. Briefly, compounds **9-11** were synthesized as described in (Mahrus and Craik, 2005; Oleksyszyn et al., 1994). Published methods describe isolation of **11** by diethyl ether precipitation, however, under the basic reaction conditions to produce **11**, the phosphonate center is not stable. Hydrolysis of one of the phenyl ester groups can occur and be replaced with either an ethyl or methyl ester adduct. Reducing reaction **c** from 5 to 2 days prevented accumulation of the side product as monitored by LC-MS. Longer incubations increased levels of the undesired product. Direct hydrogenation of **11** followed by HPLC produced pure **12**. Alternatively, **11** and **12** were separable by silica gel flash chromatography (10:1 CH_2Cl_2 :MeOH and 5:1 CH_2Cl_2 :MeOH with ninhydrin staining, respectively) at $R_f \approx 0.3$.

Improvements to the synthesis of the final biotinylated peptide diphenyl phosphonate probes include (1) separate construction of the biotinylated peptide moiety and (2) optimization of the coupling reaction of the peptide to **12** to increase yield and reduce reaction time. Instead of building the probe by extending **12** one amino acid at a time as described in (Boduszek et al., 1994) and (Jackson et al., 1998), biotinylated peptides were synthesized on 2-chlorotrityl chloride resin by standard Fmoc chemistry, cleaved under mild acidic conditions to retain the protecting groups, and coupled to the phosphonate. Previous reports indicate this phosphonate coupling reaction to be time consuming (12-48 hours) and low yielding (5-30%)(Oleksyszyn et al., 1994). Optimization of this reaction proceeded with a TFE: CH_2Cl_2 (2:5) solvent mixture to reduce the reaction time from overnight to 6 hr, where DMF had been used previously. Treatment with the coupling agent EDAC resulted in the greatest yield of product (Table 3-1) as compared to PyBOP or DCC (~20%). EDAC protects the base-sensitive phosphonate from hydrolysis since it

is typically utilized in the pH range of 4-6. Following the coupling reaction, deprotection of the amino acid side chains followed. HPLC purification was applied to both the protected and deprotected biotinylated peptide phosphonates. As a result, a combination of TFE:CH₂Cl₂ and EDAC resulted in a fast, efficient coupling that protected the integrity of the phosphonate center and improved product yield (Table 3-1).

Increasing peptide length improves phosphonate inhibition of serine proteases

Having optimized synthesis of the phosphonate inhibitors, the inhibitors were next characterized *in vitro*. Previous work using positional scanning, synthetic combinatorial library (PS-SCL) profiling had identified RKSR as the preferred P4-P1 tetrapeptide sequence for MT-SP1 and LTPR as the preferred sequence for thrombin (Bhatt et al., 2007; Harris et al., 2000). Combining this data with other validated substrates and structural information led to the creation of a series of peptide phosphonates that were designed to target MT-SP1 and thrombin (Table 3-1). Two sequences, QRVBz (**1**) and LTPBz (**2**) were rationally designed to maximize specificity for the two S1A proteases. A peptide element designed to be moderately effective against both proteases (GSGBz **3**) was also synthesized, as was a fourth sequence (EPIBz **4**) containing sub-optimal amino acids for both proteases at each P2-P4 position. Thus, a series of peptides were incorporated to create ABPs that were predicted to cover a range of activities against both MT-SP1 and thrombin.

IC₅₀ values were calculated for each inhibitor against both MT-SP1 and thrombin, and $k_{\text{inact}}/K_{\text{I}}$ values were calculated for inhibitors of a representative subset against MT-SP1 (Table 3-2). For MT-SP1, both the IC₅₀ and $k_{\text{inact}}/K_{\text{I}}$ values for the tetrapeptide inhibitors trended as expected, with the optimal sequence QRVBz-DPP (**1**) inhibiting best at 0.37 μ M, and the non-optimal sequence EPIBz-DPP (**4**) inhibiting worst at 76 μ M (Table 3-2a). These values were in agreement with k_{cat} values measured for synthetic fluorogenic substrates with sequences corresponding to each inhibitor (Supplementary Table S3-1). This correlation between k_{cat} and inhibitory potency has been previously observed (Drag et al., 2010).

Each of the peptide phosphonates tested proved to be slow inhibitors of MT-SP1. The fastest inhibitor, QRVBz-DPP (**1**), was only $200\text{M}^{-1}\text{s}^{-1}$. Previous studies have reported values approaching $37,000\text{M}^{-1}\text{s}^{-1}$ for phosphonate inhibition of serine proteases (Powers et al., 2002). The data shown here indicates that diphenyl phosphonate ABPs did not inhibit MT-SP1 rapidly, and either long incubation times or high phosphonate concentrations were needed to reach complete inhibition. While optimizing the amino acid composition of the peptide improved inhibition, we were unable to gain a large degree of selectivity. The best inhibitor for MT-SP1, **1**, was better than optimal inhibitors designed against thrombin or uPA, another S1A protease (data not shown), further evidence suggesting that sequence composition plays a minor role in inhibitory potency for certain proteases.

The minor contribution due to sequence is reiterated by the ability of the peptide phosphonates to label proteases *in vitro*. The inhibitors were incubated with MT-SP1 and thrombin at increasing concentrations for 16 hours, and biotin-labeled proteases were detected via a Western blot using avidin-HRP. Figure S3-1 shows that the ability of the ABPs to label both proteases was also not strongly dependent on sequence composition. GSGBz-DPP (**3**), designed to confer intermediate potency for MT-SP1 and thrombin, labeled more efficiently than the ABPs with optimal sequences for each protease. This observation is partly explained by the greater stability of **3** over time in aqueous solution (Table S3-1), indicating that sequence stability was an additional parameter for labeling efficiency. Additionally, QRVBz, the best kinetic inhibitor of MT-SP1, contains a second cleavage site after the P3 Arg. This cleavage removed the biotin from the ABP, rendering it undetectable by avidin-HRP and complicating analysis. This secondary cleavage event is evidenced by the appearance of an 846Da fragment upon post-incubation LC-MS analysis.

In addition to the ABPs described above that were designed to test the effects of amino acid sequence on inhibition, three additional ABPs were synthesized to test the effects of peptide length on potency. Previous reports have noted a dependence of peptide length on the mechanistic rate constant k_2 , which suggest a possible effect of length on peptidyl

DPP potency (Case and Stein, 2003). A mono-, di-, and tripeptide phosphonate was synthesized for the QRVBz-DPP probe (**1**), as this sequence proved to inhibit both proteases well (Table 3-2). A clear correlation was observed between increasing peptide length and improvement in inhibition, with a 10 fold increase between the IC₅₀ of the longest inhibitor (QRVBz-DPP, **1**) and the shortest inhibitor (Bz-DPP, **5**), from 0.37μM to 3.5μM. A similar trend was seen in the $k_{\text{inact}}/K_{\text{I}}$ data across the same parameters.

It was clear that not all positions affected MT-SP1 inhibition equally. The addition of a P3 residue increased potency by an order of magnitude (from 8μM to 0.56μM), while only modest changes were observed by the addition of P2 or P4. This was consistent with previously observed substrate:enzyme binding interactions with serine proteases, in which much of the binding energy is contributed by the P1 amino acid interacting with the S1 pocket of the protease. This also correlated with known MT-SP1 substrate data and with crystallographic observations about the S4 and S3 pockets (Bhatt et al., 2007; Friedrich et al., 2002). Friedrich et al. observed that the deep S3 pocket of MT-SP1 could accommodate a Lys or Arg residue from *either* P3 *or* P4 of a substrate while the other amino acid is solvent exposed. This phenomenon could explain the modest increase in inhibition seen when increasing from a tripeptide- to a tetrapeptide phosphonate (Friedrich et al., 2002).

A similar trend was seen in IC-50 values measured against thrombin (Table 3-2c) and uPA (data not shown). Again, it is notable that QRVBz-DPP (**1**), the ideal MT-SP1 inhibitor, was more potent than the ideal thrombin inhibitor LTPBz-DPP (**2**) by an order of magnitude (0.125μM for **1** compared to 1.1μM for **2**). Sequence data alone does not appear to be sufficient to design ABPs that can distinguish between these two proteases, though other proteases with much more stringent substrate binding pockets have shown to be amenable to sequence-derived specificity (Mahrus and Craik, 2005).

To determine if potency continued to improve beyond P4, a hexapeptide ABP was synthesized and tested against MT-SP1. The preferred P5 and P6 amino acids for MT-SP1 were added to the most stable inhibitor (GSGBz **3**) to create **13** (FTGSGBz). **13** is

25% more potent than **3** against MT-SP1, verifying that further increasing length improved potency.

Interestingly, each of the ABPs synthesized for this study inhibited thrombin at much lower concentrations than MT-SP1. We next sought to obtain a structural basis for the improvement in inhibition observed against thrombin.

Structure of MT-SP1 bound to Bz-DPP

The structure of MT-SP1 bound to Bz-DPP phosphonate was solved to 1.19Å resolution (Figure 3-2, Table 3-3). The protein was incubated with saturating ABP concentrations overnight at room temperature and purified via size exclusion chromatography. Attempts to crystallize MT-SP1 with Ac-QRVBz-DPP only produced crystals containing Bz-DPP. A possible explanation is that nonspecific hydrolysis of the peptide bond occurred during the several rounds of seeding and crystal growth that were necessary to obtain high-quality crystals, all of which took place in an aqueous environment at room temperature over several months. The truncated inhibitor may have also resulted from incomplete purification of the Bz-DPP (**12**) starting material from the full-length ABP.

This is the highest resolution MT-SP1 structure to date, which allows for visualization of all bonds. The phosphonate bound in the solvent exposed binding pocket in the expected conformation, with the phosphorous atom bound to the active site Ser195 and Bz in the S1 pocket (Figure 3-2a). The positively charged guanidine group of Bz formed two hydrogen bonds with the negatively charged Asp202. The N-terminal end of the inhibitor pointed down the substrate binding pocket, and the phenyl ring is solvent exposed.

A structure of thrombin (PDB: 1QUR) (Steinmetzer et al., 1999) was overlaid onto the MT-SP1-Bz-DPP structure, and the probe fit similarly into the binding pocket (Figure 3-2b). Inspection of the placement of the phenyl rings of the phosphonate revealed one important difference in the active site architecture. In MT-SP1 residue Phe99 lay in the region where the leaving group phenyl ring binds during catalysis. In thrombin, a smaller Leu99 occupied this location, forming a larger pocket than seen in MT-SP1. The Phe was

only 2Å away from the phosphorous, thus we hypothesized that Phe99 caused steric interference with the leaving phenyl ring, slowing orientation of the inhibitor in the active site and slowing inhibition of MT-SP1 relative to that of thrombin.

To test this hypothesis, MT-SP1 Phe99 was mutated to Ala to create MT-SP1 F99A, and IC-50 measurements with the same series of inhibitors were repeated (Table 3-2b). The IC-50 values for MT-SP1 F99A fell between that of MT-SP1 and thrombin in each case, indicating the size of the binding pocket for the leaving group in MT-SP1 influenced phosphonate inhibition.

When the structure of uPA (PDB: 3KGP) (Zhang et al., 2010), an S1A protease with slow kinetics of phosphonate inhibition similar to those of MT-SP1 was overlaid with thrombin, a similar steric hindrance was observed (Fig 3-2d). At the same pocket in uPA, His99 protruded exactly where Phe99 did in MT-SP1. Thrombin had a larger binding pocket than either MT-SP1 or uPA, due to the Leu found at residue 99. The smaller pocket in uPA, as with MT-SP1, may explain the slow inhibition of uPA by DPPs. This reinforces the idea that the steric fit of the leaving group on the prime side has an important effect on potency.

Labeling of cell surface proteases by ABPs

Having determined the kinetic and labeling properties of the ABPs *in vitro*, their potential for labeling active proteases on the surface of live immortalized cancer cells was examined. The most stable inhibitor (**13**) and the most potent inhibitor (**1**) were used to label the cell surface proteases of two different cell lines grown in culture. These cell lines represented epithelial cancer types from two different species: PC3 cells, derived from human prostate cancer, and PDAC2.1 cells, derived from a transgenic mouse model of pancreatic ductal adenocarcinoma (Nolan-Stevaux et al., 2009). Live cells were incubated with phosphonate overnight in serum free media at 37°C. Streptavidin conjugated with AlexaFluor488 dye was used to fluorescently tag the ABPs. Cells were examined for the presence of labeled proteases either by fluorescent microscopy or by flow cytometry.

As seen in Figure 3-3, green fluorescent labeling was observed in PC3 and PDAC cells that had been exposed to ABPs, indicating the presence of active S1A proteases on the cell surface. PDAC2.1 (Figure 3-3a) cells labeled discrete foci on the cell surface. In the case of PC3 cells (Figure 3-3b), these labeled proteases were localized to one end of each cell. In addition to cell surface labeling, punctate labeling was also observed just internal to the plasma membrane. These puncta co-localized with membrane staining dye, indicative of internalization of labeled surface proteases. Internalization was also occasionally observed in PDAC2.1 cells and more frequently observed in MCF7 cells, a human breast cancer cell line (Figure S3-2). This result indicates that ABPs can visualize and follow active serine proteases on the surface of live cells, a novel use for peptide phosphonates.

After demonstrating the ability to label cell surface proteases, the ability to quantify the active form of these proteases was tested. Cells were grown, exposed to phosphonate overnight at 37°C, and fluorescently tagged with labeled streptavidin. Fluorescence was quantified using flow cytometry on the live cells. Fluorescence increased relative to background when cells had been incubated with an ABP, and this labeling was reduced in the presence of protease inhibitors (Figure 3-3e). These results demonstrate that ABPs can be used to quantify active proteases on the surface of live cells, and that labeling can be directly attributed to proteolysis.

Collectively, the cell-based experiments show that peptide phosphonates can be used to quantitatively label active cell surface proteases on different cell types. Live cell imaging can also be used in conjunction with ABP labeling to determine the localization of active proteases in the context of a cell or group of cells.

Discussion

This study presents additional guidelines for the synthesis, design, and application of peptide phosphonate ABPs to those described previously (Oleksyszyn and Powers, 1994). Our results show that by focusing on peptide length, stability, and leaving group sterics,

the lifetime and utility of these ABPs can be improved dramatically. By following these guidelines, a novel protease imaging application using ABPs was developed. These experiments demonstrate that ABPs can be used to quantify, image, and follow proteases on cell surfaces.

We have improved the utility of phosphonate ABPs by combining synthetic, kinetic, and structural data. Obtaining reagent quantities of material has been a significant barrier to using these molecules in numerous applications. The improved synthesis methodology presented here both increases reproducibility of ABP production and increases yields up to seven fold compared to previous methods. The robust generation of ABPs greatly improves their utility, and synthesizing greater quantities of these probes enabled a systematic study of their potency.

Three major factors were found to contribute to peptide phosphonate potency: peptide stability, length, and leaving group sterics. Peptide sequence is often viewed as a primary determinant of potency, and reports of sequence-based selectivity exist for Granzymes A and M, two S1A proteases with highly selective and differing substrate specificities at P2-P4 (Mahrus and Craik, 2005). However, for the majority of trypsin-fold proteases, much of the substrate binding energy of is contributed via binding of a basic P1 amino acid in the deep S1 pocket of the active site. Because of the strong P1 contribution, the P2-P4 sequence often plays a minor role. Peptide stability, however, was found to contribute significantly to ABP functionality. Inhibitors containing the amino acid Pro were especially unstable and problematic for both synthesis and purification, while long, charged side chains like Arg were found to react with the electrophilic phosphonate, subsequently inactivating the inhibitor. Additionally, the use of basic residues like Arg upstream of P1 can result in a secondary cleavage site for trypsin-like proteases, which removes the probe from the reactive diphenylphosphonate moiety. Poorly fitting residues can have a detrimental effect on inhibition, as seen by the slow kinetics of the EPIBz (**4**) probe against MT-SP1, thrombin, and uPA (Table 3-2 and data not shown). Therefore, the optimal peptide element should be composed of the most stable residues tolerated by the protease.

Peptide length, rather than sequence, had a more noticeable contribution to improving inhibitory capabilities. Increasing length increased potency, most notably at the P3 position. This agrees with earlier findings (Oleksyszyn and Powers, 1991). The data suggests that when designing peptide phosphonate inhibitors, including a longer peptide will improve inhibition more reliably than modifying the sequence. The sequence composition data and stability observations indicate that phosphonate inhibitors of trypsin-fold proteases should contain at least a tetrapeptide composed solely of stable amino acids.

The third factor contributing to potency is the steric fit of the phosphonate leaving group in the binding pocket of the protease. Atomic-resolution structural data showed this pocket is smaller in MT-SP1 than in thrombin. This pocket is adjacent to the catalytic S195, exactly where the leaving group phenyl ring would reside. This smaller pocket in MT-SP1 is due to the presence of a bulky Phe at residue 99. Mutagenesis experiments confirmed that this pocket is an important binding determinant for DPPs and MT-SP1. The data indicates that the leaving group of the phosphonate can have a large effect on inhibition. When designing a phosphonate ABP specific for a protease, multiple leaving groups should be tested on a stable peptide scaffold to find the best inhibitor.

The data shown here provide important information for the design of peptide phosphonate ABPs with both broad and narrow specificity. We show that the peptide element (in stability and length) and the leaving group (in reactivity and sterics) contribute to inhibitory potency of phosphonate ABPs. When designing a broad-specificity phosphonate ABP, one should start with a scaffold containing at least four stable amino acids and then consider varying the leaving group if improved potency is desired. When designing an inhibitor for a specific S1A protease, substrate cleavage data should be viewed as a starting point. Varying the leaving group may result in larger differences in potency, even for closely related proteases. Interestingly, kinetic data indicates that varying the reaction time may label different sets of proteases, with longer incubations resulting in larger sets of labeled proteases. Therefore, reaction time may also

influence selectivity. However, these experiments suggest that only in rare instances will true specificity be engineered by varying peptide composition alone.

By following the guidelines presented here, several broad-spectrum ABPs for S1A proteases were produced in high yields. We used the most potent (**1**) and stable (**13**) ABPs to develop a novel method of imaging proteases on the surface of cancer cells. ABP-labeled proteases can be visualized and quantified with fluorescently conjugated streptavidin. This approach found that levels of protease activity vary by cell type, and that the location of labeled proteases can be tracked through the cell (Figure 3-3). Protease activity and localization information can be leveraged to obtain new information about protease function.

The ability to study the localization of active proteases is a novel use of phosphonate activity-based probes, and offers a promising way to examine the biology of cell surface protease activity. Previous studies with cysteine protease ABPs have been successful at labeling and visualizing lysosomal cathepsins and extracellular cathepsins in tumors (Blum et al., 2005; Joyce et al., 2004). The current study extends the use of ABPs to serine proteases on the surface of live cells. Differences in labeling and localization varied between the cell types, a conclusion previously observed with MT-SP1 using specific antibody-based probes (Darragh et al., 2010). These broad-spectrum ABPs may be used to highlight cell-specific differences in global S1A protease function.

For example, cell surface proteases have been implicated in metastasis, and it is interesting to note that active protease localization was polarized. Notably, high concentrations of enzymes were observed at one edge of the cells distal to cell-cell junctions. In addition, correlating the degree of labeling with a cellular phenotype such as metastatic potential may yield new information about cancer cell biology.

Though the pattern varied, internalization of proteases was observed in all cell types, as evidenced by the co-localization of membrane and ABP in puncta just inside the cell membrane. We hypothesize two explanations for this observation. First, many proteins

undergo natural trafficking to and from the cell surface, modulating cellular interactions with the outside environment. Trafficking has been implicated previously in the regulation of proteases in the cell (Ghosh et al., 2003). ABPs could thus be used to track the movement and function of active proteases in many complex biological systems, including cancer biology, where protease activity is frequently dys-regulated. Alternatively, the ABPs themselves may cause proteases to become internalized. Ligand-dependent endocytosis has been observed with other cell surface receptors (Behrendt, 2004; Ghosh et al., 2003). The molecular mechanism of cell surface protease internalization observed via ABPs invites further investigation.

In summary, through synthetic, kinetic, and structural insights, we have developed additional guidelines that define and expand the use of peptide phosphonate ABPs. By following these guidelines, we have created a potent pan-S1A protease probe and developed a general methodology for the study of active proteases at the surface of cells. This technology could allow for future insights into the role of proteases in cancer, and has potential applications to other fields in biology.

Acknowledgement

Mass spectrometry was provided by the Bio-Organic Mass Spectrometry Resource at UCSF (A. L. Burlingame, Director) supported by the Biomedical Research Technology Program of the NIH National Center for Research Resources (NIH NCRR P41RR001614 and NRCC RR014606). This work was supported by a NIH/NIGMS award (K12GM081266) to A.E.-R., a NIGMS-IMSD award (R25-GM56847) to C.T., and by the National Institutes of Health (NIH R01CA128765).

References

Adams, P.D., Grosse-Kunstleve, R.W., Hung, L.W., Ioerger, T.R., McCoy, A.J., Moriarty, N.W., Read, R.J., Sacchettini, J.C., Sauter, N.K., and Terwilliger, T.C. (2002).

PHENIX: building new software for automated crystallographic structure determination. *Acta Crystallogr D Biol Crystallogr* 58, 1948-1954.

Behrendt, N. (2004). The urokinase receptor (uPAR) and the uPAR-associated protein (uPARAP/Endo180): membrane proteins engaged in matrix turnover during tissue remodeling. *Biol Chem* 385, 103-136.

Bhatt, A.S., Welm, A., Farady, C.J., Vasquez, M., Wilson, K., and Craik, C.S. (2007). Coordinate expression and functional profiling identify an extracellular proteolytic signaling pathway. *Proc Natl Acad Sci U S A* 104, 5771-5776.

Blum, G., Mullins, S.R., Keren, K., Fonovic, M., Jedeszko, C., Rice, M.J., Sloane, B.F., and Bogyo, M. (2005). Dynamic imaging of protease activity with fluorescently quenched activity-based probes. *Nat Chem Biol* 1, 203-209.

Boduszek, B., Oleksyszyn, J., Kam, C.M., Selzler, J., Smith, R.E., and Powers, J.C. (1994). Dipeptide phosphonates as inhibitors of dipeptidyl peptidase IV. *J Med Chem* 37, 3969-3976.

Case, A., and Stein, R.L. (2003). Mechanistic origins of the substrate selectivity of serine proteases. *Biochemistry* 42, 3335-3348.

Darragh, M.R., Schneider, E.L., Lou, J., Phojanakong, P.J., Farady, C.J., Marks, J.D., Hann, B.C., and Craik, C.S. (2010). Tumor detection by imaging proteolytic activity. *Cancer Res* 70, 1505-1512.

Davis, I.W., Leaver-Fay, A., Chen, V.B., Block, J.N., Kapral, G.J., Wang, X., Murray, L.W., Arendall, W.B., 3rd, Snoeyink, J., Richardson, J.S., *et al.* (2007). MolProbity: all-atom contacts and structure validation for proteins and nucleic acids. *Nucleic Acids Res* 35, W375-383.

- Drag, M., Bogyo, M., Ellman, J.A., and Salvesen, G.S. (2010). Aminopeptidase fingerprints, an integrated approach for identification of good substrates and optimal inhibitors. *J Biol Chem* 285, 3310-3318.
- Emsley, P., and Cowtan, K. (2004). Coot: model-building tools for molecular graphics. *Acta Crystallogr D Biol Crystallogr* 60, 2126-2132.
- Farady, C.J., Egea, P.F., Schneider, E.L., Darragh, M.R., and Craik, C.S. (2008). Structure of an Fab-protease complex reveals a highly specific non-canonical mechanism of inhibition. *J Mol Biol* 380, 351-360.
- Friedrich, R., Fuentes-Prior, P., Ong, E., Coombs, G., Hunter, M., Oehler, R., Pierson, D., Gonzalez, R., Huber, R., Bode, W., *et al.* (2002). Catalytic domain structures of MT-SP1/matrilysin, a matrix-degrading transmembrane serine proteinase. *J Biol Chem* 277, 2160-2168.
- Ghosh, P., Dahms, N.M., and Kornfeld, S. (2003). Mannose 6-phosphate receptors: new twists in the tale. *Nat Rev Mol Cell Biol* 4, 202-212.
- Harris, J.L., Backes, B.J., Leonetti, F., Mahrus, S., Ellman, J.A., and Craik, C.S. (2000). Rapid and general profiling of protease specificity by using combinatorial fluorogenic substrate libraries. *Proc Natl Acad Sci U S A* 97, 7754-7759.
- Holton, J., and Alber, T. (2004). Automated protein crystal structure determination using ELVES. *Proceedings of the National Academy of Sciences of the United States of America* 101, 1537-1542.
- Jackson, D.S., Fraser, S.A., Ni, L.M., Kam, C.M., Winkler, U., Johnson, D.A., Froelich, C.J., Hudig, D., and Powers, J.C. (1998). Synthesis and evaluation of diphenyl phosphonate esters as inhibitors of the trypsin-like granzymes A and K and mast cell tryptase. *J Med Chem* 41, 2289-2301.

Jessani, N., Niessen, S., Wei, B.Q., Nicolau, M., Humphrey, M., Ji, Y., Han, W., Noh, D.Y., Yates, J.R., 3rd, Jeffrey, S.S., *et al.* (2005). A streamlined platform for high-content functional proteomics of primary human specimens. *Nat Methods* 2, 691-697.

Joyce, J.A., Baruch, A., Chehade, K., Meyer-Morse, N., Giraudo, E., Tsai, F.Y., Greenbaum, D.C., Hager, J.H., Bogoy, M., and Hanahan, D. (2004). Cathepsin cysteine proteases are effectors of invasive growth and angiogenesis during multistage tumorigenesis. *Cancer Cell* 5, 443-453.

Lim, M.D., and Craik, C.S. (2009). Using specificity to strategically target proteases. *Bioorg Med Chem* 17, 1094-1100.

Liu, Y., Patricelli, M.P., and Cravatt, B.F. (1999). Activity-based protein profiling: the serine hydrolases. *Proc Natl Acad Sci U S A* 96, 14694-14699.

Mahrus, S., and Craik, C.S. (2005). Selective chemical functional probes of granzymes A and B reveal granzyme B is a major effector of natural killer cell-mediated lysis of target cells. *Chem Biol* 12, 567-577.

McCoy, A.J., Grosse-Kunstleve, R.W., Adams, P.D., Winn, M.D., Storoni, L.C., and Read, R.J. (2007). Phaser crystallographic software. *J Appl Crystallogr* 40, 658-674.

McStay, G.P., Salvesen, G.S., and Green, D.R. (2008). Overlapping cleavage motif selectivity of caspases: implications for analysis of apoptotic pathways. *Cell Death Differ* 15, 322-331.

Nolan-Stevaux, O., Lau, J., Truitt, M.L., Chu, G.C., Hebrok, M., Fernandez-Zapico, M.E., and Hanahan, D. (2009). GLI1 is regulated through Smoothened-independent mechanisms in neoplastic pancreatic ducts and mediates PDAC cell survival and transformation. *Genes Dev* 23, 24-36.

Oleksyszyn, J., Boduszek, B., Kam, C.M., and Powers, J.C. (1994). Novel amidine-containing peptidyl phosphonates as irreversible inhibitors for blood coagulation and related serine proteases. *J Med Chem* 37, 226-231.

Oleksyszyn, J., and Powers, J.C. (1991). Irreversible inhibition of serine proteases by peptide derivatives of (alpha-aminoalkyl)phosphonate diphenyl esters. *Biochemistry* 30, 485-493.

Oleksyszyn, J., and Powers, J.C. (1994). Amino acid and peptide phosphonate derivatives as specific inhibitors of serine peptidases. *Methods Enzymol* 244, 423-441.

Powers, J.C., Asgian, J.L., Ekici, O.D., and James, K.E. (2002). Irreversible inhibitors of serine, cysteine, and threonine proteases. *Chem Rev* 102, 4639-4750.

Rawlings, N.D., Barrett, A.J., and Bateman, A. (2010). MEROPS: the peptidase database. *Nucleic Acids Res* 38, D227-233.

Sienczyk, M., and Oleksyszyn, J. (2006). Inhibition of trypsin and urokinase by Cbz-amino(4-guanidinophenyl)methanephosphonate aromatic ester derivatives: the influence of the ester group on their biological activity. *Bioorg Med Chem Lett* 16, 2886-2890.

Sienczyk, M., and Oleksyszyn, J. (2009). Irreversible inhibition of serine proteases - design and in vivo activity of diaryl alpha-aminophosphonate derivatives. *Curr Med Chem* 16, 1673-1687.

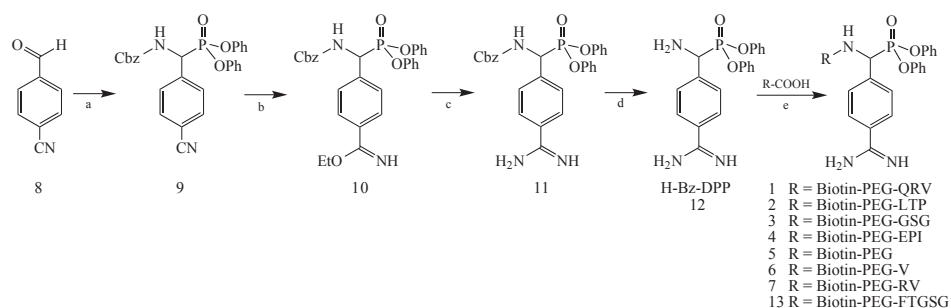
Steinmetzer, T., Renatus, M., Kunzel, S., Eichinger, A., Bode, W., Wikstrom, P., Hauptmann, J., and Sturzebecher, J. (1999). Design and evaluation of novel bivalent thrombin inhibitors based on amidinophenylalanines. *Eur J Biochem* 265, 598-605.

Takeuchi, T., Shuman, M.A., and Craik, C.S. (1999). Reverse biochemistry: use of macromolecular protease inhibitors to dissect complex biological processes and identify a

membrane-type serine protease in epithelial cancer and normal tissue. *Proc Natl Acad Sci U S A* *96*, 11054-11061.

Zhang, L., Zhang, Z.G., Buller, B., Jiang, J., Jiang, Y., Zhao, D., Liu, X., Morris, D., and Chopp, M. (2010). Combination treatment with VELCADE and low-dose tissue plasminogen activator provides potent neuroprotection in aged rats after embolic focal ischemia. *Stroke* *41*, 1001-1007.

Figure 3 - 1. General Synthesis of 4-Amidinophenyl-Glycine that Incorporates Benzamidine at the P1 Position



General synthesis of 4-amidinophenyl-glycine that incorporates benzamidine at the P1 position. Reagents and conditions: (a) P(OPh)₃, benzyl carbamate, HOAc, 1 h at rt, 1 h at 85 °C; (b) dry EtOH, CHCl₃, HCl in dioxane, 5 d at 4 °C; (c) NH₃ in dioxane, dry EtOH:dioxane (1:1), 2 d at rt; (d) H₂, cat. Pd(10% on C), HCl, EtOH, 6 h at rt; (e) EDAC, HOBt, TFE:DCM, 6 h at rt.

Table 3 - 1. Yields and Masses of Each Phosphonate Probe Synthesized

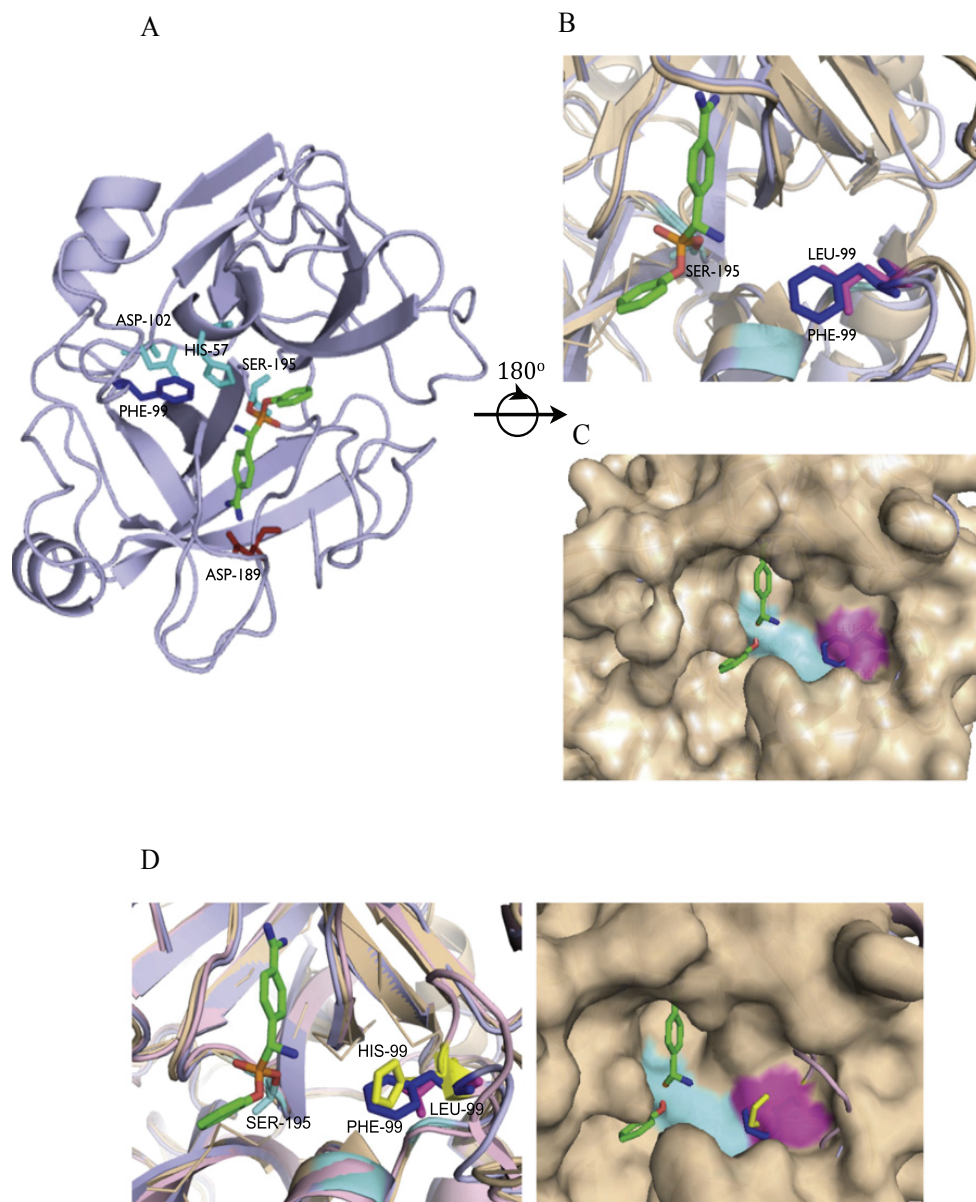
Compound (biotin-PEG- R)	Yield (%)	m/z Calculated (Found)
R = QRVBz-DPP (1)	72	1308.61 (656.34)
R = LTPBz-DPP (2)	56	1236.57 (1237.12)
R = GSGBz-DPP (3)	65	1126.46 (1126.92)
R = EPIBz-DPP (4)	57	1264.56 (1266.31)
R = Bz-DPP (5)	25	925.38 (926.7)
R-VBz-DPP (6)	20	1024.45 (1025.82)
R = RVBz-DPP (7)	77	1180.55 (1181.64)
R = FTGSGBz-DPP (13)	40	1374.57 (1376.27)

Table 3 - 2. Inhibition Kinetics of Phosphonate Probes against MT- SP1 and Thrombin

	Enzyme	Compound	Inhibitor	IC ₅₀ (mM)
A	MTSP1	5	Bz	3.5 ± 0.6
		6	VBz	8 ± 0.1
		7	RVBz	0.56 ± 0.09
		1	QRBVz	0.37 ± 0.2
		3	GSGBz	14 ± 1
		2	LTPBz	1.1 ± 0.02
		4	EPIBz	76 ± 1
		13	FTGSGBz	3.5 ± 0.5
B	MTSP1 F99A	5	Bz	1.5 ± 0.04
		6	VBz	1.3 ± 0.06
		7	RVBz	0.23 ± 0.01
		1	QRBVz	0.22 ± 0.01
		3	GSGBz	9.2 ± 0.4
C	Thrombin	5	Bz	0.097 ± 0.01
		6	VBz	0.28 ± 0.05
		7	RVBz	0.068 ± 0.04
		1	QRBVz	0.13 ± .002
		3	GSGBz	0.027 ± 0.01
		2	LTPBz	1.8 ± 0.5
		4	EPIBz	0.76 ± 0.2
D	MTSP1	Compound	Inhibitor	k _{inact} /K _I (M ⁻¹ s ⁻¹)
		5	Bz	50 ± 2
		6	VBz	60 ± 10
		7	RVBz	490 ± 40
		1	QRBVz	200 ± 60
		3	GSGBz	26 ± 0.5
		4	EPIBz	11.7 ± 3

MT-SP1 and thrombin were incubated with varying concentrations of inhibitor and activity was monitored on addition of substrate.

Figure 3-2: structure of the catalytic domain of MT-SP1 bound to benzamidine phosphonate



A: Structure of the catalytic domain of MT-SP1 bound to Benzamidine phosphonate. Numbered amino acid residues correspond to chymotrypsin protease numbering.

B: Close-up ribbon of thrombin (tan) overlaid onto MT-SP1 (light blue). Thrombin L99 purple, MT-SP1 F99 blue, catalytic triad cyan.

C: Thrombin (tan) surface overlaid onto MT-SP1 (light blue). Thrombin L99 purple, MT-SP1 F99 blue, catalytic triad cyan.

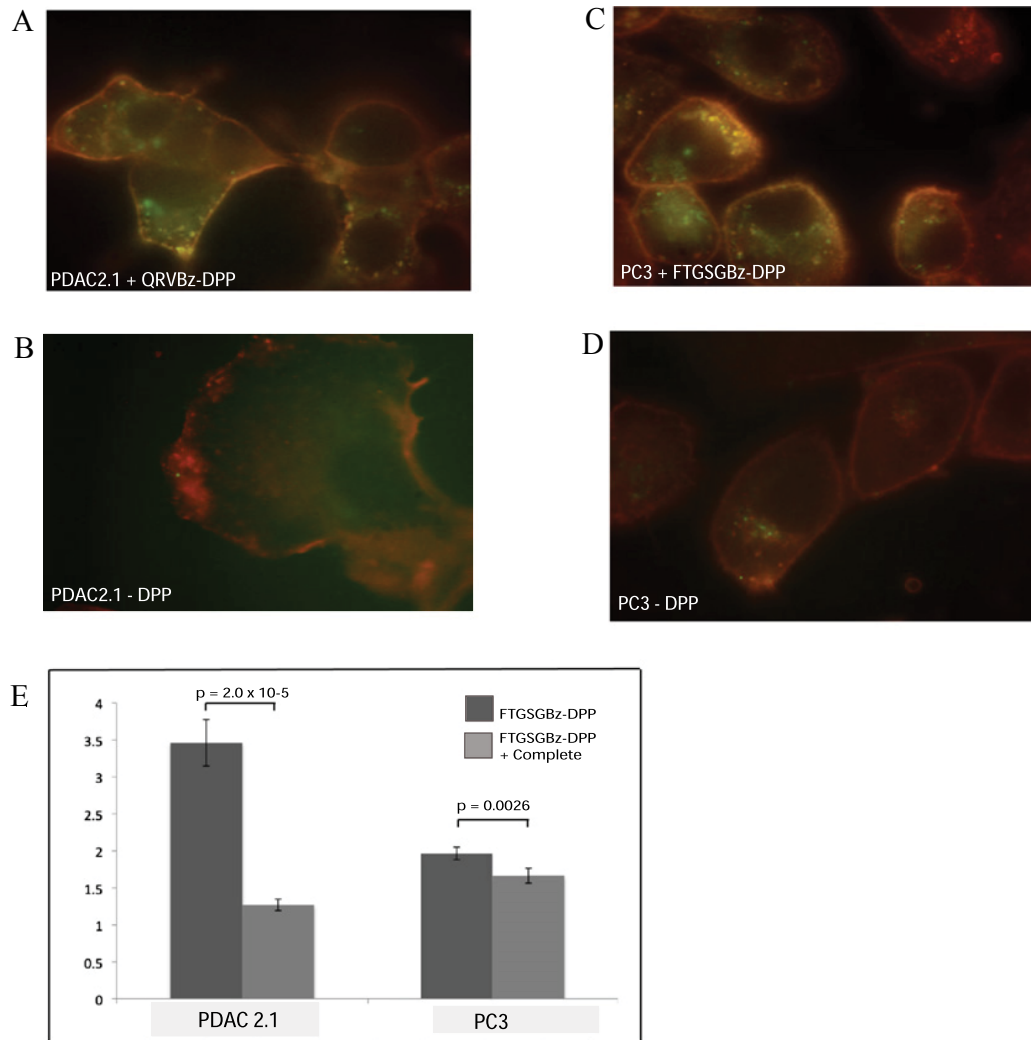
D: Thrombin surface (tan) overlaid onto MT-SP1 (light blue) and uPA (pink). uPA His99 (yellow) occupies prime-side pocket similarly as MT-SP1 Phe99 (blue). Thrombin Leu99 purple, catalytic triad cyan.

Table 3 - 3. Data Collection and Refinement Statistics

Structure	MT-SPI-covalent adduct
PDB ID	3NCL
Data set	ALS290709
Data statistics	
Wavelength	1.11587 Å
Space group	C2
Cell dimensions	a = 79.9 Å
	b = 80.2 Å
	c = 40.5 Å
	b = 95.8 °
Resolution (last shell)	54.6–1.19 Å ° (1.25–1.19 Å °)
Unique reflections	58,355 (1597)
Redundancy	6.7 (3.8)
Completeness	76.4% (14.5%)
Mean I/s (I)	21.0 (5.0)
R _{sym}	6.5% (15.0%)
Refinement statistics	
Resolution range	54.6–1.19 Å
Reflections used word (test)	56,653 (1530)
R _{free} /R _{fac}	20.3%/19.4%
Overall figure of merit	0.915
Overall B _{wilson}	12.7Å ²
Protein atoms	1900, 21.8 Å ²
Ligand atoms	21, 34.8 Å ²
Solvent atoms	221, 38.9 Å ²
Rmsd bonds	0.016 Å
Rmsd angles	1.010°
Ramachandran analysis	
Residues in preferred regions	96.4%
Residues in allowed regions	3.6%
Outliers	0%

Rmsd = root-mean-square deviation.

Figure 3-3: Cell surface labeling of active serine proteases.



PDAC2.1 and PC3 cells were imaged in the presence (3A, 3C) or absence (3B, 3D) of ABP. Cell membranes were stained with tetramethylrhodamine-conjugated wheat germ agglutinin (red), and labeled proteases were stained with streptavidin-AlexaFluor 488 (green). Colocalization of labeled proteases with membrane is seen at the cell surface and in discrete puncta, but only in the presence of ABP. Flow cytometry was used to quantify labeled streptavidin on the surface of cells (panel E). Averaged mean fluorescence intensity values are plotted normalized to background staining of labeled streptavidin in the absence of ABP. P-values correspond to a two-sample T-test, and error bars correspond to the addition of the Relative Standard Error values for the two averages multiplied by the normalized mean of each sample.

Supplementary Table S3-1: Phosphonate probe degradation

compound	$t_{1/2}$ (hours)	% remaining after 20 hours
QRGBz-DPP (1)	64	78
LTPBz-DPP (2)	17	91
GSGBz-DPP (3)	241	100
EPIBz-DPP (4)	34	71

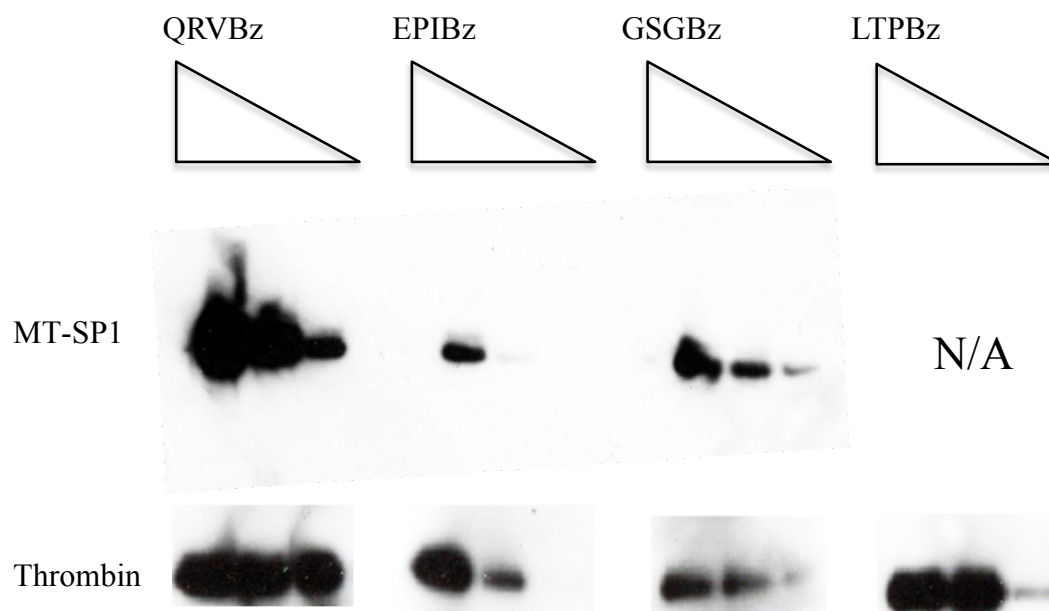
Measurement of phosphonate probe stability by LC-MS over 100 hours in aqueous buffer.

Supplementary Table S3-2: Kinetic parameters of MT-SP1 and thrombin substrates

Enzyme	Compound	Substrate	m/z (expected)	K_M (μ M)	V_M (μ M/s)	K_{cat} (1/s)	K_{cat}/K_M (1/ M_s)
MTSP1	13	Ac-QRVR-ACC	800.3 (801.42)	585 \pm 25.4	14.1 \pm 0.06	1.9 \pm 0.008	3340 \pm 131
	14	Ac-LTPR-ACC	728.3 (729.38)	152.2 \pm 9	3.6 \pm 0.08	0.99 \pm 0.023	6568 \pm 239
	15	Ac-GSGR-ACC	618.2 (619.27)	18.4 \pm 13.8	0.23 \pm 0.11	0.032 \pm 0.015	2016 \pm 682
	16	Ac-EPIR-ACC	756.3 (757.38)	326.3 \pm 102.8	1.1 \pm 0.11	0.15 \pm 0.015	482 \pm 104
thrombin	13	Ac-QRVR-ACC		306 \pm 14.1	5.16 \pm 0.1	7.1 \pm 0.14	23338 \pm 631
	14	Ac-LTPR-ACC		23.5 \pm 2.9	1.24 \pm 0.13	34.3 \pm 3.5	1462545 \pm 30496
	15	Ac-GSGR-ACC		ND	ND	ND	ND
	16	Ac-EPIR-ACC		ND	ND	ND	ND

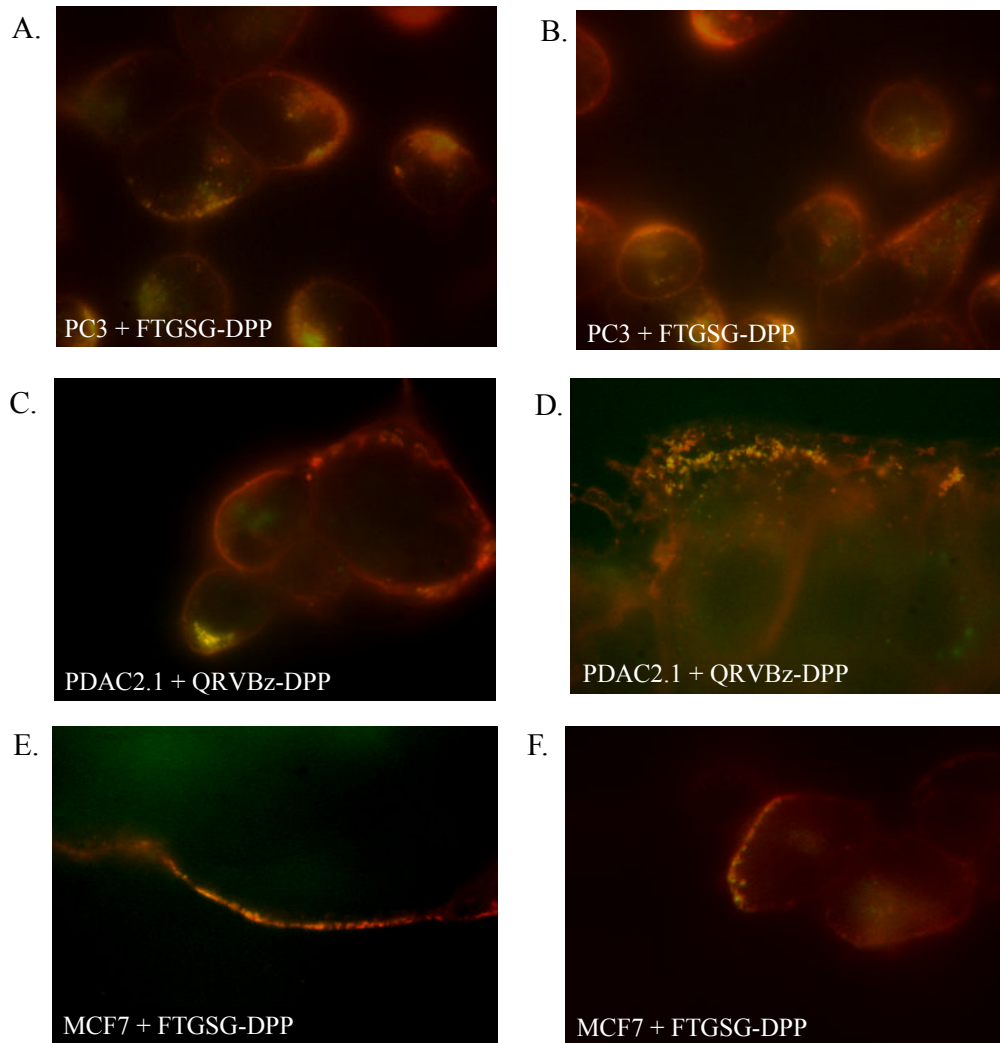
Kinetics of 4 substrates against MT-SP1 and thrombin. Each substrate was serially diluted and the reaction initiated by addition of enzyme. Velocity values were fit to the Michaelis-Menten equation to determine K_M , V_M , and k_{cat} . ND= no observable cleavage.

Supplementary Figure S3-1: Dose-dependent labeling by peptide phosphonates



Enzyme was combined with varying concentrations of phosphonate inhibitor (3mM-30uM) at room temperature overnight. The reaction was stopped by the addition of SDS loading buffer and boiling for 10 minutes.

Supplementary Figure S3-2. Additional images of cell surface labeling of active serine proteases



PC3 cells (panels A and B) show localized cell surface labeling and internalization at one end of cells. PDAC2.1 cells show internalization of labeled cell surface proteases (panel C) and further labeling at the leading edge of cells (panel D). MCF7 cells (panels E and F) show marked internalization at the leading edge of cells. Red = membrane, green = streptavidin.

Chapter 4

Identification and biochemical characterization of active proteases in bacteria

Tuberculosis is a devastating disease that infects approximately 2 billion people globally. Proteases, which can make excellent drug targets, make up 4% of the *Mycobacterium tuberculosis* (*Mtb*) genome, and of those, serine protease comprise 75%. In order to learn new information about the proteases that may regulate essential process in *Mtb*, a two pronged approach was taken: first, a chemical biology and mass-spectrometry based approach to identify all active proteases, and second, a candidate-based approach to examine the activity of proteases known to impact bacterial biology. In the first method, protease activity-based probes were developed to identify active proteases in *Mycobacterium bovis*- *bacillus Calmette-Guérin* (BCG) and *E. coli*. In parallel, the biochemistry and enzymology of ClpXP, the mycobacterial proteasome, and MycP1 were investigated. This chapter details the challenges and insights into the use of chemical biology to study bacterial proteases.

Introduction:

Mycobacterium tuberculosis (*Mtb*), the causative agent of tuberculosis, infects approximately 2 billion people worldwide, killing up to 2 million people a year (WHO | Global tuberculosis control - surveillance, planning, financing). Upon inhalation, *Mtb* infects alveolar macrophages, where the bacteria grow very slowly. *M. tuberculosis* can survive inside macrophages because it secretes proteins that allow it to evade or modulate immune response (Hsu et al., 2003), (Stanley et al., 2003). One system, the ESX-1 secretion system, is known to deliver virulence factors during infection of host cells, thus secretion makes an excellent target for therapeutic intervention in the *Mtb* life cycle (Abdallah et al., 2007). 90% of infected individuals do not develop active tuberculosis, instead, the bacteria enter a dormant state from which they can reemerge decades later. This nonreplicative persistent (NRP) state is characterized by lack of DNA replication,

decreased metabolic activity, and resistance to many antibiotics (Wayne and Sohaskey, 2001). Targeting this persistent state will be crucial to eradicating tuberculosis, therefore understanding how these bacteria enter, maintain, and exit from NRP will provide information about how to control this disease.

Proteases, enzymes that hydrolytically cleave proteins, regulate essential cellular processes in all forms of life, from viruses to humans. These enzymes generally compose 2-3% of an organism's genome, underscoring their biological importance. Proteolytic events are irreversible and therefore can represent decision-making points in biology, a property that makes proteases excellent drug targets. Proteases have been implicated in infectivity and virulence in many bacteria, such as in bacterial secretion of virulence factors, and transcriptional regulation of life cycle progression (Gottesman, 2003).

A search of MEROPS, a protease database (Rawlings et al., 2010), by species reveals that serine proteases are the most abundant class in Mtb (Figure 1-2), and they presumably play an important role in Mtb biology. This is supported by the fact that serine proteases in both Mtb and other bacteria have been implicated in a variety of essential pathways. For example, serine proteases play two major roles in bacteria: homeostatic maintenance by removing unfolded or misfolded proteins, and regulation, which may occur by cleaving transcription factors based on environmental cues (Gottesman, 2003). Since both homeostatic maintenance (the protein turnover necessary for this change), and transcriptional regulation are involved in NRP, proteases may play a regulatory role in entry, maintenance, and exit from NRP.

A two-pronged approach was taken to study the role of proteases in Mtb biology, both globally and individually. The first approach used chemical biology and biochemistry to obtain a broad "snapshot" of all active proteases in multiple states, including logarithmic growth, NRP, and during secretion. The second approach used biochemistry and enzymology to focus on candidate proteases involved in transcriptional regulation or secretion.

In order to label active serine proteases, peptide phosphonate activity based probes were used. Serine proteases form an acyl-enzyme intermediate that is covalently linked to the N-terminal fragment of the substrate. Phosphonates act as transition state inhibitors of serine hydrolases by forming a very stable bond between the serine nucleophile and the phosphonate (Powers et al., 2002). Protease activity based probes, which can measure enzyme activity in cells, consist of a reactive functional group that covalently interacts with the catalytic residue of the protease (Kidd et al., 2001). The probe mimics a peptide substrate whose amino acid composition can be tailored to the specificity of the protease (Figure 1-4). The probe also contains a linker region and a detection tag, such as biotin. These inhibitors can be made specific or general by varying the peptide side chains, as well as varying the phosphonate leaving groups. Because phosphonate inhibitors only label the active protease, this method allows detection of the functional form of the enzyme. A series of biotinylated inhibitors with varying peptide sequences were synthesized in order to bind to a wide range of serine proteases. To identify active serine proteases, these probes were added to lysates of BCG or *E.coli*, with the goal of comparing profiles of bacteria grown in different conditions. Proteins covalently attached to the probes were purified using streptavidin resins and identified by mass spectroscopy.

In the candidate-based approach, the proteases ClpXP, the mycobacterial proteasome, and MycP1 were examined. ClpP is a highly conserved ATP-dependent bacterial serine protease (Porankiewicz et al., 1999). ClpP is shaped like a barrel composed of two seven-membered rings, and proteolysis occurs inside this chamber. ClpP alone is inactive and requires binding to a class of AAA+ ATPase chaperone proteins (ClpA or ClpX in *E.coli*, homologs ClpC and ClpX found in *Mtb*). These ATPases confer specificity, which can occur by recognition of a specific degradation tag on proteins targeted for destruction. These chaperones then unfold the substrates in an ATP-dependent manner and thread substrates into ClpP for hydrolysis. ClpP functions as a housekeeping enzyme by removing misfolded proteins from the cell, but it also has been shown to play regulatory roles in many bacteria. ClpP controls sporulation pathways in *B. subtilis*, and regulates expression of virulence factors in *Y. enterocolitica* (Gottesman, 1996). The diverse roles of ClpP in other species imply that it may play a significant, and as yet uncharacterized,

regulatory role in Mtb. Organisms lacking the protease Lon have been found to possess more copies of ClpP, and this is true in Mtb, which has two homologs of ClpP. This may imply that ClpP is the major protease in Mtb, and therefore ClpP may play an important role in the entry and exit from bacterial NRP. Going into and out of a persistent state may require a drastic change in the proteome of the bacteria, and maintaining that state may require transcriptional repression of unnecessary proteins. ClpP may contribute to this protein turnover, as well as maintenance of NRP. To better understand the activity of ClpXP, both ClpX and ClpP were recombinantly expressed and purified, then assayed for activity.

The recently discovered mycobacterial proteasome offers a new potential drug target against Mtb (Lin et al., 2006). The proteasome is an essential gene, and another barrel-shaped, multi-subunit, gated protease. Drugs targeting the human proteasome, like bortezomib, have proven effective in cancer treatment (Moore et al., 2008), so it may follow that the mycobacterial proteasome is similarly drugable. Targeting the mycobacterial proteasome specifically, without also inhibiting the human proteasome, could result in a very safe and effective treatment for tuberculosis. To determine the substrate specificity of the mycobacterial proteasome, the enzyme was profiled against a library of amino acids representing the P1-P4 substrate positions. This assay was repeated with the human proteasome, and substrates that exploited differences between the two enzymes were synthesized and tested. A similar approach was also attempted with the malarial proteasome.

The third protease examined, MycP1, is a component of the ESX-1 secretion system and is responsible for regulating the delivery of certain virulence factors (Ohol et al., 2010). This regulatory ability makes MycP1 a promising drug target in *M. tuberculosis*. Both the presence and the activity of MycP1 are essential for successful ESX-1 secretion. MycP1 can both negatively and positively regulate secretion, a rare phenotype for a single protein. Genetic experiments have shown ESX-1 secretion is abolished in the absence of MycP1, indicating a chaperone-like function in the formation of the ESX-1 complex. Knocking out MycP1 from *M. tuberculosis* has been shown to decrease bacterial counts

in mice and increase survival. A drug that could interfere with the interaction of MycP1 with the other secretion components could prevent ESX-1 secretion, which could in turn attenuate virulence.

In addition to its chaperone-like role, MycP1 protease activity is also involved in ESX-1 secretion. Normal MycP1 activity leads to a downregulation of secretion through substrate cleavage. Inactivation of the MycP1 through mutating the catalytic residues leads to oversecretion. Some virulence factors, such as the ESX-1 substrate ESAT-6, are highly immunogenic. Therefore, oversecretion of virulence factors can lead to activation of the immune system against *M. tuberculosis*. This activation has been observed in macrophages, where protease-dead MycP1 mutants of *M. tuberculosis* elicit greater cytosolic signaling than wild type. These mutant bacteria also result in greater survival in mice over wild type. By altering the tight control of ESX-1 secretion, drugs that interact with MycP1 could significantly reduce *M. tuberculosis* infection.

Many questions remain about the relationship of MycP1 activity to its function. The timing of the activity and the interactions between the enzyme and the rest of the ESX-1 machinery are of particular interest. To answer these questions, peptide phosphonate activity based probes targeting MycP1 were synthesized and tested for potency. These probes could be used to assess when and where active MycP1 is located, as well to purify intact MycP1-ESX-1 complexes in their active state.

Results:

Purification and identification of active proteases from bacterial lysates

To identify proteases that govern the transition between growth states, a protocol to label, purify, and identify active proteases was developed. Bacteria were grown into log-phase, then lysed in the presence of protease inhibitors, excluding serine proteases. Bacteria have a large number of biotinylated proteins, and the presence of these proteins interfered with analysis of biotinylated active proteases in early experiments. This problem was addressed by pre-clearing the lysates with avidin beads after lysis, which reduced the

background significantly. The activity based probe was added to the cleared lysates and incubated at 4°C overnight. A wide range of probes was tested to account for differing protease specificities. To cast the broadest net, a probe with no peptide was initially used. To account for different protease specificities, a series of probes with differing P1 residues were tested, including P1 Benzamidine, P1 Alanine, P1 Norleucine, and P1 Phenylalanine. However, subsequent work presented in Chapter 3 demonstrated that a peptide element was needed for potency, so later experiments utilized a longer, more stable probe (GSGBz phosphonate). Labeling was assessed by performing Western blotting using avidin-HRP. Successful labeling was observed in BCG (Figure 4-1), as well as in *E. coli*.

However, enriching for these labeled proteins using the biotin-avidin interaction proved problematic. As discussed in previous chapters, the slow kinetics of the phosphonate ABP require long incubations at high concentrations, complicated the pulldowns. While several probe removal methods were successful when using recombinant proteins (Figure 4-2), only size exclusion columns using PD-10 desalting columns were useful in bacterial lysates. These modifications enabled successful enrichment of proteases in *E. coli* (Figure 4-3). In anticipation of modeling normal vs. NRP growth in mycobacterial, *E. coli* in log and stationary phase were compared, and recombinant ClpP was added as a positive control. However, mass spectrometry revealed very few proteases that were unique to the samples containing the probe, and the positive control was not found in many instances (Table 4-1). Additional optimization into the mass spectrometry section of the protocol will be necessary.

To capitalize on the robust labeling observed with these probes, *E. coli* strains that either contained His-tagged copies of a single protease or a knockout of a single protease (generous gifts from the lab of Dr. Carol Gross) were utilized. Expression of the His-tagged proteases worked well (Figure 4-4), but labeling was not effective, and labeling was inconclusive in the knockout strains. Labeling of nickel-purified proteases was successful. However, pulldowns with these strains was similarly unproductive. Future

work comparing the activity and phenotype of these strains under different growth conditions may enable new insights into the role of proteases during adaptive changes.

Expression, purification, and activity of Mtb ClpXP

ClpXP is an important and well-characterized protease in *E. coli* and other bacteria, and it is likely to play a role in Mtb as well. However, this mycobacterial enzyme has not been biochemically examined. To determine the activity and substrate specificity of this enzyme, the Mtb ClpX, ClpP1, and ClpP2 proteins were expressed and purified in *E. coli*. All constructs were His-tagged and purified using Ni-NTA beads. Expression of each protein was successful (Figure 4-5), with N-terminal tagged constructs expressing in higher yields than C-terminal tagged constructs. Activity was assessed using a canonical ClpXP substrate from *E. coli*, LY-AMC. As shown in Figure 4-6, ClpXP was only minimally active, though it was successfully labeled by phosphonate ABPs. Attempts to improve activity through varying buffer conditions were unsuccessful. As the activity seen in these experiments was not enough to conduct substrate profiling or enzyme kinetics, this project was not taken further.

Substrate profiling of the mycobacterial proteasome

The mycobacterial proteasome has potential as a therapeutic target if a drug could distinguish between the mycobacterial and human enzymes. This work was carried out in collaboration with the lab of Dr. Carl Nathan. To assess the difference between the two enzymes, both proteases were screened using the positional scanning synthetic combinatorial libraries developed in the Craik lab. These libraries consist of pools of peptides in which one position in the P1-P4 positions is randomized. As shown in Figure 4-7, both enzymes had fairly broad specificities, which is characteristic of a proteasome. However, there were slight differences at each position, and 8 substrates were synthesized to capitalize on these differences. The K_M of each substrate was measured for the mycobacterial enzyme (Table 4-2). Most of the substrates were not cleaved particularly efficiently, but the best inhibitor, VRRQ, could be used to generate a potentially selective inhibitor. The malarial proteasome was also screened using this

library in collaboration with Dr. Matt Bogyo's lab. The enzyme was minimally active, and only a P1 profile could be obtained (Figure 4-8). Due to the noise present with such an inactive enzyme, more sensitive mass spectrometry profiling techniques will be used for future studies.

Synthesis of a MycP1 activity-based probe

MycP1 activity is important for mycobacterial secretion, however, the exact function of the activity is unclear. To gain a better understanding of the temporal, function, and structural roles played by MycP1, an activity based probe targeting this enzyme was synthesized. Previous work showed that Gly-Pro was a substrate for MycP1, and attaching this sequence to a phosphonate resulted in an effective inhibitor (Ohol et al., 2010). An activity-based probe was synthesized based on this inhibitor, and tested for inhibitory labeling ability. As shown in Figure 4-9, the probe labeled MycP1, but it also labeled the inactive form. Additionally, some inhibition was observed. Based on the work in Chapter 3, a longer inhibitor may prove more potent against MycP1, and a probe based on the putative cleavage site of the substrate EspB (ALAP) was synthesized. Additional work is needed to determine its potency.

Conclusions and Future directions

The ability to identify proteases in two biologically distinct states would be a powerful new tool in studying bacterial transitions. In particular, discovering the proteases that play a part in the regulation of NRP could have a profound impact on the ability to understand and treat tuberculosis. However, the enrichment and mass spectrometry remain significant hurdles to this goal. The use of releasable probes may improve this methodology. Once optimized, this technique could be used to identify proteases in any system.

The MycP1 probes could allow a better insight into how MycP1 activity affects secretion. The probe could be added at different times during the induction of secretion or during macrophage infection, thus obtaining a timeline of MycP1 activity. Pulling down MycP1 interactors by taking advantage of the biotin tag could identify new components of the ESX-1 machinery. Additionally, the imaging and flow cytometry techniques developed in cancer cells could be tested in mycobacteria to gain new information about the localization of active MycP1. The thick cell wall of mycobacteria may hamper binding, however, these techniques could be used in fixed cells as well. In summary, the use of activity based probes holds great promise for studying transitions in bacteria.

References

- Abdallah, A. M., Gey van Pittius, N. C., Champion, P. A. D., Cox, J., Luirink, J., Vandenbroucke-Grauls, C. M. J. E., Appelmek, B. J., and Bitter, W. (2007). Type VII secretion--mycobacteria show the way. *Nat. Rev. Microbiol* 5, 883-891.
- Gottesman, S. (1996). Proteases and their targets in *Escherichia coli*. *Annu. Rev. Genet* 30, 465-506.
- Gottesman, S. (2003). Proteolysis in bacterial regulatory circuits. *Annu. Rev. Cell Dev. Biol* 19, 565-587.
- Hsu, T., Hingley-Wilson, S. M., Chen, B., Chen, M., Dai, A. Z., Morin, P. M., Marks, C. B., Padiyar, J., Goulding, C., Gingery, M., et al. (2003). The primary mechanism of attenuation of *Bacillus Calmette-Guérin* is a loss of secreted lytic function required for invasion of lung interstitial tissue. *Proc Natl Acad Sci U S A* 100, 12420-12425.
- Kidd, D., Liu, Y., and Cravatt, B. F. (2001). Profiling serine hydrolase activities in complex proteomes. *Biochemistry* 40, 4005-4015.
- Lin, G., Hu, G., Tsu, C., Kunes, Y. Z., Li, H., Dick, L., Parsons, T., Li, P., Chen, Z., Zwickl, P., et al. (2006). *Mycobacterium tuberculosis* *prcBA* genes encode a gated proteasome with broad oligopeptide specificity. *Molecular Microbiology* 59, 1405-1416.
- Moore, B. S., Eustáquio, A. S., and McGlinchey, R. P. (2008). Advances in and applications of proteasome inhibitors. *Current Opinion in Chemical Biology* 12, 434-440.
- Ohol, Y. M., Goetz, D. H., Chan, K., Shiloh, M. U., Craik, C. S., and Cox, J. S. (2010). *Mycobacterium tuberculosis* MycP1 protease plays a dual role in regulation of ESX-1 secretion and virulence. *Cell Host Microbe* 7, 210-220.
- Porankiewicz, J., Wang, J., and Clarke, A. K. (1999). New insights into the ATP-dependent Clp protease: *Escherichia coli* and beyond. *Mol. Microbiol* 32, 449-458.

Powers, J. C., Asgian, J. L., Ekici, O. D., and James, K. E. (2002). Irreversible inhibitors of serine, cysteine, and threonine proteases. *Chem. Rev* *102*, 4639-4750.

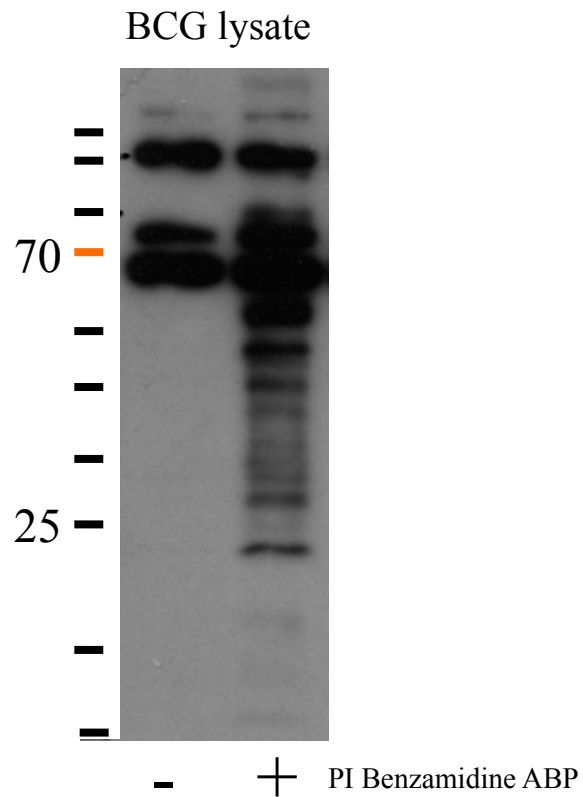
Rawlings, N. D., Barrett, A. J., and Bateman, A. (2010). MEROPS: the peptidase database. *Nucleic Acids Res* *38*, D227-233.

Stanley, S. A., Raghavan, S., Hwang, W. W., and Cox, J. S. (2003). Acute infection and macrophage subversion by *Mycobacterium tuberculosis* require a specialized secretion system. *Proc Natl Acad Sci U S A* *100*, 13001-13006.

WHO | Global tuberculosis control - surveillance, planning, financing Available at: http://www.who.int/tb/publications/global_report/2007/en/index.html [Accessed July 25, 2011].

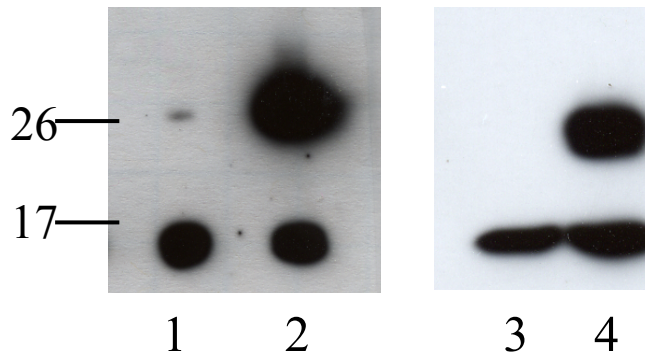
Wayne, L. G., and Sohaskey, C. D. (2001). Nonreplicating persistence of *mycobacterium tuberculosis*. *Annu. Rev. Microbiol* *55*, 139-163.

Figure 4-1: Labeling active proteases in BCG



BCG lysates were pre-cleared of biotinylated proteins with avidin beads. Lysates were then incubated with PI-benzamidine phosphonate or a control. Labeled proteases were visualized by avidin blot.

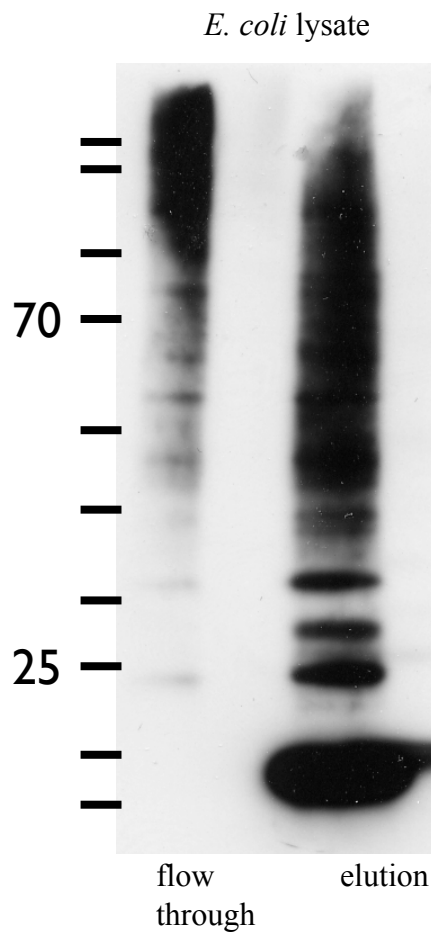
Figure 4-2: Excess probe removal methods



- 1: Desalting spin column
- 2: Dilution/concentration
- 3: Dialysis
- 4: TCA precipitation

Recombinant elastase was incubated with P1 Alanine phosphonate. Excess probe was removed using various methods, then pulled down using streptavidin beads and visualized by avidin blot.

Figure 4-3: Pulldown in *E. coli*

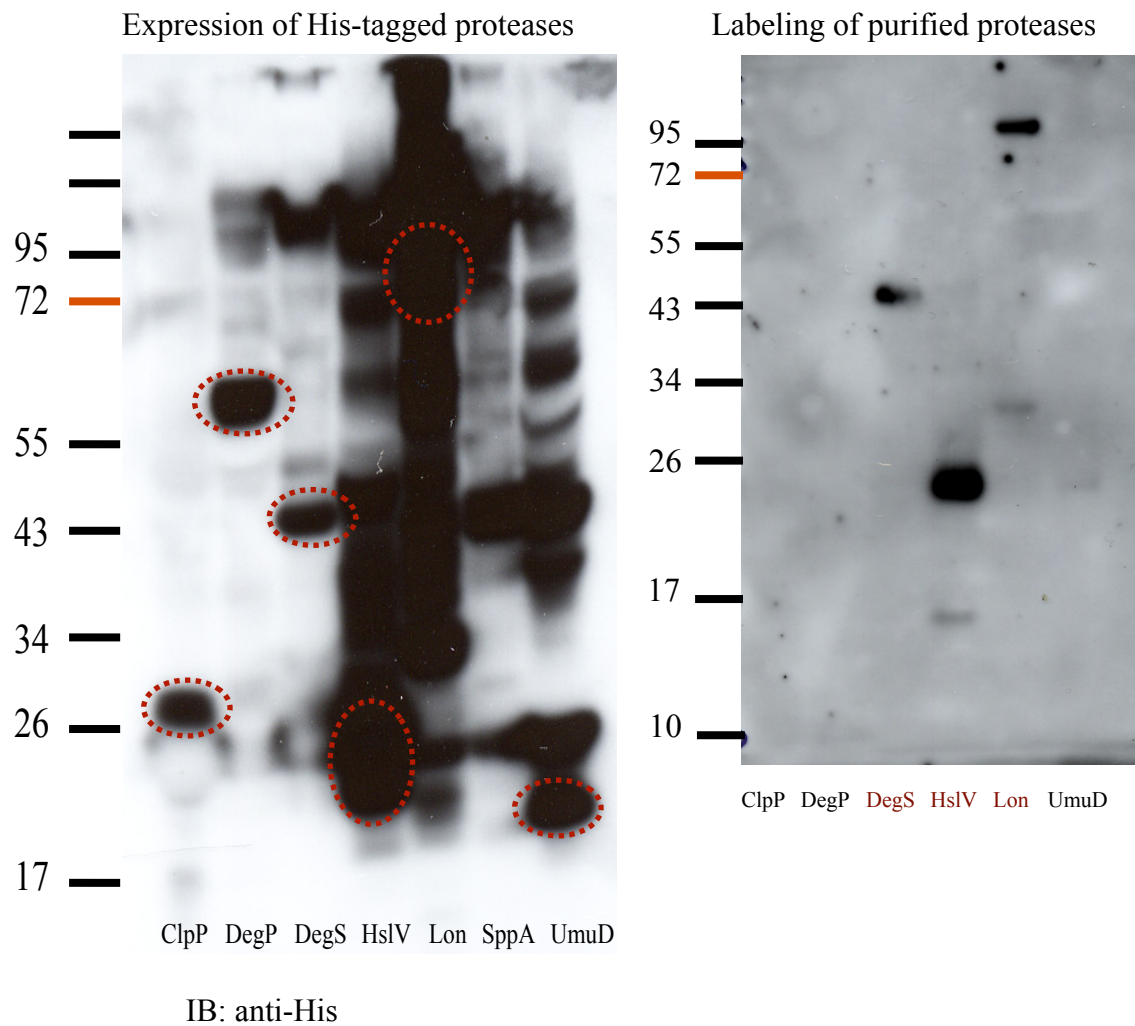


E. coli lysates were labeled with P1-Bz phosphonate and enriched for active proteases using the optimized protocol. Enriched proteases were eluted by boiling and visualized by avidin blot.

Table 4-1: Summary of proteins identified by mass spectrometry

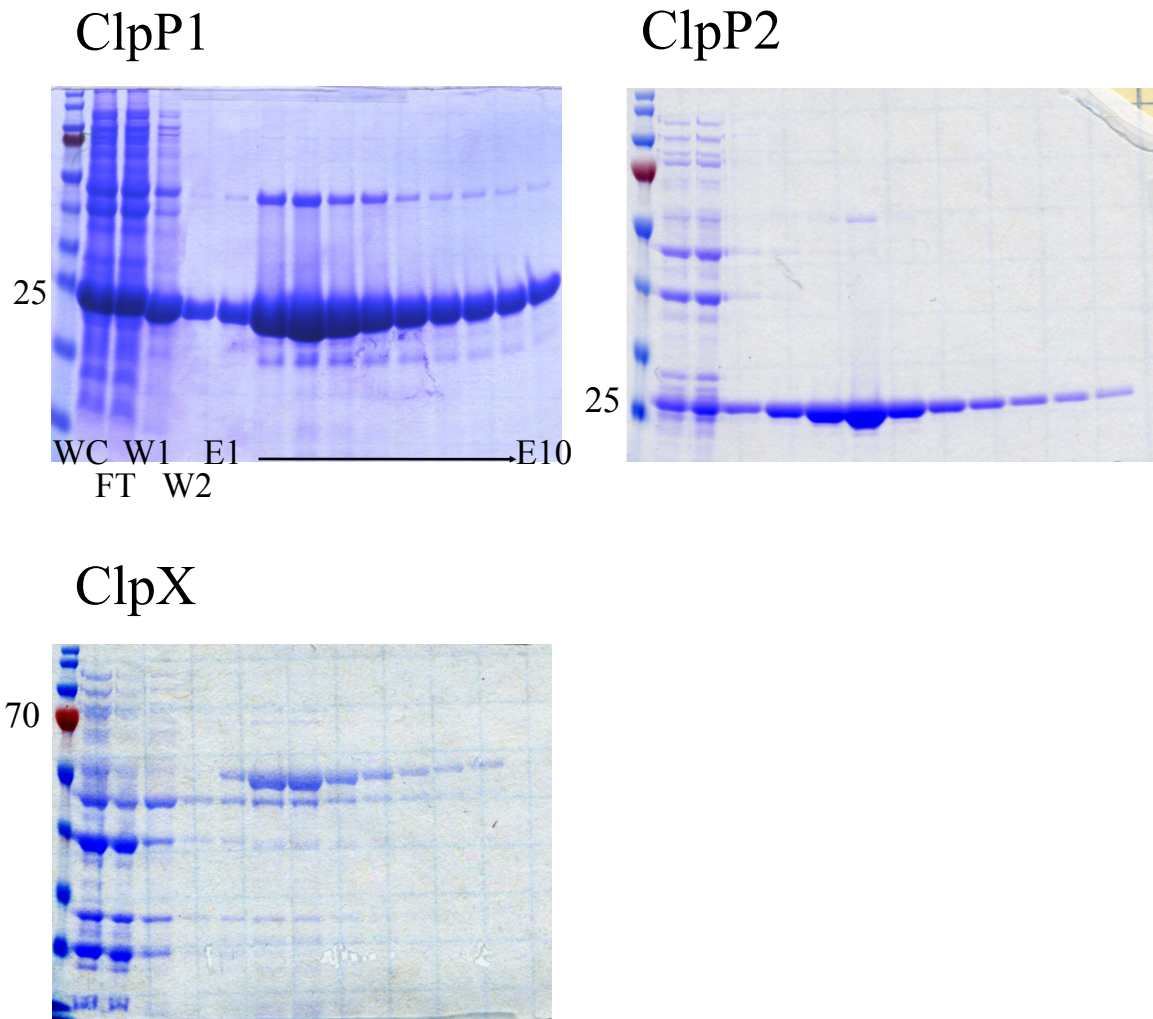
	E.coli -	E.coli +	E.coli log -	E.coli log +	E.coli stationary -	E.coli stationary +	BCG -	BCG +
# proteins identified	58	90	152	104	109	127	54	33
# unique	17	49	~50			~20	~20	
# proteases	3 FtsH, HslU, ClpX	5 FtsH, HslU, ClpA, DegP, ClpX	5 HslU, FtsH, ClpX, Peptidase B, ClpA	4 HslU, FtsH, ClpX, ClpA	2 HslU, Xaa- Pro dipeptidase	2 HslU, ClpX	4 FtsH, ClpP1, ClpX, ClpP1	3 ClpP1, ClpX, ClpP2
# unique		2	1				1	
ClpP controls?	no	yes	yes	yes	yes	yes		

Figure 4-4 Expression and labeling of His tagged proteases in *E. coli*



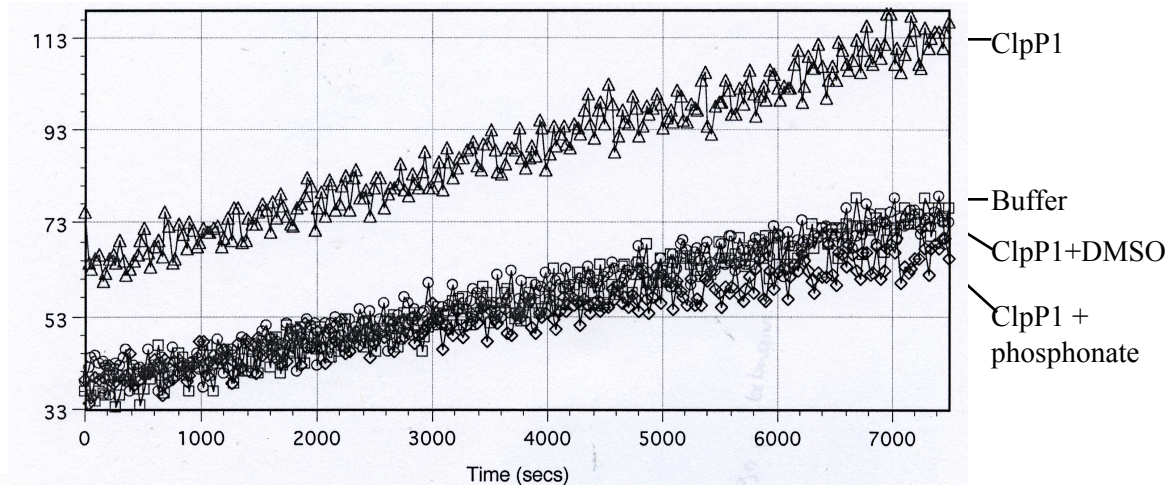
E. coli strains containing His-tagged proteases were induced with IPTG and expression was confirmed by Western blot with an anti-His antibody. Proteases were purified using nickel beads, and purified proteases were labeled with P1-Alanine phosphonate.

Figure 4-5 Expression and purification of ClpP1, ClpP2, and ClpX



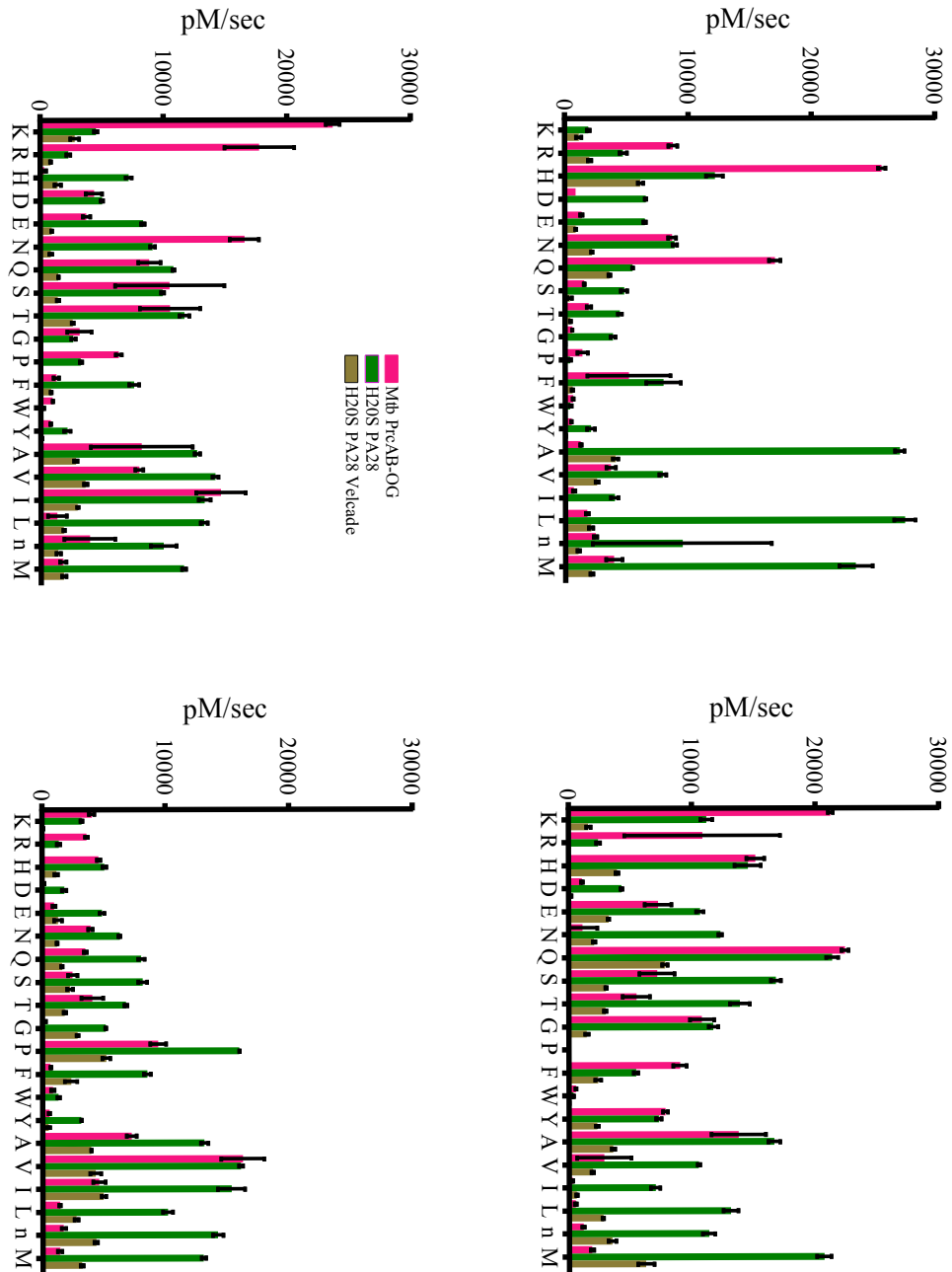
Each His-tagged construct was expressed in *E. coli* and purified using nickel beads followed by a MonoQ column.

Figure 4-6: ClpP1 activity and inhibition



Purified ClpP1 (22 μ g) was combined with suc-LY-AMC. Addition of a phosphonate probe with no peptide decreased activity.

Figure 4-7: Substrate profiles of the Mtb proteasome, human proteasome, and human + velcade



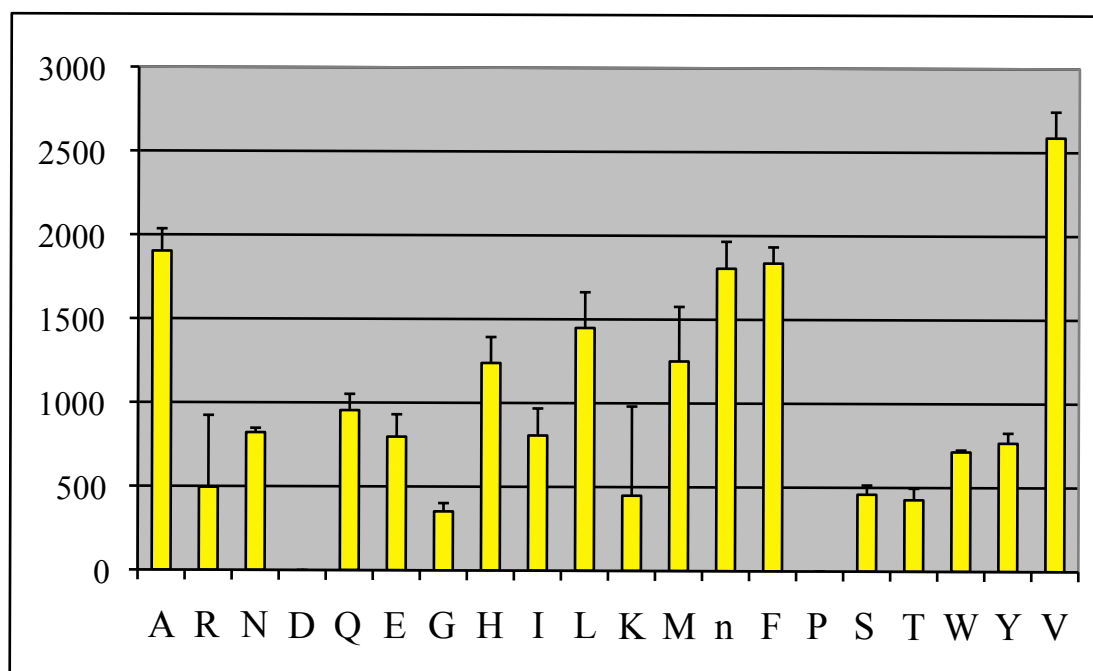
The human and mycobacterial proteasome were profiled against a complete diverse substrate library to determine the P1-P4 amino acid preference. For comparison, the human proteasome was also tested in the presence of velcade, a proteasome inhibitor

Table 4-2: Substrate cleavage by the Mtb proteasome

Substrate	K _m (μM)	K _{cat} /K _m (1/Ms)
VRRQ	2	1.98E+06
VK _F H	351	2.96E+04
VN _K Q	48	2.85E+04
VK _A H	276.4	6.49E+03
VK _A Q	654	1.23E+03
VK _Q H	188.5	7.26E+03
VR _Q H	44	8.11E+04
VR _Q Q	174	6.12E+03
VK _Q Q	21	1.30E+05

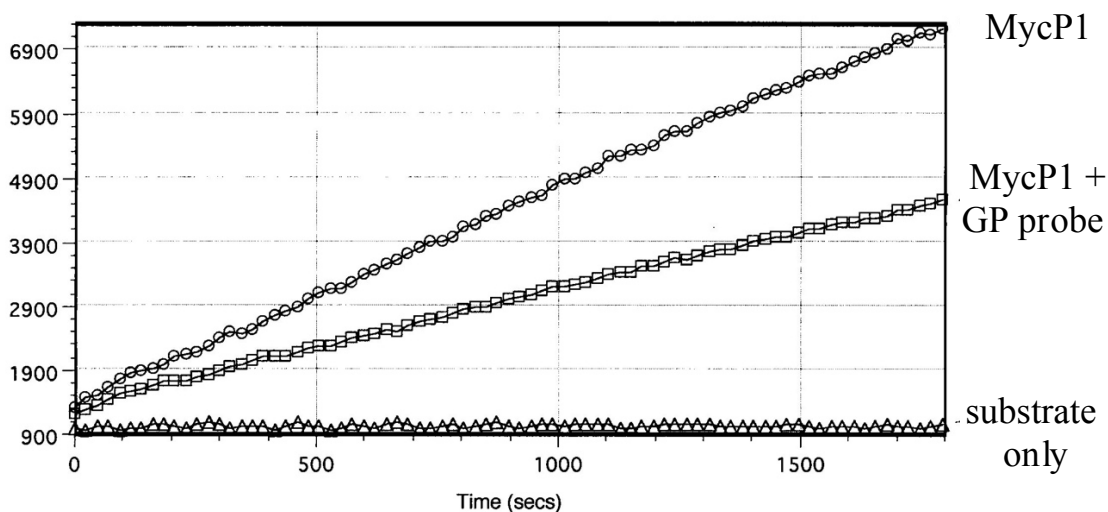
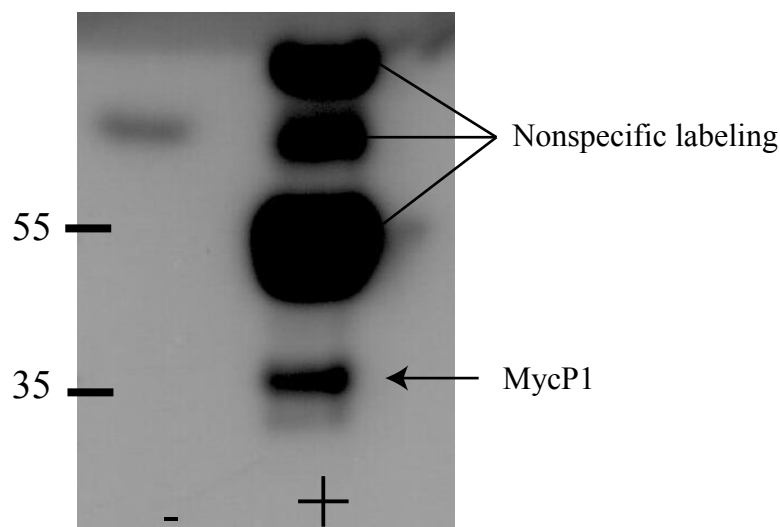
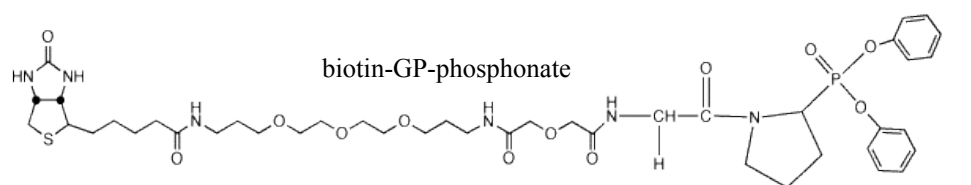
Peptides were attached to a resin linked to ACC using the Quartet peptide synthesizer the purified by HPLC. Kinetic values were tested against the Mtb proteasome.

Figure 4-8: P1 profile of the Pf proteasome



The *Plasmodium falciparum* proteasome was profiled against the P1 complete diverse library. Due to the slow kinetics of the enzyme and long lag times observed, the final 600 sections of the 1800 second assay were used to determine the activity of each amino acid at the P1 position.

Figure 4-9: Labeling and inhibition of MycP1 by biotin-GP-phosphonate



Purified MycP1 was combined with biotin-GP-phosphonate and tested for labeling by avidin blot and inhibition by the addition of GP-AMC.

Conclusions and Future Directions

In this thesis, the role of protease inhibitors was explored in a cancer biology and a chemical biology setting. Dysregulation of the normal roles of macromolecular protease inhibitors can lead to dramatic, cancer-promoting changes in cells. However, using chemical biology, the use of small molecule protease inhibitors can be successfully functionalized and used to study proteolytically driven processes like cancer metastasis more effectively. By gaining a better understanding of protease inhibitors, important biological pathways can be elucidated, giving rise to potential future therapies for afflictions as wide ranging as cancer and infectious diseases.

PI-9 and prostate cancer treatment

In exploring the role of protease inhibitor PI-9 in prostate cancer, it was found that PI-9 is a key contributor to evading immunosurveillance. PI-9 was present in aggressive prostate cancer cells lines and was capable of inhibiting Granzyme B in those cell lines. This ability of PI-9 to block Granzyme B reduced apoptosis induced by Natural Killer cells, indicating that cells that contain PI-9 are resistant to immunosurveillance. When examining human prostate tissue, PI-9 levels were found to be generally dysregulated in tumors, but consistently upregulated in high grade prostatic neoplasia (HGPIN), an early, benign form of prostate cancer, and upregulated in inflammatory and atrophied cells, conditions that are strongly associated with the development of prostate cancer. This data implies that PI-9 is needed early in the progression of prostate cancer to protect cells from the apoptotic response. Later in cancer progression, protective mechanisms such as the shedding of MIC, a receptor found on the surface of cancer cells that binds NK cells and activates granule exocytosis, develop, allowing the cells to evade recognition by immune cells. Importantly, since PI-9 is induced in response to inflammation, PI-9 upregulation may be the link in prostate cancer progression between pre-cancerous inflammation and prostate tumors.

The protective role of PI-9 has important implications for the diagnosis and treatment of prostate cancer. There are currently a battery of prostate cancer treatments that range

from watchful waiting to therapies with extreme side effects such as chemotherapy and chemical castration (Heidenreich et al., 2008). These treatments are often employed sequentially, causing the patient to endure side effects from many treatments over time. The level of the prostate-specific antigen (PSA) is currently the most widely used diagnostic for prostate cancer, however, this test has come under scrutiny and may not be an effective or accurate indication of prostate cancer severity (Croswell et al., 2011). Better diagnostic information on the severity and aggressiveness of the prostate tumor, as well as better prognostic markers to guide doctors to the most successful treatment would benefit the entire field. Preliminary data implied that PI-9 could be used as a diagnostic biomarker to distinguish between low and high grade prostate tumors. However, a more comprehensive analysis showed that PI-9 can be dysregulated in both types of tumors. Additionally, PI-9 is located inside the cell, so invasive biopsies would be necessary to examine PI-9 levels.

Alternatively, PI-9 may be useful as a prognostic marker to guide treatment. Immunotherapy, activating the body's own immune cells to target tumors, has emerged as a promising new treatment in several types of cancer. This approach was recently approved as a "vaccine" to treat prostate cancer (Small et al., 2006). The presence of PI-9, which allows the tumor to block the immune cell response, would render this therapy ineffective. PI-9 could therefore be used as a metric to determine whether immunotherapy would be a useful treatment, potentially saving significant expense and time. Another avenue to treatment could be eliminating PI-9, which would remove the block to apoptosis. Evidence from the literature shows that Granzyme M, another protease located inside cytotoxic lymphocytes, can cleave and inactivate PI-9 (Mahrus et al., 2004). If Granzyme M could be increased in an isolated population of immune cells, possibly through treatment with cytokines, these immune cells could be introduced into the patient to both inactivate PI-9 and induce apoptosis in cancer cells. In combination with an extracellular protease inhibitor to block MIC shedding (Liu et al., 2010), this combination would have the potential to treat both mechanisms of immunoevasion. Additionally clinical studies are warranted to explore the possibilities of treating prostate cancer with upregulated PI-9.

Phosphonate Activity Based Probes: tools for labeling and beyond?

In this thesis, a systematic approach was taken to elucidate the parameters governing the potency of peptide phosphonate activity based probes, as well as their use as tools to study active proteases. This study resulted in a series of guiding principles for the design of peptide phosphonate ABPs targeting S1A proteases. The composition of the peptide element alone did not confer enough specificity to distinguish between similar S1A proteases, but the composition did strongly influence the stability of the probe in aqueous solution. Since most of the binding energy in S1A proteases comes from the binding of the P1 residue in the S1 pocket, additional residues should be chosen to optimize stability where possible. The length of the peptide element was more indicative of potency, where longer peptides inhibited the proteases more effectively, most likely due to additional contacts between the protease and the probe. The shape and size of the leaving group in fact governs potency more effectively, which could be exploited to obtain specificity.

While creating a probe specific to a single protease proved challenging, using these principles, a pan-S1A probe was created and used to label active proteases in several systems. Active proteases were visualized at the cell surface, and these proteases could be quantified by flow cytometry and followed by microscopy within the cell. The ability to quantify active proteases allows comparisons of proteolysis levels between different cell types and under different conditions. These measurements could be correlated with a phenotype, such as metastatic potential, creating a new approach to studying cancer. Additionally, observing the location and pattern of active surface proteases within the cell gives new information about the function of these proteases. For example, proteases in PC3 cells were located along one edge and were internalized, whereas proteases in PDAC cells were observed in tight puncta. It will be interesting to correlate these patterns with the phenotype of each cell type and the function of the protease. Future experiments using matrigel assays for cellular invasion in the presence and absence of protease inhibitors could further define the role of these surface proteases in cancer cells. This technique could be applied to any cell type to learn new information about the function of proteases in any system.

The next frontier for these activity based probes will be to identify the labeled proteases. The ability to identify active proteases in a complex system, or to get a “snapshot” of proteolysis, will provide a wealth of new information on diverse cellular functions. Particularly, comparing the proteases active under different conditions, such as normal and cancerous cells, or active and dormant bacteria, could identify the proteases governing these phenotypic switches. Learning more about the proteases and pathways controlling human diseases will lead to the discovery of new drug targets and intervention points.

However, identification by mass spectrometry has proved challenging. Attempts to assign identities to the labeled proteases have resulted both in poor enrichment and a dearth of proteases or serine hydrolases identified by mass spectrometry. Proteases are generally not needed in large abundance, making detection difficult under any circumstances. Enrichment of labeled proteases is complicated by the slow kinetics of phosphonate ABPs. Overcoming the slow kinetics requires the use of high concentrations of probe and long incubation times in the absence of serine protease inhibitors. These excess biotinylated probe binds to the avidin beads used for enrichment, swamping the much smaller pool of labeled proteases. The excess probe can be removed through the use of both precipitation and size exclusion techniques, making the pulldowns more effective. However, any remaining probe, if designed to target S1A proteases, could also inhibit the trypsin used for generating peptides, one of the first steps in preparing protein samples for mass spectrometry. Multiple rounds of probe removal or larger amounts of trypsin may be necessary to overcome the issue of excess probe.

Much of the work in identifying proteases has focused on whole cell lysates, both mammalian and bacterial. The shift in focus to cell surface proteases may solve many of the problems associated with these pulldowns. By labeling only the outside of intact cells, excess probe can be removed in washing steps before lysis, preventing the complications during the enrichment and trypsinization steps. Additionally, most of the steps in the enrichment protocol can be carried out using intact cells, decreasing the time unstable

lysates are used and improving the overall stability of labeled proteases. Proteases at the cell surface are key players in communication between the cell and its outside environment. Focusing on cell surface proteases holds much promise for the development of successful protocols to identify active proteases that are involved in key processes like cancer metastasis.

Lastly, creation of a releasable detection tag may improve the protein samples generated for mass spectrometry. The work presented here uses a biotin-avidin system for enrichment, and this tight interaction offers many advantages, such as the ability to withstand harsh washing conditions. However, this interaction can only be broken by extreme conditions like boiling in SDS or very high or low pH, which also removes any other protein bound to the pulldown beads. This results in high nonspecific background in the mass spectrometry protein samples, and along with the low abundance of protease, identification becomes difficult. Synthesizing a releasable element into the activity based probe would allow for the specific elution of labeled proteases and a much cleaner protein preparation. Attempts to create a specifically cleavable probe included the use of iminobiotin, which elutes at high pH, a base-cleavable linker, and a UV light-cleavable linker. However, these probes were either less stable or less potent than their corresponding non-releasable probes. Current research into more stable cleavable elements is ongoing.

In conclusion, although technical limitations remain, it is clear that by gaining greater insight into the mechanism of serine protease inhibition, new discoveries in the pathways and treatments of human diseases may unfold.

References

- Croswell, J. M., Kramer, B. S., and Crawford, E. D. (2011). Screening for prostate cancer with PSA testing: current status and future directions. *Oncology (Williston Park, N.Y.)* 25, 452-460, 463.
- Heidenreich, A., Aus, G., Bolla, M., Joniau, S., Matveev, V. B., Schmid, H. P., and Zattoni, F. (2008). EAU Guidelines on Prostate Cancer. *European Urology* 53, 68-80.

Liu, G., Atteridge, C. L., Wang, X., Lundgren, A. D., and Wu, J. D. (2010). The membrane type matrix metalloproteinase MMP14 mediates constitutive shedding of MHC class I chain-related molecule A independent of A disintegrin and metalloproteinases. *J. Immunol* 184, 3346-3350.

Mahrus, S., Kisiel, W., and Craik, C. S. (2004). Granzyme M is a regulatory protease that inactivates proteinase inhibitor 9, an endogenous inhibitor of granzyme B. *J. Biol. Chem* 279, 54275-54282.

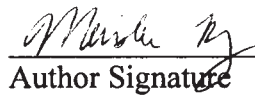
Small, E. J., Schellhammer, P. F., Higano, C. S., Redfern, C. H., Nemunaitis, J. J., Valone, F. H., Verjee, S. S., Jones, L. A., and Hershberg, R. M. (2006). Placebo-Controlled Phase III Trial of Immunologic Therapy with Sipuleucel-T (APC8015) in Patients with Metastatic, Asymptomatic Hormone Refractory Prostate Cancer. *Journal of Clinical Oncology* 24, 3089 -3094.

Publishing Agreement

It is the policy of the University to encourage the distribution of all theses, dissertations, and manuscripts. Copies of all UCSF theses, dissertations, and manuscripts will be routed to the library via the Graduate Division. The library will make all theses, dissertations, and manuscripts accessible to the public and will preserve these to the best of their abilities, in perpetuity.

Please sign the following statement:

I hereby grant permission to the Graduate Division of the University of California, San Francisco to release copies of my thesis, dissertation, or manuscript to the Campus Library to provide access and preservation, in whole or in part, in perpetuity.



Author Signature

7 | 27 | 11

Date